PALACKY UNIVERSITY

FACULTY OF MEDICINE AND DENTISTRY

Doctoral program: Pediatrics

Identification of meningioma prognostic biomarkers using transcriptomic profiling

Hanuš Slavík, M.Sc.

Supervising department:

Laboratory of Experimental Medicine,

Institute of Molecular and Translational Medicine,

Faculty of Medicine and Dentistry,

Palacky University Olomouc

Supervisor:

Josef Srovnal, M.D., Ph.D.

Olomouc 2021

Statement:

I declare that this thesis has been written solely by myself and that all the relevant resources are cited and included in the references part. The research was carried out at the Laboratory of Experimental Medicine, Institute of Molecular and Translational Medicine, Faculty of Medicine and Dentistry, Palacky University in Olomouc, and in the cooperation with the University Hospital in Olomouc and other participating institutions.

Acknowledgment:

First, I would like to thank my supervisor Josef Srovnal, M.D., Ph.D. for his professional leadership, support, helpful approach, many fruitful scientific discussions, and especially for the opportunity to work on the presented project, which allowed me to scientifically grow in many ways. I would also like to thank Vladimír Balik, M.D., Ph.D. for his help, willingness, and diligence in our joint scientific work on this project. Moreover, I would like to thank the entire staff of the Laboratory of Experimental Medicine, especially the members of our team within the RNA laboratory, for friendly work environment. Namely, I would like to mention Alona Řehulková, M.D., Pavel Stejskal, M.Sc., Monika Vidlařová, M.Sc., Kateřina Štaffová, M.Sc., and Veronika Černohorská, M.Sc. Special thanks go to Zuzana Macečková, M.Sc. and Natálie Kudlová, M.Sc. My thanks also go to all the co-authors of our joint publications. The most important people and their specific contributions are mentioned in the methodological part of this thesis. Last but not least, I would like to thank my loved ones, especially Lucie Borková, Ph.D., Melanie Slavíková, Eng., and Wiesław Fierla, for their continuous support.

This study was supported by Ministry of Health of the Czech Republic (15-29021A), Ministry of Education, Youth and Sport of the Czech Republic (LM2018132), Palacky University Olomouc (LF 2021_019), Technological Agency of the Czech Republic (TN01000013), and European Regional Development Fund (ENOCH CZ.02.1.01/0.0/0.0/16_019/0000868 and ACGT CZ.02.1.01/0.0/0.0/16_026/0008448).

In Olomouc

November 2021

Hanuš Slavík, M.Sc.

Bibliographical identification:

Author´s name and surname:	Hanuš Slavík
Title:	Identification of meningioma prognostic biomarkers using transcriptomic profiling
Type of thesis:	Dissertation
Department:	Laboratory of Experimental Medicine, Institute of Molecular and Translational Medicine, Faculty of Medicine and Dentistry, Palacky University Olomouc
Supervisor:	Josef Srovnal, M.D., Ph.D.
The year of defense:	2021
Keywords:	meningioma, prognosis, miRNA, mRNA, lncRNA, recurrence
Number of pages:	87
Language:	English

Bibliografická identifikace:

Jméno a příjmení autora:	Hanuš Slavík
Název práce:	Identifikace prognostických biomarkerů u meningeomů pomocí transkriptomického profilování
Typ práce:	Dizertační
Pracoviště:	Laboratoř experimentální medicíny, Ústav molekulární a translační medicíny, Lékařská fakulta Univerzity Palackého v Olomouci
Vedoucí práce:	MUDr. Josef Srovnal, Ph.D.
Rok obhajoby práce:	2021
Klíčová slova:	meningeom, prognóza, miRNA, mRNA, lncRNA, rekurence
Počet stran:	87
Jazyk:	Anglický

Abstract:

Meningiomas represent more than 20% of all intracranial tumors and their growth rate is highly variable. Even some benign forms may grow faster and progress at a later stage. Biomarkers that could identify aggressive and potentially recurrent meningiomas early and thus allow prediction of their biological behavior are scarce in current clinical practice.

This thesis is primarily focused on the screening (microarray, NGS) and validation (RT-qPCR) of new prognostic biomarkers in meningiomas using coding and non-coding ribonucleic acids. Moreover, RNA in-situ hybridization was used for the MEG3 tracking within the meningioma tissue. Archive tissue samples of surgically removed meningiomas were used in all analyses.

Multivariate Cox models identified decreased miR-331-3p expression and increased lnc-GOLGA6A-1 expression as the most effective markers for the recurrence risk estimation. Additionally, decreased cluster formation and increased nuclear localization of MEG3 were correlated with a higher probability of meningioma recurrence.

Our findings might lead to improvement of postoperative care by optimization of follow-up surveillance as well as the discovery of new therapeutic targets.

Abstrakt:

Meningiomy představují více než 20% všech intrakraniálních nádorů a jejich rychlost růstu je velmi variabilní. I některé benigní formy mohou rychleji růst a v pozdější fázi progredovat. Biomarkerů, které by včasně identifikovaly agresivní a rekurentní meningiomy a umožnily tak predikci jejich biologického chování, je v současné klinické praxi nedostatek.

Tato práce je primárně zaměřena na screening (microarray, NGS) a validaci (RT-qPCR) nových prognostických biomarkerů u meningiomů pomocí kódujících a nekódujících ribonukleových kyselin. Kromě toho byla pro sledování MEG3 ve tkáni meningiomu použita RNA in situ hybridizace. Ve všech analýzách byly použity archivní vzorky tkáně chirurgicky odstraněných meningiomů.

Multivariátní Coxovy modely identifikovaly jako nejúčinnější markery pro odhad rizika recidivy sníženou expresi miR-331-3p a zvýšenou expresi lnc-GOLGA6A-1. Navíc snížená tvorba klastrů a zvýšená nukleární lokalizace MEG3 korelovaly s vyšší pravděpodobností recidivy meningiomu.

Naše zjištění by mohla vést ke zlepšení pooperační péče v průběhu dispenzarizace a k objevu nových terapeutických cílů.

Contents

1. Detailed introduction to the thesis

Clinical, histopathological, and biological characteristics of meningiomas and already available prognostic markers are described in this chapter. Due to the fact that the experimental work is based on the analysis of various types of RNAs (ribonucleic acids), non-coding RNAs are also introduced. The emphasis is placed on microRNAs (miRNAs) and long non-coding RNAs (lncRNAs) in the context of coding genes, thus messenger RNAs (mRNAs) are included as well.

1.1 Meningiomas

These tumors arise from brain envelopes (meninges), most probably from the arachnoid layer, which represents the thinnest and softest meninges [1]. This fact explains, why the meningiomas are often localized near to the inner side of the skull (Fig. 1A) and rarely within the spine, where meninges are also located [2]. It was generally supposed that these tumors are derived from cap cells located in leptomeninges (arachnoid matter and pia mater representing soft and thin meninges) [1] [2] [3] [4], but this hypothesis has never been proven and the cellular features of these tumors are reflecting various cell types [2] [5]. Only one study, which was focused on the origin of meningioma cells experimentally proved that meningiomas are more probably originated in meningeal precursor cells with high expression of prostaglandin D synthase (PGDS) [6]. Nevertheless, this study was performed using PGDS-Cre model mice and only two benign meningioma histological subtypes were derived. Deciphering the origin of meningiomas complicates also the fact that meninges can have both mesodermal and neural crest histogenetic origin according to their cranial localization [6] [7]. The presence of cancer stem cells (CSC) in meningiomas was also identified according to the cultivation experiments and expression of the markers such as nestin, vimentin, and CD133 [4]. Yet, the biological context of CSC in meningioma pathogenesis is still not fully elucidated, as in the case of the other benign tumors [4] [8]. Although approximately 80% of all surgically resected meningiomas are benign, grow slowly, and do not invade the brain itself, more aggressive forms of those tumors also exist [3] [9]. According to the actualized WHO (World Health Organization) classification of brain tumors from 2016, there are three histopathological grades of meningiomas according to their degree of differentiation corresponding to their invasiveness, growth rate, and the probability of recurrence [9] [10]. Besides benign meningiomas (WHO grade I), there are also atypical meningiomas (WHO grade II), which can grow more rapidly and can invade the brain itself (18% of diagnosed meningiomas). The rarest cases (2% of

diagnosed meningiomas) are represented by malignant, so-called anaplastic meningiomas, which recur more frequently than lower grade meningiomas and are typical for their invasion into the brain [9] [11] [12]. However, future recurrence itself cannot be estimated only according to WHO grade; surgically removed benign tumors can also recur. In approximately 25% of patients with WHO grade I meningiomas recur during 10 years after surgical resection of the tumor [11].

The extent of surgical resection also influences the probability of meningioma recurrence [11]. Total resection is defined as the removal of the whole tumor with attached dura mater (the hardest meninges; Fig. 1C) and potentially affected bone. This procedure is not possible to perform in each case because of the risk of blood supply disruption, brain injury, or inaccessible location of the tumor [13]. Thus, in 1957, Simpson grade (SG) was defined according to extent of surgical resection and this parameter is determined by the surgeon [14]. SG I represents total resection with the lowest probability of recurrence (Fig. 1B). SG II – III are gross total resections, where the tumor itself is removed completely, but parts of the attached structures (bone, dura mater) remain [9] [13] [14]. SG IV is incomplete resection of the tumor, where the risk of recurrence is almost five times higher than in SG I. Only biopsy and decompression of the affected area are marked as SG V [11].

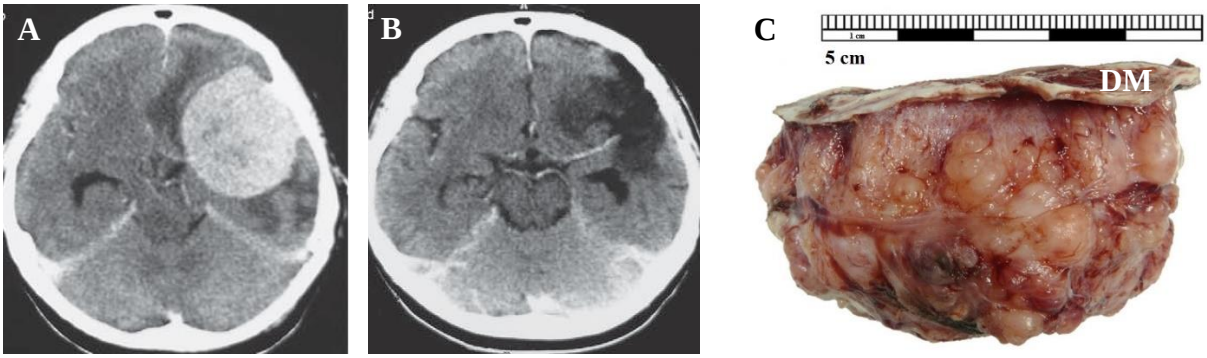

Figure 1. *Pre-operative (A) and postoperative (B) CT scans show a left-sided meningioma-like contrast-enhancing tumor, originating at the left sphenoid wing. Postoperative CT scan 1 year after surgery shows that the tumor was completely removed and does not recur (images kindly provided by Dr. Vladimir Balik). Completely resected meningioma with attached dura mater (DM; C) adapted from Shivapathasundram's review article* [4].

Neurosurgery is the most often way how to effectively treat meningiomas, but there is a high risk of postoperative complications and further consequences, such as the development of anxiety and depression (up to 40% of the patients) [9] [15]. Thus, the "watch and wait" approach is often chosen for patients with non-aggressive, asymptomatic, or mild symptomatic

meningiomas. Regular medical examinations using computed tomography (CT) and magnetic resonance (MRI) serves for the monitoring of these patients. These methods are also used for primary diagnostics and pre-operative and post-operative management of the patients [9] [13] [15].

In case of incomplete resection, presence of inoperable meningioma, or growth slowdown of an aggressive tumor, radiotherapy is the next choice in the treatment of these tumors [16]. However, ionizing radiation is one of the most significant risk factors for the development of meningioma [17]. Because of this paradox, there is an effort to avoid radiotherapy. Unfortunately, there is no routinely used systemic therapy of meningiomas. Nevertheless, there are few drugs currently in clinical trials. For instance, nivolumab and pembrolizumab are tested for treatment of residual and recurrent meningiomas of higher WHO grades [13]. These two drugs activate T-lymphocytes and their utility is based on the assumption that higher-grade meningiomas have impaired immune microenvironment [13] [18]. Moreover, inhibitors of the mTORC1 pathway (everolimus, temsirolimus, vistusertib) showed satisfactory results in the treatment of meningiomas even in phase II clinical trials [13]. This pathway is often over-activated in meningiomas, which is mainly caused by a mutation in the NF2 gene producing a protein merlin that influences the mTOR pathway [19].

NF2 represents the most often altered gene in meningioma with an abundance of more than 50% cases of sporadic meningiomas of all WHO grades. NF2 is supposed to play a crucial role in the proliferation of meningeal cells and is located on a 22q chromosomal locus, often prone to alterations in meningiomas [20]. The abbreviation NF2 is derived from the name of the disease Neurofibromatosis type II, which is characterized by the germinal mutation in the NF2 gene leading to a higher probability of development of meningiomas or other tumors [21]. Meningiomas without NF2 mutation usually carry at least one of the following described mutations.

Tumor necrosis factor receptor-associated factor 7 (TRAF7) is mutated in about 20% of meningiomas and is involved in many signaling pathways. The mutations in KLF4, AKT1, SMO, or PIK3CA are typical for meningiomas with an occurrence of less than 10% [3] [20]. There are also promotor mutations, such as in the telomerase transcriptase gene (TERT), which has a negative prognostic value and is associated with recurrence and progression [20]. Two possible alterations have been found in RNA polymerase II (specifically in POLR2A gene for the largest protein subunit) exclusively in WHO grade I meningiomas [3] [20]. Other types of alterations, such as complex deregulation of signaling pathways also exist. A typical representative of this phenomenon in meningiomas is Wnt signaling pathway [22] [23] [24].

On the chromosomal level, there are various types of alterations, especially on 1, 6q, 10, 14q, 18, and 22q loci, associated with a worse prognosis including the possibility of recurrence. These chromosomal loci have often altered the methylation profiles, which seems to be crucial in the development of prognostic tools in meningiomas [25] [26]. Gene expression signature of meningiomas seems to be quite complex and variable among different studies and that aspect will be discussed in further chapters (1.1.4). Nevertheless, investigation of meningiomas on molecular levels helped us to understand the biological substantiality, but there is still a lack of specific prognostic and predictive biomarkers and treatment of this disease.

1.1.1. Histopathological classification

Meningiomas are divided into 15 subgroups according to their morphological features based on hematoxylin-eosin FFPE tissue slices staining [4]. These subgroups are divided into 3 histopathological grades by WHO according to a degree of differentiation [10]. WHO grade I, so-called benign, contains 9 subgroups showing a relatively high degree of differentiation and signs of organized tissue architecture, which is specific for each subgroup (Fig. 2). These subgroups are meningothelial, fibrous, transitional, psammomatous, secretory, angiomatous, microcystic, lymphoplasmacyte-rich, and metaplastic meningiomas. Importantly, WHO grade I meningiomas do not contain the features of higher grades (Fig. 2), such as increased mitosis, spontaneous necrosis, prominent nucleoli, increased cellularity, or higher nucleus to cytoplasm ratio [4] [9] [12]. In the final consequence, tumors with those features are clinically more aggressive, can recur more frequently, and can invade the brain itself [12]. WHO grade II meningiomas, generally called atypical meningiomas include atypical, clear cells, and chordoid subtypes and show an 8 times higher recurrence rate than benign meningiomas [11] [12]. The most aggressive meningiomas from a histopathological point of view are referred to as malignant or anaplastic. There are 3 subtypes in the WHO grade III category: anaplastic, papillary, and rhabdoid. WHO grade III meningiomas are the rarest (2-4% of all meningiomas), but they are associated with adverse prognosis [11] [12] [27]. Only approximately 30% of WHO grade III meningiomas have recurrence-free survival (RFS) higher than 5 years; overall survival (OS) usually does not reach 10 years [11]. Nevertheless, even benign lesions after total resection can recur in 12-19% within 10 years [28]. The histopathological classification itself is therefore insufficient in meningioma prognostication and this type of diagnosis is inaccurate by a subjective error. Interestingly, WHO grade III meningiomas can show similar morphological patterns as melanomas or carcinomas. Additional markers are currently being introduced in

histopathological practice using immunohistochemical (IHC) staining [29]. For instance, the combination of somatostatin receptor (SSTR2A) and epithelial membrane antigen (EMA) IHC staining can specifically distinguish the meningioma tissue [30]. However, Ki-67 IHC staining is the most relevant additional marker routinely used during histopathological classification these days. Ki-67 is expressed in the nucleus during the active phase of the cell cycle, and it is a tool for determining the proliferation index in various cancers (Fig. 2). Proliferation index > 4% is associated with worse OS and RFS in meningiomas [29] [31].

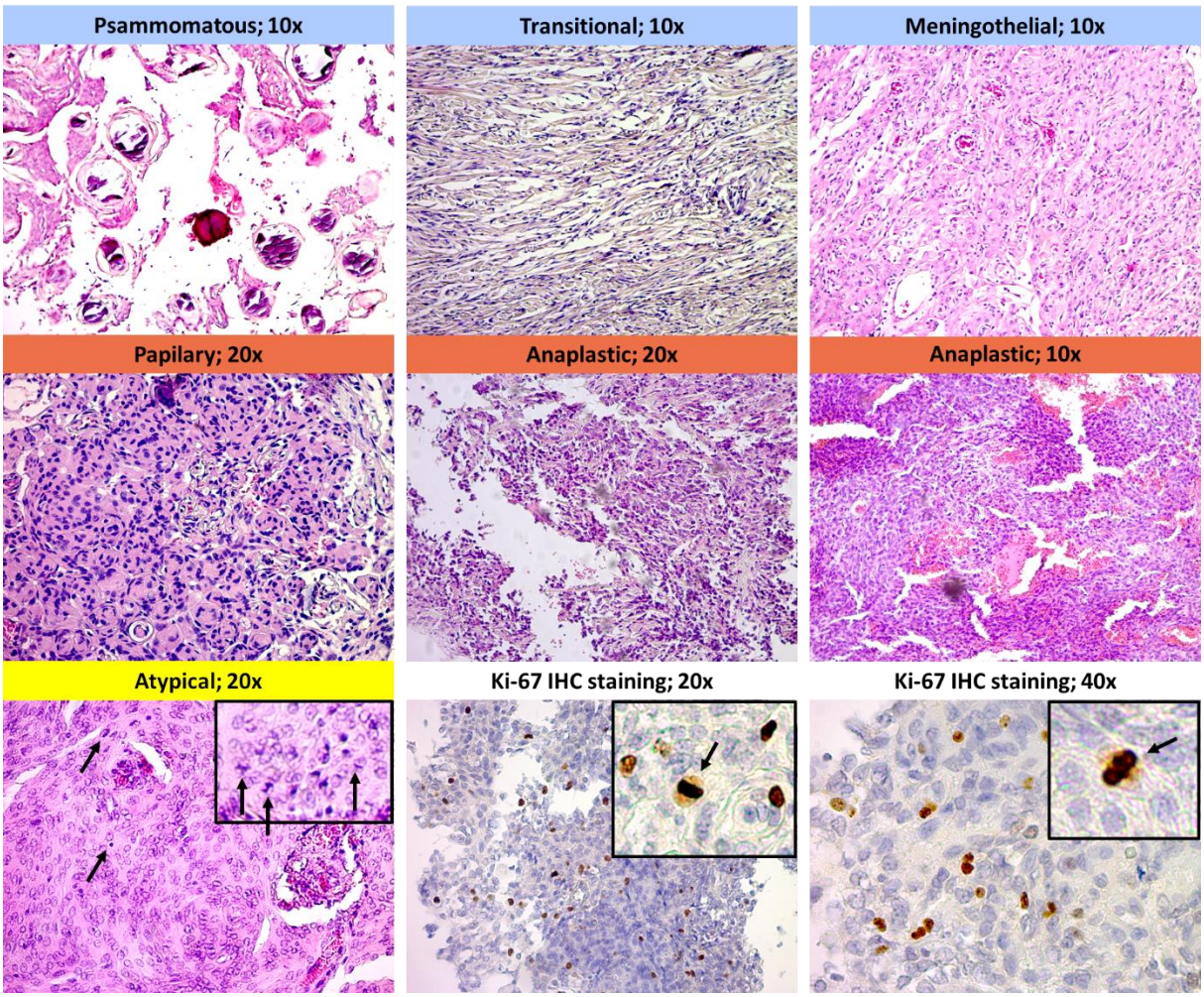

Figure 2. *Selected histopathological features in meningiomas. Certain histological subtype with respective image magnification is introduced above each image in the color of respective WHO grade (I-blue; II-yellow; III-red). The first line represents morphological variability of WHO grade I tumors with a common feature of low cellularity and sparse representation of nuclei. Contrary, there are high cellularity, prominent nuclei, and a larger area of nuclei in the second line of malignant meningiomas. The black arrows show mitoses. The samples are stained with the hematoxylin-eosin method (ping – cytoplasm / intercellular space; dark-blue –*

nuclei / DNA) and immunohistochemistry (IHC) for proliferation index determination by Ki-67 marker (brown) co-stained with hematoxylin (dark-blue).

Meningiomas after surgical resection can progress into higher WHO grades if they recur. This phenomenon is sometimes called atypical or malignant transformation. There is a 19.5% risk of recurrence in all meningioma patients, who need therapeutic intervention. Only about 1% of recurrent patients will progress [32]. Loss of 1p36 chromosomal loci and CCNB1 and CDC2 coding genes are molecular patterns associated with progression. The expression pattern of mRNA GREM2 and small nucleolar RNAs (snoRNAs) SNORA46 and SNORA48 can also distinguish between benign meningiomas, which will progress, and those, which will not [18]. Nevertheless, the complex molecular mechanism of meningioma progression is unknown [3] [18].

Molecular differences among various histological types are also present. For instance, gains on chromosome 5 are typical only for angiomatous meningiomas, whereas mutations in AKT1, TRAF7, and KLF4 are typical for WHO grade I of all histological subtypes [3] [12]. WHO grade I tumors are also more strongly infiltrated by immune system components in comparison with higher grades [18]. High-grade meningiomas (WHO grade II and III) exhibit a higher mutation rate and more complex chromosomal changes [33]. Regarding proteomic characterization, WHO grade I tumors are enriched by proteins for extracellular matrix formation and mitochondrial metabolism. Oncogenes involved in RNA metabolism and signaling pathways, including TNF-α and c-Myc, were identified in tumors of higher grades [27].

1.1.2. Location and histo-genetic origin

The vast majority of meningiomas are intracranial and extracerebral lesions lining the edges of meninges and subdural cavities. Especially WHO grade I meningiomas are encapsulated and well-defined [34]. Only less than 2% of meningiomas are spinal [35]. Intracranial meningiomas can be divided into central (medial) and peripheral (lateral) tumor locations [34]. The most common central meningiomas are falcine and parasagittal, which together represent about 25% of all meningiomas [34] [35]. There are also suprasellar and olfactory groove locations, both representing 10% of diagnosed meningiomas, whereas central meningiomas located intraventricularly and petroclivaly are very rare [35]. Lateral meningiomas represent convexity (20%) and posterior fossa (10%). Sphenoid wing tumors can

be either central or peripheral, depending on the exact position relative to the sphenoid bone [34] [35]. Most often meningioma intracranial locations are summarized in Fig. 3. Central meningiomas are associated with worse clinical outcomes because of difficult surgical accessibility and dense vascularization within this location [34]. Nevertheless, skull-based meningiomas, which are placed at the bottom of the skull (sphenoid wing, posterior fossa, olfactory, etc.; Fig. 3) are not generally associated with higher mortality or morbidity due to surgical intervention in these days [36]. On the other hand, convexity meningioma, which is surgically most accessible, because of its location on the upper side of the brain, is associated with the worst outcome. Tumors on the convexity are most often malignant and recurrent in comparison with other localizations [34] [37].

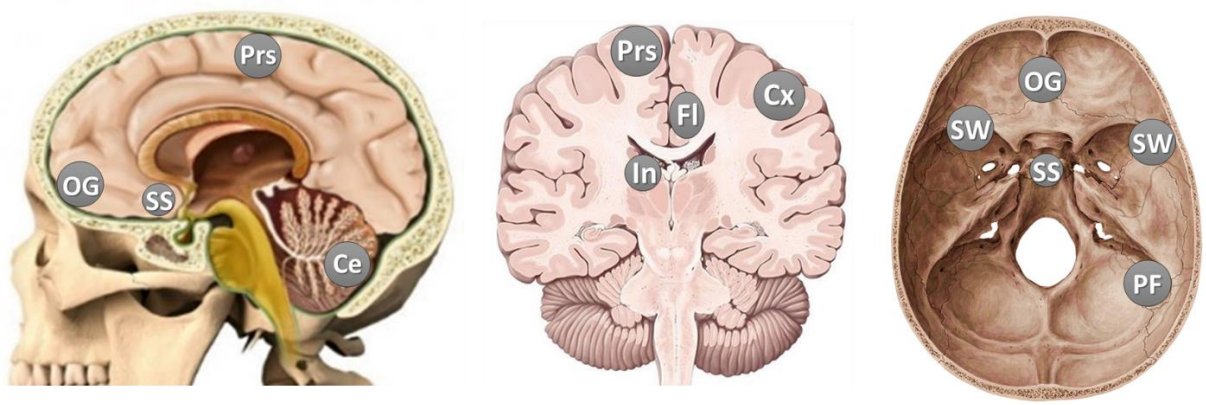

Figure 3. *Selected usual locations of intracranial meningiomas: Parasagittal (Prs), Olfactory groove (OG), Suprasellar (SS), Cerebral (Ce), Falcine (Fl), Convexity (Cx), Intraventricular (In), Sphenoid wing (SW) and Posterior fossa (PF). Images were adapted and prepared according to the websites hopkinsmedicine.org and cz.pinterest.com.*

A possible explanation for the increased aggressiveness of convexity meningiomas is their location in the area of exclusive neural crest-derived histogenetic origin. In general, tumors arising from the neural crest are more likely aggressive and malignant, because neural crest-derived cells have a higher capacity of migration and proliferation, and the ability of differentiation [38]. Regional variability in the meningeal histogenesis with various meningeal progenitors suggests that it plays a role in the development of meningiomas and their variable behavior. The precursor is of mesoderm origin at the skull base and of neural crest-derived at the convexity [6]. At the early prenatal stage, a neural crest-mesodermal interface is located where the frontal neural crest-derived and parietal mesoderm-derived bones meet (Fig. 4). When the telencephalon begins to expand caudally, it carries with it the borderline [39]. The neural crest-derived meninges thus cover the convexity up to the posterior/caudal edge of

cerebral hemispheres, whereas meningeal layers of the posterior cranial fossa (around brainstem and spinal cord) arise from the mesoderm [40]. This process is preceded by neurulation - the stage when the neural tube is developed during embryogenesis (Fig. 4). The neural crest cells then begin to migrate and later differentiate into other cell types [41]. Nowadays, molecular mechanisms of those processes are already well-understood, but it has never been studied in the context of meningioma development.

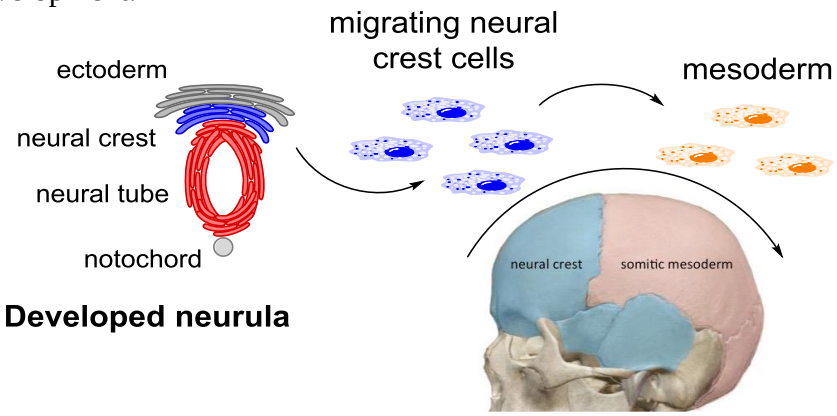

Figure 4. *Migration of neural crest-derived cells after the neurulation explains the location-based histogenetic origin of the skull and potentially developed meningioma. The image of the skull is adapted from the Medical Embryology website of Drexel University (webcampus.drexelmed.edu) and adjusted according to Méndez-Maldonado's review* [41].

1.1.3. Gender aspects and hormonal dependency

Women are more likely to be affected by non-malignant meningiomas with a female:male ratio of 2.3:1 [42]. Based on 702 aggregated samples, low-grade meningiomas occurred significantly more frequently in females [33], while in a cohort of 300 meningiomas, higher-grade lesions were observed more often in males [43]. Interestingly, spinal meningiomas have the strongest female predominance with 75-90% of all diagnosed cases [44]. This male predominance in higher-grade lesions was also reported in terms of DNA methylation profile [45]. Regarding genotyping, meningiomas with NF2 loss and/or NF2 mutation, but without TRAF7, AKT1, KLF4, or PIK3CA mutations were predominantly observed in the male population, while TRAF7/KLF4 lesions exhibited female dominance [46]. Testing of affected and unaffected relatives of a patient with clear cell meningiomas with a large deletion of the 5′ end of SMARCE1 gene identified the same deletion in two affected female siblings and their unaffected father, implying incomplete penetrance of meningioma disease in males [47]. On the epigenetic level, miR-224 was found to be more expressed in females, most probably because miR-224 maps to chromosome X [48].

The most likely explanation for the prevalence of female meningiomas is their hormonal dependence: 88% of meningiomas are positive for progesterone receptors (PR) and about 40% are positive for androgen (AR) or estrogen receptors (ER). Even though there is no difference in hormonal receptor expression according to age and sex [49], there is still a higher risk of meningioma development for breast cancer patients, users of progestins, and patients during risky pregnancy suggesting the link between meningioma and sex steroid hormones [44]. Also, there is a higher expression of PR in meningioma patients treated by cyproterone acetate (anti-androgen and progestin medication) [44]. Similarly, 83% of women with a special homogenous group of spheno-orbital osteomeningiomas exhibits significant exogenous progesterone uptake. These tumors are positive for PR in 96% of cases, are benign and recur after surgical resection in 25% of cases [50]. Hormonal intake can influence the mutation landscape of the tumor with hormonal dependence, which was previously described in breast or endometrial cancers. This phenomenon was reported also in meningiomas when long-term progestin therapy results in tumors with a higher frequency of PIK3CA mutations and a lower frequency of NF2 mutations [51].

Expression of sex hormonal receptors is more typical for WHO grade I than for higher grades. Those receptors are linked with higher proliferation (Fig. 5), which possibly supports the phenomenon of recurrence events in benign meningiomas [49].

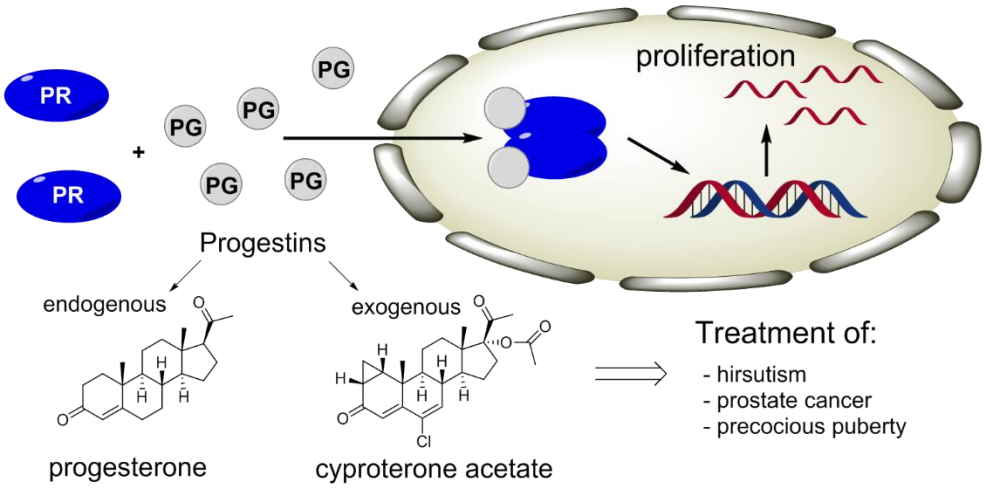

Figure 5. *Progesterone receptor (PR) induces transcription of specific genes after binding of progestin. During this process, PR dimer is created and translocated into the cell nucleus, where transcription is induced with the binding of PR dimer to the specific DNA region. Lack of natural endogenous progestin, mostly composed of progesterone, or more often excess of androgen stimulation, can be treated with exogenous progestins. However, tissues with high*

expression of PR are prone to hormonally induced carcinogenesis after the stimulation with progestin. This phenomenon is typical for breast cancer and probably also for meningioma.

1.1.4. New potential molecular prognostic biomarkers

The molecular and genomic landscape of meningioma is already well-explored, especially on the level of DNA (chromosomal abnormalities, small scale mutations, and methylation profiles). Regarding transcriptomic and proteomic investigations, there are still a lot of uncertainties [3]. Moreover, most of the known molecular patterns cannot be used universally for meningioma prognostication. For instance, NF2 is most commonly affected in meningioma, but this feature has no prognostic value [3] [26]. Therefore, only the molecular signatures with prognostic potential will be discussed within this subchapter. Local recurrence is the most relevant prognostic parameter for biomarker discovery in meningioma, thus most of the effort in meningioma clinical research is focused on this aspect. Nowadays, only proliferation index (Ki-67 or phospho-histone H3 at serine residue 10 staining) is routinely used for meningioma prognostication during histopathological evaluation [3].

On the cytogenetic level, copy number alterations (CNA) on 1p, 6q, 9p, 10, 14q, 17, 18p, and 22q chromosomes are associated with recurrence risk [25]. CNA losses on 1p, 6q, and 18q and gains on 1q were associated with recurrence in a prognostic unfavorable group according to DNA methylation status. This investigation revealed the methylation status of 64 CpG loci (Fig. 6), which were identified as important for meningioma prognosis when combined with CNA data and adjusting for clinical factors. The identified loci with different methylated status depending on the prognosis included 44 genes involved in G-protein coupled receptor signaling, axonal guidance signaling, cAMP-mediated signaling, Wnt and AMPK signaling, thrombin and glucocorticoid signaling, protein-kinases, PI3K/AKT and PTEN signaling, mTOR, p53, NF-κB signaling, and also in interleukin signaling [26]. Focusing on certain genes, TIMP3, CDKN2A, and NDRG2 methylation were associated with a shorter time-to-recurrence (TTR). Co-methylation of homeobox-related genes was also associated with aggressive tumors and progression. Hypermethylation of p53 and its binding partners (for instance MEG3 non-coding gene) can cause meningioma progression. Last but not least, methylation of IGF2BP1 and PDCD1 increases the malignant potential. Most of the methylation sites were found within promotor regions (Fig. 6). Hypomethylation of physiologically methylated regions has never been studied in terms of meningioma prognostication [52] as well as another DNA epigenetic

marker - hydroxymethylation (Fig. 6). CpG methylation represses transcription, but the specific biological function of hydroxymethylation remains unknown [53].

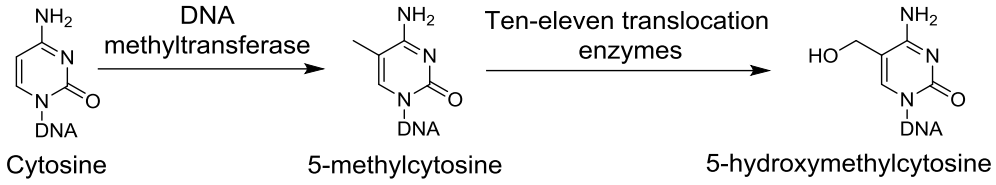

Figure 6. *DNA methylation and hydroxymethylation as a common epigenetic mark with potential utility in disease prognostication. Scheme of the frequent biochemical reactions on CpG regions, densely represented and already methylated or hydroxymethylated in gene's promotors according to Johnson's review article* [53].

DNA mutation status in meningioma is correlated with histopathological features and tumor location, but most of the driver and sporadic mutations, typical for meningioma, have no additional benefit in potential prognostication of RFS or OS. Only the previously described promotor mutation in the TERT coding gene is associated with poor clinical outcomes, such as recurrence and progression. This mutation has an incidence of approximately 9% and leads to activation of telomerase activity [3]. NF2 driver mutation is associated with a higher proliferation index, increased tumor size, and incidence of vasogenic edema, but it has no independent influence on RFS or OS in patients with meningioma [54].

Analysis of the coding transcriptome is evolving tool for meningioma prognostication. However, there is still a low number of studies, which are limited by a small number of patients involved. Moreover, there is a low overlap of the results among those studies [3]. This phenomenon can be probably caused by high variability in methodological screening approaches including microarray, NanoString, qPCR arrays, and various set-ups for NGS. Microarray screening with following independent qPCR validation revealed that downregulation of LEPR and upregulation of PTTG1 are associated with worse clinical outcomes, including recurrence and progression, independently on WHO grade, gender, or extent of resection [55]. Another study introduced a validated panel of 36 genes for recurrence risk estimation. The transcriptional signature of those genes, investigated using NanoString pre-designed cancer panel, is associated with RFS and OS [56]. Patel et al. distinguished meningiomas into the 3 molecular subtypes according to their RNA-seq data. The last type, C, is characterized by shorter RFS from the clinical point of view and decreased function of the DREAM complex on the molecular level. DREAM complex represses the cell cycle activation

and contains the proteins, which are bound to Rb-like proteins, and modulate their activity. The expression of genes that form the cell cycle-activating DREAM complex is also increased in C-type tumors [57]. For instance, FOXM1 is associated with such a function and has also been linked to aggressive behavior in meningioma, where it causes activation of Wnt signaling leading to increased proliferation [22] [57]. This explains, why C-type tumors showed the highest proliferation index [57]. Viaene et al. used the RNA-seq approach as well with further RT-qPCR validation. The study identified GREM2 mRNA as a potential marker of the progression of benign meningiomas. Additionally, two snoRNAs, SNORA46 and SNORA48, showed the same feature [18].

1.2. Non-coding RNAs

All RNAs, which are not translated into the proteins are called "non-coding", thus only mRNAs do not fall into this category. There are various types of non-coding RNAs and they have usually regulatory and catalytic functions. This type of cellular, intercellular, and distant regulation is involved in all-controlling processes in living organisms. Because of the wide variability of non-coding RNA species, they are divided into two major groups according to their length: small or short non-coding RNAs (< 200 - 300 nt) and long non-coding RNAs (> 300 nt) [58]. Even though this thesis is focused only on a few specific types of RNAs, the following table summarizes also the other most commonly known RNA species (Tab. 1).

Non-coding transcriptome has developed rapidly with NGS, microarray, and other high-capacity methods. Further detection and analysis are simplified, despite the low expression of some RNA species, by easy and accurate examination with RT-qPCR. These days it is generally known that some non-coding RNA species have better-discriminating potential than histology and immunohistochemistry. Thus, some non-coding RNAs, especially miRNA and lncRNA, are intensively studied in cancer.

Table 1. *Overview of selected RNA species according to Cech's review* [59].

Name	**Function and characteristics**	**Transcribed by**	**Length**
mRNA	Only protein-coding RNA	RNApol II	2 - 5 k nt
tRNA	Adaptor connecting an mRNA codon and amino acid	RNApol III	70 – 90 nt
rRNA	Ribozyme activity on the ribosome (4 strains); translation	RNApol I, III	120 – 5025 nt
miRNA	Endogenous negative regulation of gene expression	RNApol II, III	17 - 24 nt
siRNA	Exogenous negative regulation of gene expression	-	Cca 22 nt
snRNA	Splicing of pre-mRNA in the cell nucleus	RNApol II	100 – 300 nt

snoRNA	Processing and modification of pre-rRNA	RNApol II	> 60 nt
scaRNA	Modification of other sRNAs (especially snRNA)	RNApol II	200 – 300 nt
piRNA	Negative regulation of transcription	RNApol II	Cca 27 nt
telomeRNA	Template component for telomerase reaction	RNApol II	451 nt
hnRNA	Intron-containing pre-mRNA stabilization	RNApol II	2 – 40 k nt
Rnase P RNA	Processing of pre-tRNA and RNA degradation	?	400 nt
***RNA species legend**; messenger (mRNA), transfer (tRNA), ribosomal (rRNA), micro (miRNA), small interfering (siRNA), small nuclear (snRNA), small nucleolar (snoRNA), Small Cajal body-specific (scaRNA), PIWI-interacting (piRNA), heterogeneous nuclear (hnRNA)*			

1.2.1. Small non-coding RNAs (sncRNAs)

Most of the sncRNAs are involved in the process of maturation, regulation, and modification of other RNA species. For instance, there are small nuclear RNA (snRNA), PIWI-interacting RNA (piRNA), or Small Cajal body-specific RNA (scaRNA). However, there are a few exceptions, such as transfer RNA (tRNA), which is crucial in the process of translation [59]. Yet, the most intensively studied sncRNAs are miRNAs, which are also involved in the process of regulation of other RNA species.

MiRNAs are sncRNAs (17-24 nt), which negatively regulates most of the known mRNAs by antisense RNA interference (RNAi) mechanism. These days, more than 1,100 miRNA species have been identified in humans according to the miRBase v22 database, but it is estimated that there may be about 2,300 actual human miRNAs [60]. MiRNA-based regulation covers most of the processes in mammals, such as apoptosis, differentiation, proliferation, immune system, stem-cell features, and neoplastic transformation. Genes for miRNA are strongly conserved in genomes, located on all chromosomes (independently or in clusters), except Y, and transcribed by RNA polymerase II or III. Good temperature, pH, ribonuclease stability, and simple structure make miRNAs ideal candidates for biomarkers from an analytical point of view [61].

MiRNA biogenesis and function

Transcription of miRNA genes leads to primary miRNA transcript with a length of > 80 nt (pri-miRNA), which can be composed of one or more final miRNAs [59]. Pri-miRNA is processed with a microprocessor complex composed of Drosha and Pasha (DGCR8) proteins. This leads to cleavage of the targeted loop from pri-miRNA. The split loop is called precursor miRNA (pre-miRNA) with a total length of 60 nt and 2 nt unpaired overlaps at the 3’ termini [59] [62]. Pre-miRNA is then actively exported from the nucleus by Exportin-5 (EXP5) through

GTP-binding protein. Endonuclease DICER localized in cytoplasm cleaves the terminal loop from pre-miRNA, thus double-stranded miRNA is created. This miRNA duplex is loaded into the RNA-induced silencing complex (RISC) and one strand is removed (passenger strand). Mature one-strand miRNA remains attached to RISC until targeted long RNA is reached. RISC with mature miRNA usually binds to mRNA at 3'UTR (untranslated region at the 3' termini). Based on the principle of antisense mechanism, in the case of partial complementarity, translation of the targeted mRNA is stopped. In the case of complete complementarity, the targeted mRNA is degraded [62] [63]. The whole pathway of miRNA is summarized in Fig. 7.

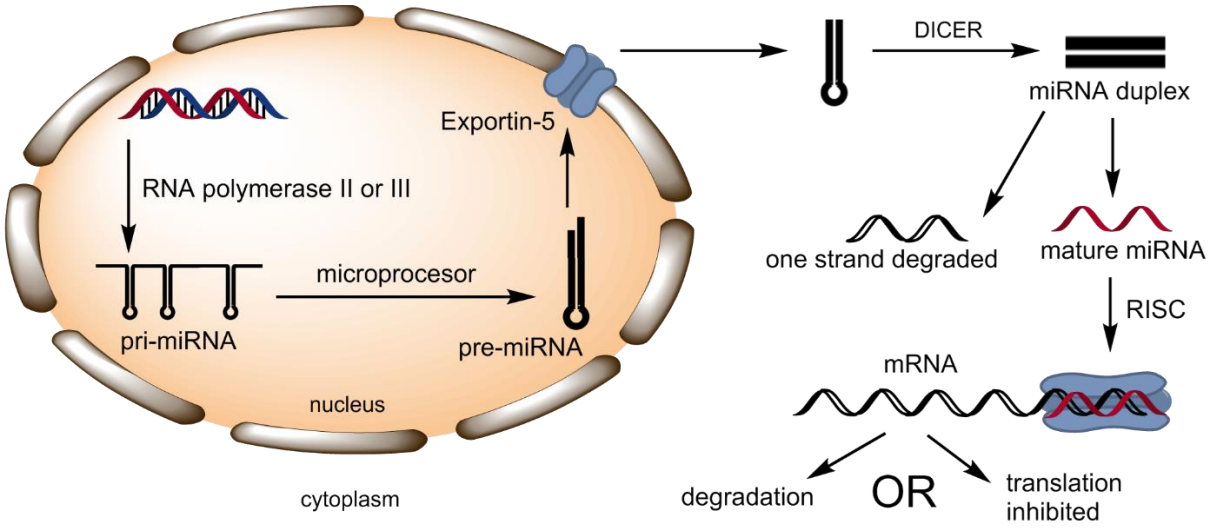

Figure 7. *Simplified scheme of miRNA maturation and function in mammals.*

Expression of miRNAs is regulated on the level of transcription by common transcription factors, such as p53, c-Myc, or NF-κB, or by promotor methylation, which is typical for malignancies. Also, miRNA maturation can be deregulated by influencing the activity of the microprocessor complex or DICER. For instance, heterogeneous nuclear ribonucleoprotein A1 (hnRNP A1) speeds up the processing of pri-miR-18a by a specific increase of accessibility to Drosha protein. This works similarly for some other miRNAs, such as the let-7 family [61].

After the maturation into the single strand miRNAs, they can be released from the cell of origin into the extracellular space, which usually results in the elevation of miRNAs in cell-free body fluids as circulating miRNA. MiRNAs are released from tissues actively (ATP activity) through vesicular particles or passively from the damaged cells, usually due to apoptosis or necrosis. Active transport carries miRNAs through exosomes, microvesicles, lipoproteins (HDL), or other protein complexes. The probable biological reason for the presence of miRNA in cell-free body fluids is distant communication and regulation among tissues in multicellular

organisms [64]. Each tissue and cell-free body fluid have a unique miRNA signature, which can be used in diagnostics or forensic applications [64] [65]. For instance, it is possible to distinguish between menstrual and non-menstrual blood or identify sperm-free semen according to specific miRNA signature [65]. The specific content of extracellular miRNA can be changed in case of the presence of the tumor or any other disease in the body. This feature can be used in non-invasive and easy diagnostics because extracellular miRNAs are stable and, in general, have better distinguishing potential than mRNAs [65]. For example, miR-21 is one of the most studied cancer-related miRNAs. Increased expression of miR-21 is typical for many types of malignant tumors, which is often reflected in plasma or serum of affected patients. Generally, the higher the miR-21 level is associated with a worse prognosis [67]. This can be used for the identification of early-stage patients using serum samples [66].

MiRNA nomenclature

There are no other natural nucleotide species with so unique nomenclature allowing the precise deciphering of the origin of the molecule according to the simple naming, as in the case of miRNA (Fig. 8). They are named according to the order of discovery, family, and the origin direction of the final leading strand after the maturation. There are few exceptions, such as let-7 or lin28, which were named before the official nomenclature was set up [61]. Most of the aspects of miRNA nomenclature are summarized in Fig. 8.

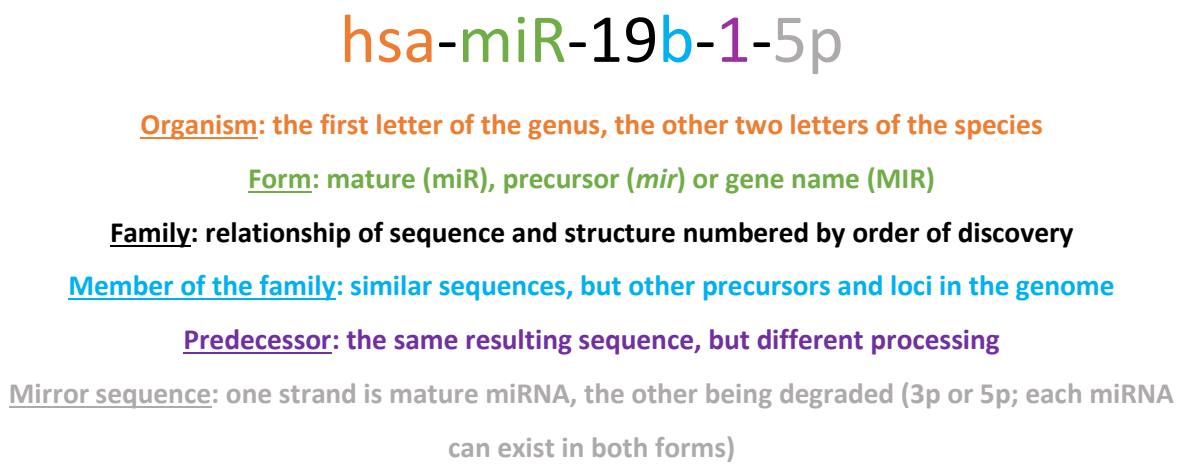

Figure 8. *Scheme of the miRNA nomenclature using the example of miR-19b-5p.*

MiRNA in cancer

MiRNAs can be divided into two groups. Those negatively regulating tumor suppressor genes are called oncogenic, whereas those targeting oncogenes are known as tumor suppressors.

The typical oncogenic miRNA is miR-21, while suppressor miRNAs are represented by, for example, the let-7 family. Usually, there is a balanced stable expression of both groups, but when neoplastic transformation starts to appear, the levels of oncogenic miRNAs increase, and the levels of tumor suppressors decrease [68]. Loss of miRNA expression during cancer development is more common due to damage at the genomic level [61]. The process of cancer development is influenced by miRNAs by various mechanisms. Cell proliferation and apoptosis suppression are promoted by miR-155. Loss of let-7 or miR-200 can promote cancer stem cell production and spread. Epithelial-mesenchymal transition (EMT), important for the creation of distant metastases, is blocked by miR-429 and miR-27, but also by miR-200. On the other hand, EMT is promoted by miR-9. Tumor cell invasion is promoted by miR-9 or miR-181 but it is blocked by miR-15a, miR-145, or miR-340 [69]. As an example of certain molecular targeting, miR-138 down-regulates the TERT mRNA level at physiological conditions. However, in anaplastic thyroid cancer, miR-138 is down-regulated, resulting in no longer regulated higher expression of TERT, which causes cell proliferation and immortalization. Previously described oncogenic miR-21 is, on the other hand, targeting many pathways in various types of cancer [61].

Because of their important role in cancer development, stability in FFPE and cell-free body fluid samples, and simple structure, miRNAs are ideal candidates for utilization as prognostic and predictive biomarkers. For instance, miR-205 was utilized for better classification of lung carcinomas, miR-21 is a reliable marker of poor prognosis, especially in colon cancers, and let-7 increased expression predicts better response to radiotherapy [61] [69]. There is a high potential for miRNAs, or RNAi in general, to be used as therapeutic targets or therapeutics themselves. There are two general strategies, miRNA inhibition (Anti-miR) and miRNA overexpression (miRNA mimic). Inhibition of miRNA was already utilized in the treatment of HCV infections, where miR-122 protects the viral RNA against degradation and enables the replication of the virus. Miravirsen is a drug, which inhibits the function of miR-122 by antisense RNAi mechanism [70]. One of the most promising miRNAs mimics candidates is miR-34a. This tumor suppressor miRNA targets many processes important for cancer development, such as cell cycle, differentiation, migration, proliferation, or invasion. Thus, it was tested in two clinical trials as a drug MRX34 and showed remarkable outcomes in various types of cancer. Nevertheless, significant adverse immune reactions appeared. The most challenging aspect of RNAi-based therapy remains an effective non-toxic delivery system (nanoparticles, liposomes, viral vectors) that will not elicit immune responses and possible RNA degradation [71].

Brain tumors also showed various miRNA deregulations and important roles of miRNA in their formation. Brain tumors differ from the others mainly in that they do not usually form distant metastases. This feature is attributed to the blood-brain barrier (BBB), which filters the particles needed for secondary tumor formation. Even though BBB does not block the miRNA transport, there is still a higher elevation of circulating miRNA in cerebrospinal fluid (CSF) than in blood. MiRNA signature, even in cell-free body fluids, can distinguish between healthy individuals, high-grade glioma, low-grade glioma, glioblastoma, and patients with other brain tumors [72]. There is a wide range of studies focused on miRNA in brain tumors, but there is still no clinically utilized targeted therapy or miRNA-based differential diagnostics. For instance, Kopkova et al. revealed the panel of 5 miRNAs, which can distinguish healthy individuals, brain metastasis, glioblastoma, low-grade glioma, and meningioma patients according to the RT-qPCR measurement of CSF samples from those individuals. They also showed increased levels of miR-10b and miR-196b associated with shorter OS in glioblastoma patients [73]. Nevertheless, there is a low number of studies focused on miRNA especially in meningioma [3]. Typically, miR-200a, which targets the Wnt signaling, is strongly down-regulated in meningioma. Tumor suppressor miR-145, usually down-regulated in various types of cancer, is down-regulated in WHO grade II and III meningiomas [3] [74]. Regarding oncogenic miRNAs, miR-21 is up-regulated in meningiomas compared to healthy tissue and is also up-regulated in WHO grade II and III in comparison with WHO grade I. Another oncogenic miRNA, miR-224 is up-regulated in meningioma tissues, especially in WHO grade III. Higher expression of miR-224 is also associated with shorter RFS and OS in meningioma patients. Nevertheless, serum levels of miR-224 decrease with increasing WHO grade. Most of the current studies are focused on the determination of the miRNA profiles distinguishing the particular histopathological types or distinguishing the meningioma tissue from the others [74]. However, there is a lack of studies focused on the association between meningioma recurrences and miRNA expression. For instance, Zhi et al. revealed that high miR-409-3p and low miR-224 serum levels are associated with higher recurrence rates [48]. Moreover, miR-190a, miR-29c-3p, and miR-219-5p expression in meningioma tissues were identified as a biomarker of the recurrence risk estimation in a multivariate model [75]. Nevertheless, none of the previous studies focusing on meningioma recurrence contained unbiased miRNA screening for independent selection of the best hits.

1.2.2. Long non-coding RNAs (lncRNAs)

Beyond DNA methylation and miRNA expression, long non-coding RNAs (lncRNAs) represent another rapidly evolving field of epigenetics. LncRNAs are structurally similar to mRNAs but are not translated. They usually show low expression and complex processing into many isoforms. Comparison between mRNA and lncRNA is summarized in Tab. 2. While their molecular mechanisms and cellular functions remain largely unknown, the few candidates that have been characterized so far often interact by sequence complementarity with other RNA species. For instance, they can either bind mRNAs, and inhibit their translation, or miRNAs, and block their activity. LncRNA can also bind to and modulate the conformation and activity of protein complexes, including those implicated in chromatin formation and regulation [58].

Table 2. *Common and different characteristics of mRNA and lncRNA.*

mRNA	**lncRNA**
Tissue-specific expression	
Form secondary structure	
Undergo post-transcriptional processing, i.e. 5' cap, polyadenylation, splicing	
Important roles in diseases and development	
Protein coding transcript	Non-protein coding, regulatory functions
Well conserved between species	Poorly conserved between species
Present in both nucleus and cytoplasm	Predominantly nuclear, others nuclear and/or cytoplasmic
Total 20-24,000 mRNAs	More than 50,000 lncRNA transcripts
Expression level: low to high	Expression level: very low to moderate
Presence of an open reading frame	Absence of an open reading frame

LncRNA expression shows exceptional cell and tissue specificity in comparison with other RNA species. This may be partially caused by more complex transcription and processing regulation. Most lncRNAs are processed in the same way as mRNAs, but they are more sensitive to regulatory factors and have some additional regulatory factors. For instance, transcription elongation of lncRNA is more sensitive to regulation by the transcription factor MYC than mRNA, and this process is additionally regulated by DICER. Also, lncRNA can be transcribed into both directions in the genome whereby one of those directions is enhanced by the proteins SWI/SNF and repressed by the CAF-1 [58]. This results in the sense (mRNA or lncRNA) or antisense (lncRNA) transcripts. When both directions result in the final RNA transcript, the particular lncRNA is supposed to be bidirectional. Depending on their position on the genome, lncRNA transcripts are intergenic if they do not overlap with the mRNA gene,

or intronic if they overlap with the mRNA gene but do not overlap with particular mRNA exons at the genomic level. Sense overlapping lncRNAs are located on the same strand as the mRNA gene but overlap the exons of particular mRNA. One lncRNA gene may fall into more than one of the described categories, but each of the final transcriptional variants can be classified into one specific category [76]. All those mentioned lncRNA categories are summarized in the following Fig. 9.

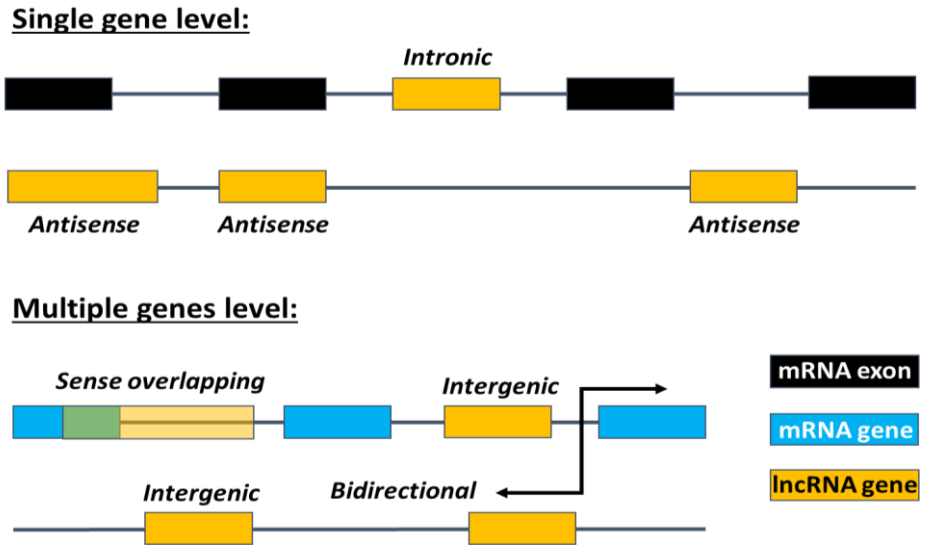

Figure 9. *Five types of lncRNAs are divided according to their positions in the genome according to the LNCipedia database version 5.2* [76].

After the transcription mediated by RNA polymerase II, lncRNAs undergo similar posttranscriptional processing as mRNAs, such as 5'-capping, 3'-polyadenylation, and splicing. Nevertheless, there are various exceptions. For instance, polyadenylation can be replaced by RNase P cleavage, which is more typical for tRNA processing. In the case of metastasis-associated lung adenocarcinoma transcript 1 (MALAT1), the primary transcript has a tRNA-loop-like structure placed on 3'-termini (Fig. 10). This structure prevents polyadenylation and is therefore cleaved by RNase P. This reaction leads to MALAT1-associated small cytoplasmic RNAs (mascRNAs) and mature MALAT1 with triple helix structure at the 3'-termini (Fig. 10). This modification makes RNA more stable and durable against endonucleases than polyadenylation [58]. Mature MALAT1 is localized in nuclear speckles (Fig. 10), where it participates in alternative splicing of mRNAs and is important in ontogenetic development [77]. MALAT1 also sponge the tumor suppressor miR-124, which has an oncogenic effect in various cancers. MALAT1 is mutated, for example, in bladder and liver cancers. Moreover, this

mutation leads to up-regulation of its expression in lung and esophageal cancers as well [78]. Nevertheless, the function and biological context of mascRNAs is still unknown.

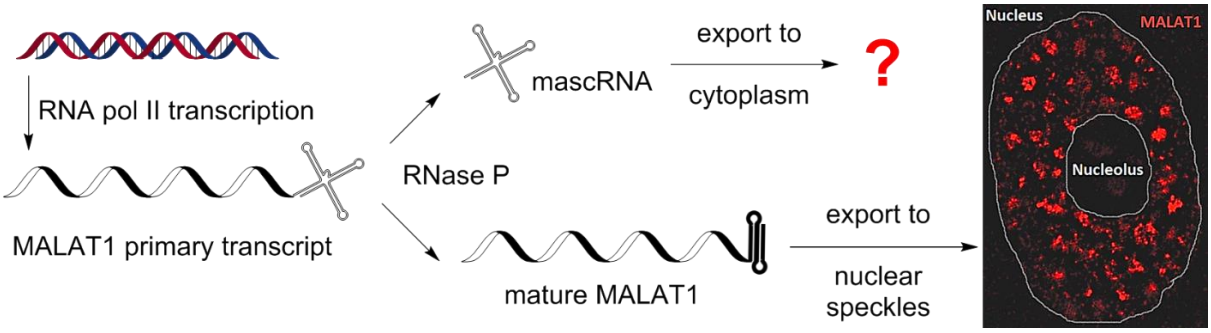

Figure 10. *Simplified* ***l****ncRNA MALAT1 processing and cellular localization were prepared according to Quinn's review* [58] *and with a microscopic image adapted from Chen's original article* [77].

Other examples of alternative lncRNA posttranscriptional processing are more variable splicing mechanisms. The most distinctive one is back-splicing leading to the circularized RNAs (circRNAs). The process is regulated by the QKI alternative splicing factor and is typically associated with EMT [58] [79]. CircRNA is a unique class of lncRNA, usually originating from the protein-coding gene, where alternative splicing of the mRNA can lead to circRNA. Thus, circRNAs contain both exons and introns from the gene of origin and can be transcribed from the same or opposite (antisense) DNA strand. Therefore, various transcripts may exist in both linear and circular forms. The main biological role of circRNA, according to the current level of knowledge, is miRNA regulation, when one circRNA can have multiple binding sites for various miRNAs. For instance, circHIPK3 can sponge at least 9 different specific miRNA molecules. This transcript is derived from the coding gene for homeodomain interacting protein kinase 3 and is abundantly present in the cytoplasm. CircHIPK3 has oncogenic features and was found to be overexpressed in hepatocellular carcinoma [79].

Besides miRNA sponging, there are various biological functions and roles of lncRNAs. Regarding genomic localization, they can be divided into two regulatory groups, the first being *trans*-regulatory mechanisms regulating targets from distant genomic loci, but more common and frequent are *cis*-regulatory mechanisms operating at parallel chromosomal coordinates [80]. The second mechanism is typical for antisense lncRNAs, which often bind to their sense mRNA transcripts and regulate their function. This type of regulation is usually negative in a similar way as in the case of miRNA, thus targeted mRNA can be degraded or its translation is

inhibited. However, antisense targeting can also lead to splicing modulation [58] [81]. For instance, ZEB2-AS hybridizes its ZEB2 mRNA counterpart in the intron at 5'-untranslated termini containing an internal ribosome entry site. This bondage prevents splicing of the respective intron and leads to translation of ZEB2, which down-regulates E-cadherin. Down-regulation of E-cadherin at both mRNA and protein levels leads to the EMT [82]. Nevertheless, antisense *cis*-regulation does not have to be based on hybridization principles. ANRIL lncRNA recruits transcriptional repressors PRC1 and PRC2, which block expression of CDKN2B, sense for ANRIL, and CDKN2A, which is transcriptionally located behind the CDKN2B on the same strand [58].

Another functional type of lncRNAs is chromatin modifiers, which regulate the transcription of surrounding genes on a chromosomal level. These lncRNAs are often bidirectional and their expression is linked to the enhancer of the respective mRNA gene. Thus, this group of lncRNA is generally called enhancer RNAs (eRNAs) [58] [83]. For example, homeobox-related genes are located at the four HOX genomic loci and encode the transcription factors important during ontogenetic development. The expression of certain HOX genes is accurately regulated mainly by these 4 lncRNAs: HOX antisense intergenic RNA (HOTAIR), HOX antisense intergenic RNA myeloid 1 (HOTAIRM1), HOXA transcript at the distal tip (HOTTIP), and Mistral. Each of them regulates the expression of certain HOX genes, HOTAIR negatively, the others positively. These 4 lncRNAs work as scaffolds for chromatin-remodeling complexes recruiting certain regulatory proteins and mediating chemical modifications of histones [81]. Chromatin-enriched lncRNAs (cheRNAs) are a subgroup of eRNAs, but they are usually longer (cheRNA > 2,000 nt versus other eRNA ~ 350 nt). CheRNAs regulate the transcription of surrounding coding genes by interaction with chromatin and RNA polymerase II. In comparison with other eRNAs, cheRNAs are not bidirectional but have an intergenic or antisense position to the genes they regulate [83] [84]. For example, Xist (X-inactive specific transcript) is actively transcribed from one female X-chromosome and transcriptionally inactivates surrounding genes, which leads to the inactivation of this chromosome. On the second X-chromosome, Xist expression is inactivated by the Tsix lncRNA, thus the second X-chromosome is active [58]. Nevertheless, most of the intergenic cheRNAs have an activating function and antisense cheRNAs have been predicted to have a repressive function [84].

Besides previously described interaction with other RNAs and chromatin, lncRNAs can also interact with other proteins and molecules. Most of their interactions are based on secondary structure and folding. The secondary structure of lncRNA is more conserved and its primary structure is less conserved compared to mRNA. Therefore, lncRNA can be part of

complex ribonucleoproteins (RNPs) serving as a biosynthetic template, structural assembly scaffold, or ribozyme catalytic domain [58]. The most common examples are rRNA in ribosomes for mRNA translation and TERC in TERT for telomere elongation.

At the present level of knowledge, the effort to precisely classify lncRNAs into individual groups and subgroups is still in vain, also due to the large overlap of functions of individual transcripts. Nevertheless, following Fig. 11 summarizes basic and previously discussed functional groups of lncRNAs.

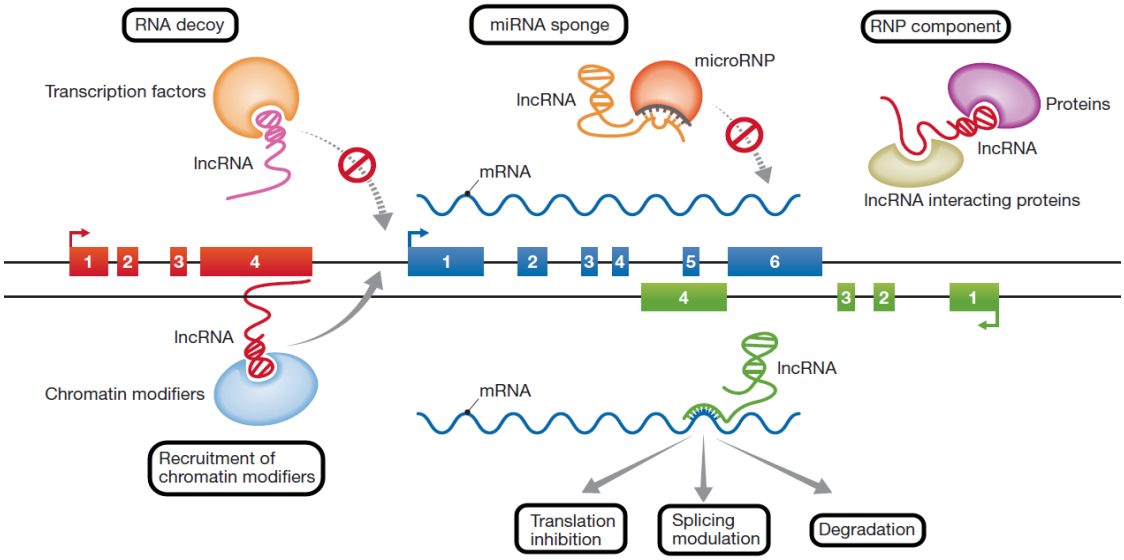

Figure 11. *Overview of lncRNA known functions adapted from Hu's review article* [81].

LncRNA in cancer

LncRNAs can induce oncogenic or tumor suppression effects by the regulation of certain cellular processes. For instance, previously described ANRIL blocks the expression of cyclin-dependent kinase inhibitors. Over activation of this process promotes the cell cycle and uncontrolled growth leading to neoplastic transformation. Overexpression of ANRIL can be caused by mutation; various of those mutations were detected in esophageal cancer, melanoma, and acute lymphoblastic leukemia. ANRIL up-regulation was detected also in other types of cancer suggesting this transcript as oncogenic. Previously described MALAT1 manifests the oncogenic features as well. On the other hand, PCNA-AS1 can serve as an example of tumor suppressor lncRNA. This transcript is antisense to proliferating cell nuclear antigen (PCNA), which is involved in DNA damage repair. PCNA-AS1 hybridizes to PCNA mRNA and stabilizes it. PCNA-AS1 has been found as down-regulated in hepatocellular carcinoma [78].

Utilizing of lncRNAs as biomarkers can be potentially challenging due to their low expression. Nevertheless, some of them, such as H19 or HULC, may be detected in cell-free

body fluids [78]. HULC is up-regulated in various cancers and its increased expression is associated with shorter OS in most of the studied malignancies. HULC activation is caused by certain mutations, which are further associated with a high risk of cancer. Mechanistically, HULC cancer-associated features are related to the sponging of various tumor suppressor miRNAs leading to EMT and cancer progression. Thus, HULC is one of the most promising prognostic and diagnostic cancer biomarkers on the level of lncRNA as well as a potential therapeutic target [85]. HOTAIR is another lncRNA intensively studied in cancer. It's up-regulation is associated with shorter OS in various cancers. HOTAIR may serve as a potential prognostic biomarker in both primary tumor tissue and cell-free body fluids. HOTAIR can also serve as a predictive biomarker when it's up-regulation is associated with reduced radiosensitivity. Additionally, HOTAIR is a very promising therapeutic target because its expression can be modulated with various drugs. For instance, natural compounds, such as isoflavones and anthocyanins, can down-regulate HOTAIR levels, but treatment with exogenous estrogens leads to HOTAIR up-regulation [86] [87]. HOTAIR is also up-regulated in brain tumors, such as gliomas and glioblastomas, and deregulates their cell cycle and apoptosis. Moreover, the expression of HOTAIR is associated with the WHO grade of gliomas and glioblastomas and can serve as a diagnostic tool in brain tumor classification [88]. LncRNAs are intensively studied in brain tumors [88], but there are only a few mechanistic studies focused on lncRNA in meningiomas. For instance, LINC00460 expression is increased in meningiomas compared to meninges. LINC00460 is also elevated in malignant meningioma cell lines (IOMM-Lee and CH157-MN) compared to the benign cell line (Ben-Men-1). Loss of LINC00460 function reduces proliferation and increases apoptosis. MiR-539 was identified as a potential target of LINC00460 [89]. Several other studies confirm the importance of Wnt signaling in meningioma development and the involvement of lncRNAs in this process [23] [24]. Nevertheless, MEG3 is the most frequently discussed lncRNA in meningiomas [90].

MEG3

Maternally expressed gene 3 (MEG3) is imprinted along the maternal line. One of the two alleles is expressed from genes regulated by genomic imprinting, and this mechanism is typical in lncRNAs [58] [90]. MEG3 is a gene that consists of 10 exons producing at least 28 potential transcriptional variants, according to Ensembl Genome Browser [91]. MEG3 belongs to the DLK1-MEG3 locus, which lies in human chromosome 14q (Fig. 12). DLK1 is involved in cell signaling and differentiation. It was found that the absence of DLK1 expression correlates with loss of differentiation and increased malignancy. DLK1 is paternally expressed and encodes a

protein belonging to the growth factor-like family. MEG3 is maternally expressed and produces lncRNA [92]. Gene expression of the DLK1-MEG3 region is tightly regulated by imprinted control regions (ICRs). The ICR of the DLK1-MEG3 locus is known as IG-DMR [90], which is unmethylated on the maternal allele and hypermethylated on the paternal allele of the chromosome (Fig. 12). In addition to the IG-DMR region, there is a second methylated region, MEG3-DMR [93]. Loss of MEG3 expression in cancer is not associated with genomic abnormalities such as gene deletion or mutation. Rather, the loss of MEG3 gene expression is attributed to the promoter of the MEG3 gene and the hypermethylation of the enhancer. Thus, MEG3 is a gene whose loss of expression may play a crucial role in tumorigenesis [94].

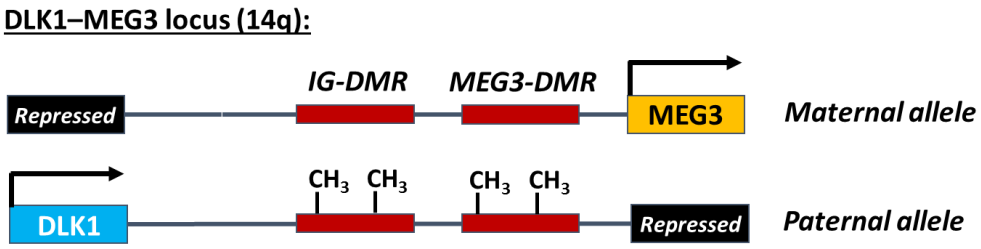

Figure 12. *The DLK1-MEG3 locus with imprinted control regions IG-DMR and MEG3-DMR, which overlap with the promotor of the MEG3 gene. Both control regions are methylated at the paternal allele.*

MEG3 is a tumor suppressor transcript, which is expressed in brain tissues, but down-regulated in meningiomas with more frequent gene methylation in WHO grades II and III tumors [95]. MEG3 interacts with other molecules and activates their tumor suppression features. The interaction complex of MEG3 with PRC2 and the JARID2 cofactor initiates the histone methylation at the MDM2 and CDH1 genes, which leads to the repression of their transcription. Reduced levels of CDH1 obstruct the EMT and reduced levels of MDM2 leads to p53 activation. MEG3 also activates p53 directly and their binding stabilizes the p53. Consequently, decreased MEG3 level promotes proliferation and metastasis and halts the apoptosis of cancer cells. MEG3 down-regulation is associated with poor prognosis and worse clinical outcomes in several types of cancer [96].

It was discovered, that MEG3 has a crucial role in p53 functional activation and the proper folding of MEG3 is the important factor increasing the p53 activity. Thus, various MEG3 isoforms have different quantitative activation potentials in terms of p53-induced tumor suppression [93]. MEG3 also regulates the retinoblastoma protein (Rb), which is crucial in the

transition from the G1 to S phase of the cell cycle and inhibits angiogenesis. Additionally, MEG3 interacts with various miRNAs and regulates them both negatively and positively. In the case of MEG3 up-regulation, this mechanism contributes to increased sensitivity to chemotherapy. Nevertheless, because of plenty of interactions with other molecules, MEG3 manifests oncogenic features in occasional cases. For instance, MEG3 sponges miR-127, which negatively regulates Wnt signaling by targeting ZEB1 mRNA. This process was observed in osteosarcomas, where MEG3 promoted proliferation and metastasis [93].

MEG3 is predominantly localized in the cell nuclei in a similar pattern to that previously described for MALAT1. Both non-coding transcripts show a significant co-localization pattern suggesting their potential direct or indirect interaction [97].

2. Specific aims of the thesis

The results of this work are divided into 3 main parts, each separately leading to the discovery of new potential biomarkers of meningioma recurrence and altogether providing novel insight into meningioma biology and pathogenesis.

Aim 1: Identification and validation of miRNAs predicting meningioma recurrence.

Aim 2: Identification and validation of mRNAs and lncRNAs associated with meningioma recurrence, histogenesis, sex, and WHO grade.

Aim 3: Characterization of MEG3 crucial features connected to meningioma recurrence and pathogenesis.

3. Methods and patients

3.1. Patients description

This retrospective study was approved by the Institutional Research Ethics Committee and includes the patients, who underwent meningioma surgery between 1990 and 2012. FFPE tumor tissue samples for this study were preliminary obtained from the Brain Tumor Database of the Department of Clinical and Molecular Pathology, Faculty of Medicine and Dentistry, Palacky University, and University Hospital Olomouc. In total, 330 FFPE samples from 166 patients with corresponding clinical data were enrolled. Comprehensive clinical-pathological data were obtained from study participants who signed informed consent. All FFPE samples were reviewed by the pathologist and proposed WHO grades were verified (ensured by prof. Jiri Ehrmann). Recurrence after total or gross total (SG I, II, or III) and incomplete (SG > III) resection was defined as a reappearance of the meningioma or any growth of remaining meningioma tissue detected during follow-up imaging after primary surgery (3 and 12 months after surgery, every 24 - 72 months thereafter). Patients with no such events during at least 5 years' follow-up were considered *non-recurrent*. Meningiomas detected after primary surgery with evidence of radiographic recurrence during the follow-up period are called *primary recurrent samples/tumors*. Meningiomas from the recurrent patients obtained after any other surgical resections in a sequence are called *secondary samples/tumors* in this study. All clinical data were obtained from the Department of Neurosurgery, Faculty of Medicine and Dentistry, Palacky University, and University Hospital Olomouc, Czech Republic (ensured by Dr. Vladimir Balik). This included age at diagnosis, sex, body mass index, risk factors, treatment details, tumor location and diameter, proposed tumor histogenesis, and other diseases. All experiments were performed at the Laboratory of Experimental Medicine, Institute of Molecular and Translational Medicine Faculty of Medicine and Dentistry, Palacky University Olomouc. A description of patient cohorts is listed within the particular subchapters.

3.2. Biological material processing

Slices with a thickness of 10 μm were cut from each FFPE tissue for nucleic acid extractions. Each aliquot contained 5-10 slices depending on the amount of tissue within the FFPE block. Substantially, 33 tissue microarrays (TMA) of original macrodisected FFPE blocks were prepared for microscopy-based investigations. Each TMA contained 10 samples in doublets and 2 controls in doublets. Thus, each TMA contained 24 tissue samples.

Total RNA was isolated from FFPE samples using the miRNeasy Mini kit (Qiagen, Hilden, Germany) according to the manufacturer's instructions. Before isolation as such, FFPE sections were incubated overnight in 500 µl of Proteinase K mixture at 60 °C. This lysis mixture consisted of 1% SDS (Merck Millipore, Burlington, MA, USA), 250 µg Proteinase K (Bioline, London, UK), 250 U RNAsin (Promega, Madison, WI, USA), 20 mM EDTA (Serva, Heidelberg, Germany), 100 mM Tris-buffer pH 7,4 (Sigma-Aldrich, St. Louis, MO, USA), and DEPC water (Ambion, Austin, TX, USA). After thorough mixing, 700 µl of QIAzol Lysis Reagent was added to the samples. After mixing and incubation at room temperature, 140 µl of chloroform was added and continued according to the manufacturer's standard protocol. The resulting total RNA was eluted to a volume of 30 µl by washing the columns twice.

RNA concentration and purity were assessed using NanoDrop 1000 Spectrophotometer (ND 1000) from Thermo Fisher Scientific (Waltham, MA, USA). Data from ND1000 were used for the calculations of proper RNA input for all following described analyses. Also, RNA integrity and level of degradation were assessed using Bioanalyzer 2100 (Agilent Technologies, Santa Clara, CA, USA) with RNA Pico Chips according to the manufacturer's instructions. The aim was to select the highest quality RNA samples for advanced applications such as NGS. One of the outputs is the RIN (RNA integrity number), from which the degree of RNA degradation can be derived. For almost all samples, this value was around 2.0 - 3.5, which indicates a high degree of degradation, which is typical for FFPE samples (Fig. 13). Also, DV_{200}(%) values were calculated demonstrating the percentage of transcripts longer than 200 nt (Fig. 13). In this way, samples applicable to some NGS approaches can be effectively selected.

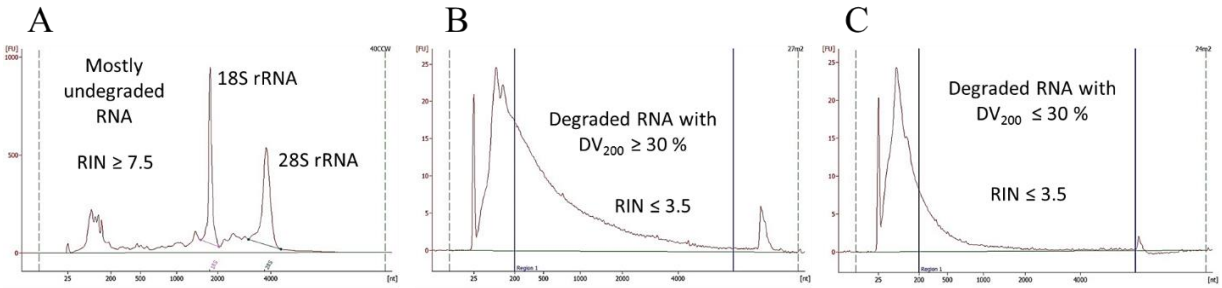

Figure 13. *Representative outputs from Agilent RNA Pico Chips measurements using Bioanalyzer 2100 instrument (x-axis: size in nucleotides; y-axis: fluorescence): (A) Undegraded RNA sample with distinguishable rRNA subunits. (B) Degraded FFPE sample with rRNA spliced into shorter fragments, but efficient numbers of the transcripts are still longer than 200 nt. (C) Highly degraded FFPE sample inappropriate for NGS.*

3.3. Microarray for miRNAs

The isolated RNA was processed according to the manufacturer's instructions using an Affymetrix GeneChip miRNA 4.0 Array (Applied Biosystems, Foster City, CA, USA) with 130 ng input of total RNA. The FlashTag Biotin HSR RNA Labeling Kit (Applied Biosystems) was used to label RNA in samples prior to application to chips. Briefly, RNA samples are first polyadenylated and biotinylated. The labeled fragments are then hybridized to an array overnight, after which the bound sections are stained. Arrays were scanned using an Affymetrix Gene Scanner 7G. The raw data were obtained in .CEL format using the Affymetrix GeneChip CommandConsole software. CEL files were then processed using "R" software v. 3.5.0 and the Bioconductor package. More detailed information about the processing of microarray data is described further (3.7). The miRNA 4.0 Array contained 30,434 probe sets for mature miRNAs. The array is suitable for 203 organisms and there are pre-designed 2,578 mature miRNAs, 2,025 precursor miRNAs, and 1,996 other small RNA species for human samples according to the manufacturer.

3.4. Transcriptomic sequencing for long RNAs

Only the RNA samples with $DV_{200}(\%) \geq 30$ were selected for cDNA libraries preparation for RNA-seq. Samples were diluted to 10 µl using nuclease-free ultra-pure water with 1000 ng total RNA input. Then, cDNA library preparation was performed using the TruSeq Stranded Total RNA Library Prep Kit with RiboZero Gold - Set A (Illumina, San Diego, CA, USA) according to the manufacturer's instructions with adjustment for degraded samples. Briefly, denaturation and specific rRNA depletion were performed. Then, fragmentation was performed in a cycler at 94 °C for 4 minutes with a subsequent hold at 4 °C only for the samples containing RNA fragments above 1000 nt. Furthermore, both strands of cDNA were synthesized separately. Adenylation and ligation of specific adapter sequences were then performed. Finally, the prepared cDNA was amplified by PCR. Between steps, cDNA samples were purified using AMPure XP Beads (Beckman Coulter, Brea, CA, USA). The final solution was transferred and stored in 0.2 ml tubes in a volume of 30 µl. Prepared cDNA libraries were stored at -20 °C. Quality control was performed using Bioanalyzer 2100 with DNA 1000 Chips. A properly prepared cDNA library should report one specific smeared peak with the average size of fragments around 260 nt (Fig. 14). Our prepared cDNA libraries had smear peaks at 246 nt on average and were quantified using Qubit 2.0 Fluorometer (Thermo Fisher Scientific) for the determination of cDNA input of each sample in NGS pools.

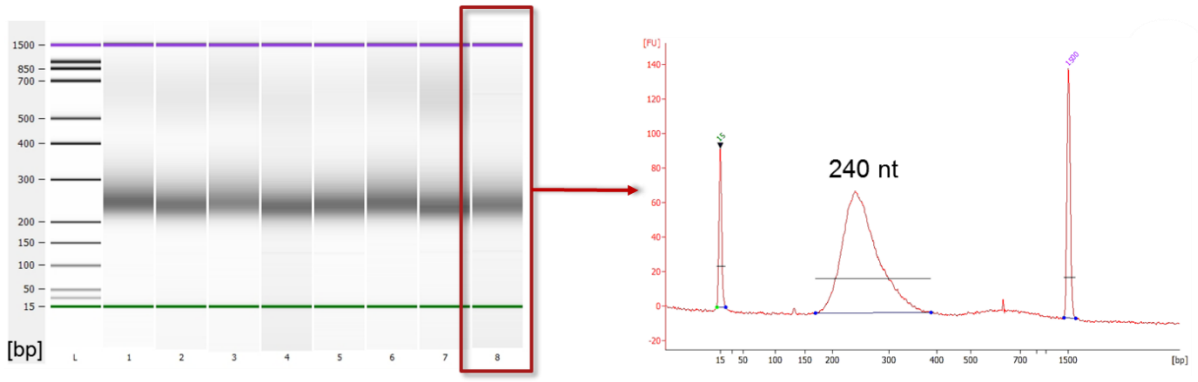

Figure 14. *Representative outputs from Agilent DNA 1000 Chips measurements using Bioanalyzer 2100 instrument for high-quality cDNA libraries. Gel-like view of 8 samples and detailed processed view of one sample.*

Quantified samples of cDNA libraries were pooled based on their molarity using 4 or 5 samples per pool. After NaOH (0.2M) denaturation, each pool was diluted with HT1 solution to a concentration of around 7.5 pM, and pools were clustered in a separate line using the cBot 2 System and the TruSeq SR Cluster Kit v3 - cBot – HS (Illumina). Sequencing was performed in duplicate on a HiSeq 2500 instrument in single read high output mode with 101 bases and 6 index bases using the TruSeq SBS Kit v3-HS (50 cycles). The first run yielded 148.2 Gbases (>Q30 reflecting efficient quality) and 1.496 x10^9 pass-filter reads (51.6 million reads/sample on average) and the second run yielded 153.9 Gbases (>Q30) and 1.523 x10^9 pass-filter reads (37.1 million reads/sample on average). Both sequencing runs were in good concordance with recommended specifications and none of the samples were removed due to low sequencing output. FastQ files were generated using BaseSpace (Illumina). All parameters were classified as satisfactory for analysis of differentially expressed genes/lncRNA (transcript) according to quality control. Sequencing runs were performed in cooperation with Dr. Rastislav Slavkovsky at IMTM Genomics Core Facility. The obtained raw FastQ data were transferred to Research Centre for Applied Molecular Oncology (RECAMO) at Masaryk Memorial Cancer Institute in Brno and processed by Dr. Filip Zavadil Kokas for determination of differentially expressed transcripts among studied subgroups and splicing variants analysis. More detailed information about the processing of NGS data is described in further chapters (3.7).

3.5. RT-qPCR approaches

All qPCR reactions were performed on a LightCycler 480 (Roche, Basel, Switzerland) with fluorescence detection in the FAM channel. All qPCR reactions were prepared in 384-well

plates in a semi-high-throughput regime with Echo 555 (Labcyte, San José, CA, USA) and Freedom EVO 150 (Tecan, Männedorf, Switzerland) automatic pipettors (in cooperation with Dr. Sona Gurska). All reactions were performed in a volume of 10 µl in triplicates and cDNA samples were prepared separately prior to qPCR measurements. The raw qPCR triplets of Ct values were summarized by average and normalized against selected reference sequences using the ΔCt method.

For miRNA expression measurement, 10 ng of total RNA was used for cDNA preparation with TaqMan Advanced miRNA cDNA Synthesis Kit (Thermo Fisher Scientific). DEPC water (Ambion) for dilution of the samples and 0.3 µl RNAsin (Promega) in the initial polyadenylation reaction were used to avoid RNA degradation during cDNA preparation. All following steps were performed according to the manufacturer's instructions. Briefly, ligation of a specific adaptor was performed after the polyadenylation. Then, reverse transcription and final PCR pre-amplification were conducted. Prepared cDNA samples were stored at -20 °C until qPCR measurement. Each miRNA was measured with respective TaqMan Advanced miRNA Assay (Thermo Fisher Scientific) in a mixture of TaqMan Fast Advanced Master Mix (Thermo Fisher Scientific) and DEPC water (Ambion) according to the manufacturer's instructions. The following optimized thermal program was used: 95 °C / 20 s with 1.9 °C / s ramp rate, then 40 cycles of 95 °C / 10 s (1.9 °C / s ramp rate) and 60 °C / 40 s (1.6 °C / s ramp rate).

For long RNAs expression measurement, 3,000 ng of total RNA was used for cDNA preparation with our in-house developed protocol. The samples were mixed with 300 ng of Random Primers (Promega) and diluted with DEPC treated water (Ambion) in a total volume of 19.5 µl. Samples were denatured at 70 °C / 5 min, and then immediately placed on ice. Then, a freshly prepared reaction mixture (9.75 µl) was added to each sample. The reaction mixture for one sample contained 6 µl of RevertAid 5x RT buffer (Fermentas), 3 µl of 10 mM deoxyribonucleotide triphosphates (dNTPs), and 0.75 µl of 40 U/µl RNAsin ribonuclease inhibitor (Promega). Each sample was incubated for 5 min / room temperature after adding the reaction mixture. During the final step, 150 U (0.75 µl) of RevertAid Moloney Murine Leukemia Virus reverse transcriptase (Fermentas) was added and the samples were incubated at room temperature for 10 minutes. Finally, samples were incubated in a cycler at 42 °C / 60 min and then at 70 °C / 10 min. Prepared cDNA samples were stored at -20 °C until qPCR measurement. Each mRNA and lncRNA were measured with respective TaqMan Gene Expression assays (Thermo Fisher Scientific) in the mixture of LightCycler 480 Probes Master

(Roche) according to the manufacturer's instructions. Amplification products were verified using the Bioanalyzer 2100 with DNA 1000 Chips (Agilent).

3.6. RNA in situ hybridization for MEG3

Five µm thick FFPE slices were freshly cut from TMA and placed to the positively charged microscope slides. Then, the slides were heated at 60 °C / 90 min. RNA in situ hybridization (RISH) in single-molecule resolution was performed with ViewRNA ISH Tissue 1-Plex Assay and ViewRNA™ Chromogenic Signal Amplification Kit (1-plex) in combination with specific probe ViewRNA Tissue Probe Set – MEG3 (Thermo Fisher Scientific) according to manufacturer's instructions. Briefly, after deparaffinization, protease treatment was optimized for 3.5 µl Protease QF and 40 ºC / 15 min treatment for one microscope slide. Then, specific probe and amplifier were hybridized. Prepared oligonucleotide *in situ* construct was labeled with 10.5 mg Fast Red Substrate dissolved in 500 µl Naphthol Buffer. Then, nuclei were stained with 300x diluted DAPI (Thermo Fisher Scientific) water solution. After the final wash, microscope slides were dried at room temperature for 30 min and mounted with Histomount Mounting Solution (Thermo Fisher Scientific). Prepared slides were preliminarily investigated using an Axio Observer.Z1/Cell Observer Spinning Disc microscopic system (Zeiss, Oberkochen, Germany) with 63x oil objective (Fig. 15).

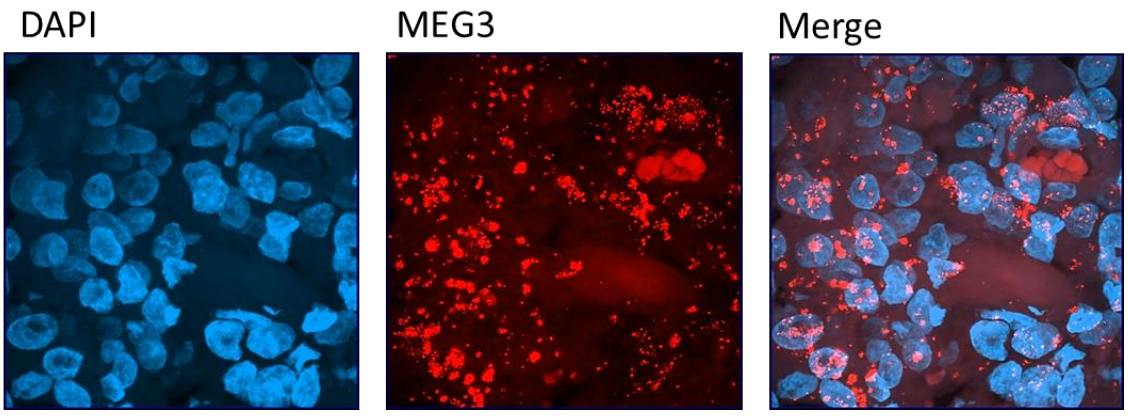

Figure 15. *Representative images of MEG3 visualization in FFPE tumor tissue using a confocal spinning disk microscope with a 63x oil objective. MEG3 transcripts are spread in the nuclei or around them and presented both in single-transcripts and aggregated clusters.*

Images for quantitative evaluation were taken using Olympus IX83 automated fluorescent microscope (conducted by Dr. Karel Koberna). The individual tissue images, placed on TMA slices, were taken in the DAPI and Cy3 channel, which the system automatically focused on.

Using CellSens Dimension software (Olympus), 20 individual images with a size of 2048 x 2048 pixels (px) were obtained from one tissue sample, and then combined into a larger image (overlap of individual images was 20%). During the evaluation process, 3 – 6 regions of interest (ROIs) were selected from each image for further analyses. Those ROIs were selected manually according to visually evaluated qualities: clear areas of tumor tissue with a good resolution of nuclei and signals, without any artifacts such as blood vessels, calcification, connective tissue, weak or overexposed fluorescent signals. Subsequently, manual signal thresholding was performed for each image separately. After thresholding, the numbers of signals and their areas for individual size categories (1, 15, 30, 60, 100, 250, 500 px) were automatically calculated for each ROI in all images. The area and location of the nuclei were not taken into account, they only helped to orient in the tissue and also to select suitable areas for analysis. However, the distribution of the signal from single transcripts (1 – 15 px; more than 60 % of the signal on average) was investigated between nuclei and space outside of the nuclei. Single signals were manually counted for this type of analysis in newly selected ROIs within the images with the best resolution. All image analysis steps were performed by Dr. Ivo Uberall, Department of Clinical and Molecular Pathology, Faculty of Medicine and Dentistry, Palacky University Olomouc.

3.7. Data processing

All data analyses were performed in cooperation with experienced biostatisticians Dr. Jana Vrbkova, Dr. Pavla Kourilova, and Dr. Filip Zavadil Kokas. Affymetrix miRNA 4.0 array data were normalized with the Robust Multi-Array Average method. The microarray expression dataset was analyzed using the univariate Cox proportional regression model of time-to-recurrence (TTR). The significance threshold was set at a raw $p < 0.05$, and only mature human miRNAs were analyzed. The condition selection of a miRNA for further experiments was that the corresponding median of the intensity of fluorescence (IF) on the array was at least five on a logarithmic scale (median log2 IF ≥ 5). MiRNAs for data normalization were selected based on a non-significant result of Wald's test in a univariate Cox regression model and IF ≥ 5. Pairwise differences of miRNAs IF from arrays corresponding to paired matched primary recurrent and secondary recurrent samples of meningiomas were tested with the usage of the Wilcox exact one sample test. The significance threshold for the pairwise analysis has been set at 1 % (raw $p < 0.01$). A final set of differently expressed miRNAs in primary recurrent and secondary tumors was selected as a subset of significantly changed miRNAs by two additional

criteria: the absolute value of the median of the difference $\log2(IF)_{secondary} - \log2(IF)_{primary} > 1$ and minimal value of medians log2 intensities at least $IF \geq 5$.

RNA-seq data were mapped to the reference genome of *Homo Sapiens* GRCh38.p13 using the TopHat2 v.2.0.12 splice-read aligner with default parameters. The reads mapped to the transcripts annotated in the reference genome were quantified using HTSeq v.0.6.0 for the stranded library. The GTF GRCh38.p13 file from the Ensembl database was used for the analysis of differential gene expression. Analysis of lncRNA was performed using a GTF file from LNCipedia v5.1 as a reference. The tests for differential expression were performed using the DESeq2. A transcript was considered significantly differentially expressed if its adjusted p-value was ≤ 0.05 and its log2 Fold Change was ≥ 2 or ≤ -2. The presented networks were created in Cytoscape 3.7.2 using the differential expression analysis results, the free web tool String version 11.0, DAVID Bioinformatics Resources, the Panther Classification System, and LNCipedia v5.1 or miRNet 2.0. Coding transcripts and lncRNAs were considered to be connected based on their chromosomal coordinates if they were within 10,000 nt of one another.

The RT-qPCR data were processed using the ΔCt method and further analyzed concerning recurrence status, sex, histogenesis, WHO grade, and tumor location using common statistical methods (Student's t-test and the Wilcoxon's test, or Pearson's chi-square test and Fisher's exact test for testing marker positivity). For each marker, a univariate Cox regression model of TTR was fitted with adjustment for the following clinical factors: age at diagnosis, WHO grade, sex, extend of resection, and tumor location (convexity). The models' outputs were hazard ratio (HR) estimates with associated 95% confidence intervals and p-values. The HR is associated with a one-unit change in the ΔCt value for the miRNA, mRNA, or lncRNA marker in question. The additive effects of measured markers were investigated by creating multinomial logistic regression models. Final multivariate Cox regression models were created using stepwise selection with fixed or unfixed adjusting clinical factors.

For statistical processing of MEG3 image data, the number of points of size categories in the total number of illuminated points was evaluated for each ROI as shares. The data were normalized to the area of all ROIs within the whole data set. Averages were then calculated for each sample from the proportions of the individual ROIs for each sample. Student's t-test and Wilcoxon's test were used to comparing the proportions of points of each size category to recurrence and other clinically relevant factors. Also, Wilcoxon's test was used for signal localization distribution (nuclei / outside the nuclei) between recurrent and non-recurrent samples. Finally, Cox regression models were created to evaluate the TTR in accordance with MEG3 transcript distribution within the meningioma tumor tissue.

4. Results

4.1. Aim 1: miRNA profiling

The purpose of this aim was to identify meningioma patients at high risk of recurrence using miRNA-based biomarkers. The data was published at Neurosurgery (Oxford Academic; IF: 4.85; [98]) and the article is attached as Appendix 1. Potential biomarkers were selected using the initial unbiased microarray screening phase, following the training phase performed by RT-qPCR on an independent cohort. Finally, the best hits were validated on the expanded cohort of 172 patients. The whole experimental design and description of particular patient cohorts are described in detail in the following Fig. 16.

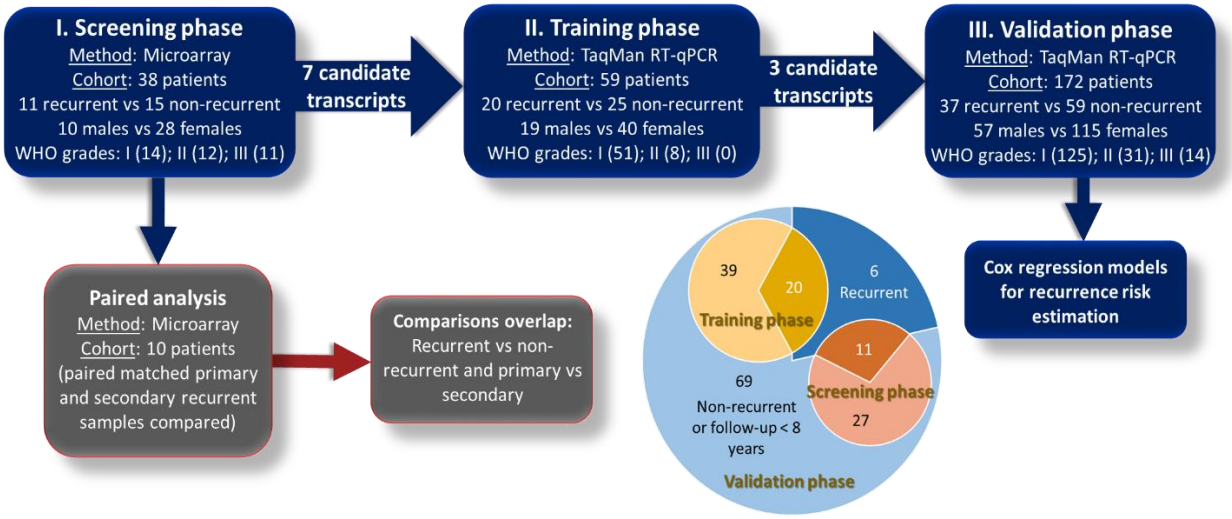

Figure 16. *Schematic overview of the study designed for selection of an appropriate miRNA-based model for recurrence risk estimation. Only patients after > 8 years' follow-up were considered non-recurrent in the diagrams, but all patients and their overlap between the experimental phases are shown in the circular cohorts-overview visualization. Nevertheless, all markers are selected and analyzed using Cox regression models using TTR parameter, thus categorization to recurrent and non-recurrent patients is not relevant for this aim and has only an informative purpose.*

I. Screening phase

The microarray analysis of primary recurrent and non-recurrent samples revealed that the expression of 49 abundant miRNAs strongly correlates with TTR ($p < 0.05$) in meningiomas at

various risks of recurrence, quantified with HR, according to the Cox regression models of TTR (Fig. 17). Thirty-seven miRNAs showed down-regulated gene expression with an increased risk of recurrence. On the other hand, 12 miRNAs were up-regulated following recurrence. The highest HR values were reveled in miR-320 family, particularly for miR-320c (HR = 8.8; p = 0.003), miR-320b (HR = 8.8; p = 0.005) and miR-320a (HR = 5.7; p = 0.032). On the other hand, the most significant miRNA in the Cox model with the lowest HR, reflecting decreased expression with a higher risk of recurrence, was miR-7975 (HR = 0.4; p = 0.003).

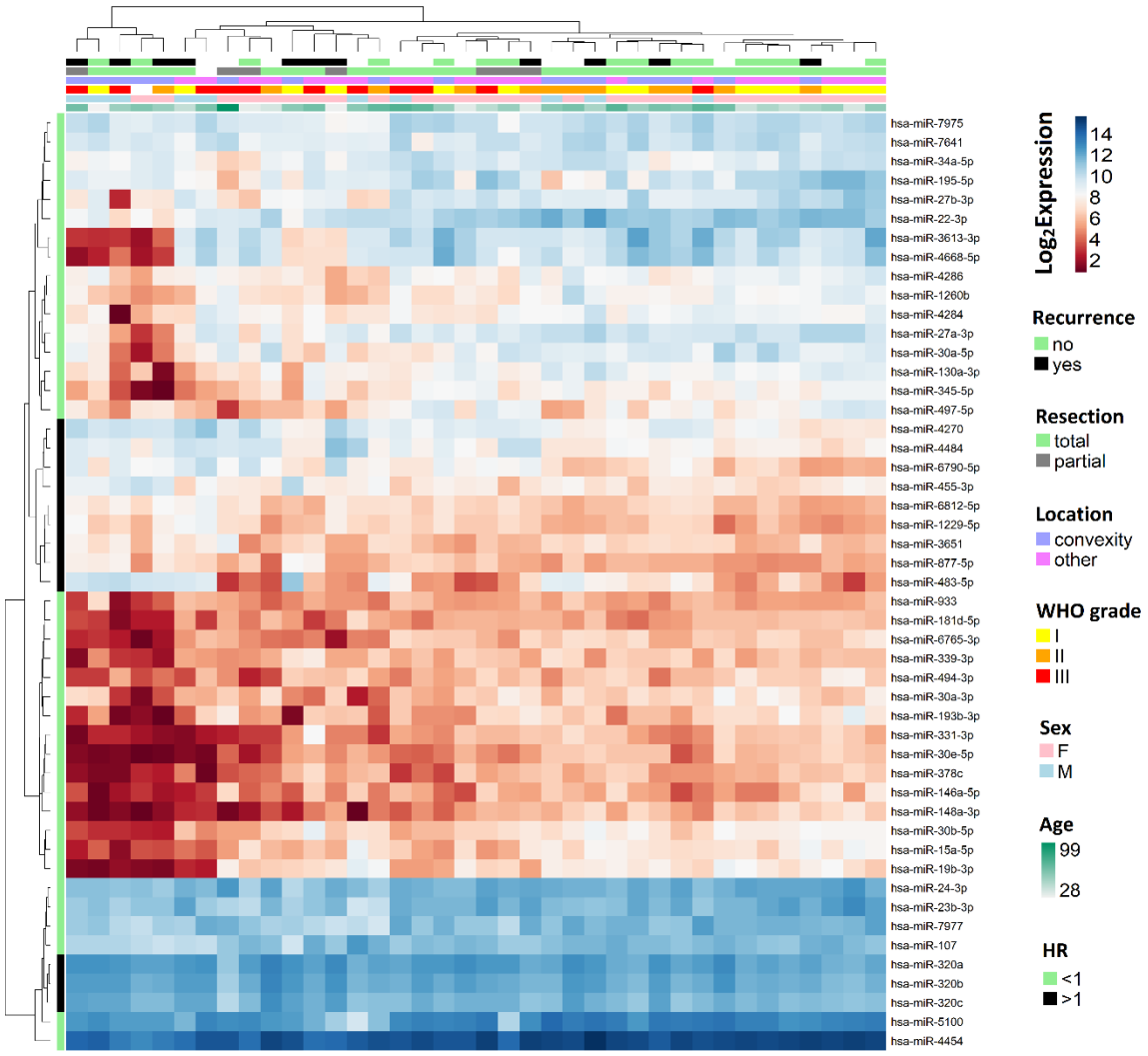

Figure 17. *Hierarchical clustering of 49 mature and highly abundant miRNAs, which have their expression dependent on TTR ($p < 0.05$) according to the univariate Cox regression model. Only patients after > 8 years' follow-up were considered non-recurrent in the heatmap, but all patients included in the analysis are shown. Hazard ratio (HR) is marked for each miRNA (y-axis) as well as relevant clinical characteristics for each patient (x-axis).*

Seven highly abundant and biologically relevant miRNAs were subsequently selected for the further training phase of the study. That set included miR-15a-5p, miR-19b-3p, miR-30e-5p, miR-107, miR-146a-5p, miR-320c, and miR-331-3p. Their characteristics from the microarray screening are shown in the Fig. 18. Also, four miRNAs that exhibited stable expression and did not correlate with recurrence status or other clinical characteristics were selected for normalization of RT-qPCR data in the following experimental phases (let-7b-5p, let-7c-5p, miR-181b-5p, and miR-1281).

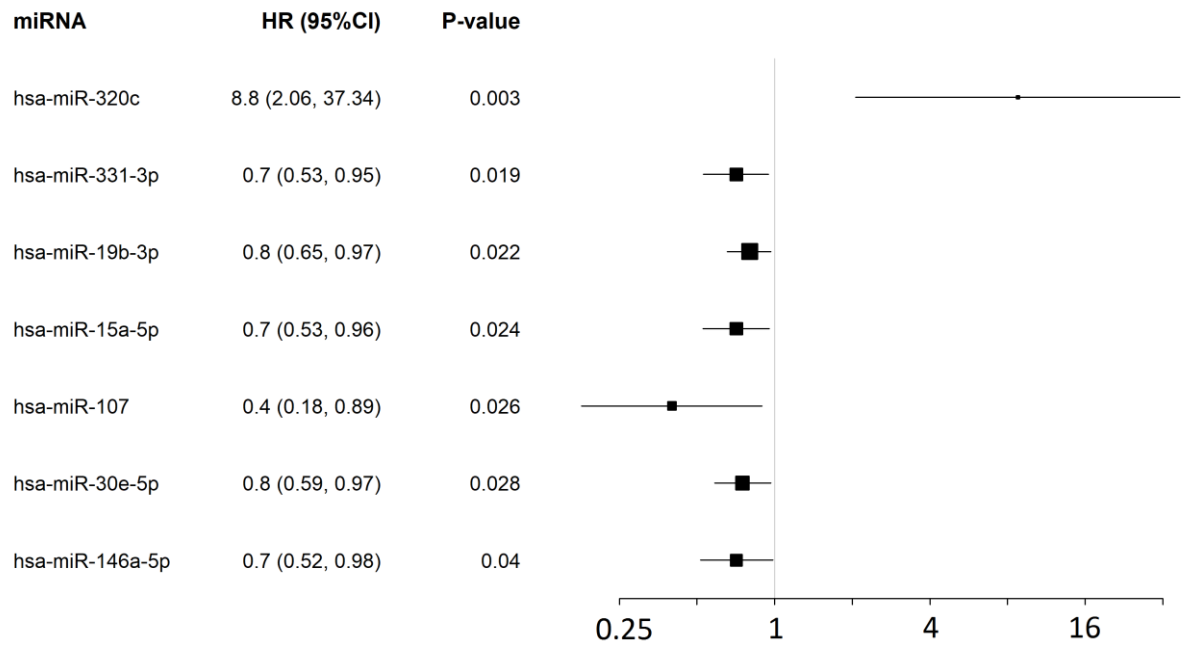

Figure 18. *Selected miRNAs for the training phase and their characteristics from a univariate Cox regression model of TTR. Hazard ratio (HR) with 95% confidential intervals (CI) are showed in the forest plot.*

Paired analysis

Only 10 recurrent patients with available both primary and secondary tumor samples were included in this microarray analysis. Forty-one mature miRNAs showed differential expression in paired matched primary and secondary recurrent samples (Fig. 19). Twenty-eight miRNAs were less expressed in the secondary recurrent samples whereas only 13 miRNAs were more strongly expressed in secondary recurrent samples (Fig. 19). Interestingly, the sample pairs formed two main clusters according to differentially expressed miRNAs, with some miRNAs changing their levels of expression in opposite ways. One of these clusters contained only patients with convexity meningiomas who were generally older and had higher WHO histopathological grades at diagnosis. Only two miRNAs, miR-193b-3p and miR-27a-3p, were

deregulated between primary and secondary recurrent samples and showed dependence on TTR in the screening phase comparing the primary recurrent and non-recurrent samples. Both of those miRNAs exhibited increased expression in secondary samples in comparison with primary recurrent samples and decreased expression in primary recurrent samples in comparison with non-recurrent samples (according to the Cox models of TTR). These two miRNAs were not chosen for further experimental phases. Interestingly, miR-30c-5p was up-regulated in secondary recurrent samples, while expression of the closely related miR-30e-5p, miR-30b-5p, and miR-30a-5p was found to be dependent on TTR in the screening phase. This observation indicates that miR-30 is significantly involved in meningioma pathogenesis and was therefore selected for the further training phase. Moreover, the miR-30 family showed decreased expression pattern following recurrence. According to this data, miRNAs with tumor suppressor features in meningiomas reported increased expression in tumors following recurrence.

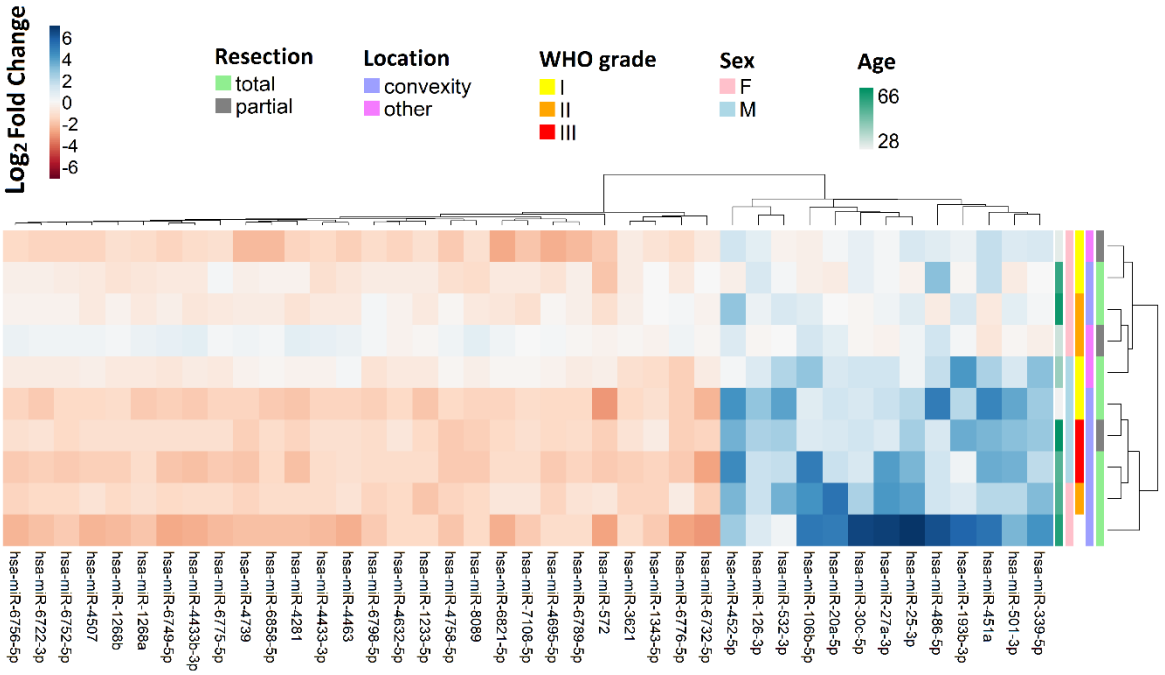

Figure 19. *Hierarchical clustering of 41 mature and highly abundant miRNAs, which exhibited differential expression between paired matched primary and secondary recurrent samples.*

II. Training phase

RT-qPCR was performed for 7 candidate miRNA recurrence predictors and 4 candidate normalizators. The expression of selected miRNA biomarkers was finally normalized against miR-181b-5p that exhibited the most stable basal expression over all samples within the training

cohort. A univariate Cox regression model confirmed the differences in some of the miRNAs expression in primary recurrent and non-recurrent samples observed in microarray experiments. The following miRNAs exhibited significant dependence on TTR using adjusted or non-adjusted models in their expression: miR-15a-5p, miR-146a-5p, and miR-331-3p (Tab. 3). Non-adjusted models are calculated only with certain miRNA as a prognostic factor and the adjusted one includes also clinical factors, such as age at diagnosis, sex, WHO grade, tumor location, and extent of surgical resection. All 3 miRNAs were selected for the final validation phase.

Table 3. *Univariate models for recurrence risk prediction from the training phase for each measured miRNA. Significant miRNA-based models are marked with a bold. Hazard ratio (HR) is reflecting the one unit of ΔCt increase with respective 95% confidential intervals (CI).*

	Non-adjusted model					**Adjusted model**				
Factor	**HR**	**1/HR**	**95% Cl range**		**p-value**	**HR**	**1/HR**	**95% Cl range**		**p-value**
miR-107	1.25	0.80	0.86	1.80	0.240	0.94	1.06	0.63	1.41	0.761
miR-331-3p	**1.76**	**0.57**	**1.14**	**2.70**	**0.010**	1.57	0.64	0.93	2.65	0.090
miR-15a-5p	1.15	0.87	0.97	1.35	0.103	**1.25**	**0.80**	**1.01**	**1.55**	**0.038**
miR-19b-3p	1.27	0.79	0.90	1.78	0.175	1.25	0.80	0.88	1.77	0.214
miR-30e-5p	1.11	0.90	0.89	1.38	0.357	1.21	0.83	0.90	1.64	0.209
miR-320c	1.23	0.81	0.79	1.92	0.364	0.89	1.12	0.49	1.62	0.710
miR-146a-5p	**1.55**	**0.65**	**1.13**	**2.13**	**0.007**	**1.42**	**0.70**	**1.00**	**2.02**	**0.053**

III. Validation phase

Three markers, namely miR-331-3p, miR-146a-5p, and miR-15a-5p, were selected for the final validation phase and tested in an expanded cohort of 172 patients including cohorts from the screening and training phases. Cox regression models were developed using the complete set of ΔCt values for this cohort that had an unbalanced reality-like ratio of recurrent and non-recurrent patients. Adjusting clinical factors, such as age at diagnosis, sex, WHO grade, tumor location, and extend of resection, were also included in the final analysis of TTR. Univariate analyses confirmed the miR-331-3p as the most promising prognostic factor. Analyzing each marker separately, miR-331-3p reports the highest hazard ratio (HR = 1.45) and level of significance (p = 0.001) among other miRNA-based univariate models; miR-146a-5p showed significant prognostic features (HR = 1.34; p = 0.003), too. Additionally, those analyses were performed also for the group of patients with only total resection to exclude the influence of such strong prognostic factor with probably no molecular background. Of note, this analysis provided similar results. Moreover, miR-15a-5p did not reach statistical significance in the presented models. Investigating the influence of clinical adjusting factors, extend of resection

has the strongest prognostic value in all models. Results from univariate Cox regression models are summarized in the following Tab. 4.

Table 4. *Univariate models for recurrence risk prediction from the validation phase for each measured miRNA. Significant factors are marked with bold. Hazard ratio (HR) is reflecting the one unit of ΔCt increase with respective 95% confidential intervals (CI).*

All patients (n = 172)					**Patients after total resection (n = 127)**				
Factor	**HR**	**95% Cl range**		**p-value**	**Factor**	**HR**	**95% Cl range**		**p-value**
Age at diagnosis	0.99	0.97	1.01	0.436	Age at diagnosis	1.01	0.98	1.00	0.709
Sex male	1.68	0.84	3.37	0.142	Sex male	1.15	0.47	2.80	0.759
WHO grade	1.63	1.07	2.50	0.024	**WHO grade**	1.86	1.06	3.20	0.029
Non-convex. loci	0.63	0.33	1.18	0.148	Non-convex. loci	0.54	0.23	1.30	0.150
Partial resection	3.16	1.67	6.00	4.24E-04	-	-	-	-	-
miR-146a-5p	1.34	1.10	1.63	0.003	**miR-146a-5p**	1.37	1.07	1.80	0.014
Age at diagnosis	0.99	0.97	1.01	0.254	Age at diagnosis	0.99	0.97	1.00	0.656
Sex male	2.77	1.45	5.27	0.002	Sex male	1.69	0.72	4.00	0.228
WHO grade	1.37	0.91	2.08	0.132	**WHO grade**	1.85	1.07	3.20	0.027
Non-convex. loci	0.69	0.37	1.28	0.236	Non-convex. loci	0.65	0.28	1.50	0.310
Partial resection	3.67	1.92	7.02	8.52E-05	-	-	-	-	-
miR-15a-5p	0.94	0.84	1.05	0.283	miR-15a-5p	0.96	0.82	1.1	0.573
Age at diagnosis	1.00	0.97	1.02	0.827	Age at diagnosis	1.01	0.98	1.00	0.443
Sex male	1.43	0.67	3.03	0.354	Sex male	1.12	0.44	2.90	0.811
WHO grade	1.33	0.86	2.05	0.200	WHO grade	1.53	0.86	2.70	0.146
Non-convex. loci	0.58	0.31	1.10	0.095	Non-convex. loci	0.46	0.19	1.10	0.085
Partial resection	3.87	2.03	7.38	4.11E-05	-	-	-	-	-
miR-331-3p	1.45	1.17	1.79	0.001	**miR-331-3p**	1.43	1.10	1.90	0.007

Furthermore, the multivariate model was created to prove that miRNA represents real added value in meningioma recurrence prognostication. A stepwise selection method with fixed clinical adjusting factors was used to select the most important prognostic factors in this model. Final model contains only miR-331-3p with HR = 1.44 and $p < 0.001$ among other measured miRNAs and type of resection is the only significant clinical factor (HR = 3.90; $p < 0.001$). The other clinical factors have only a supportive role. The final model is shown in the Fig. 20.

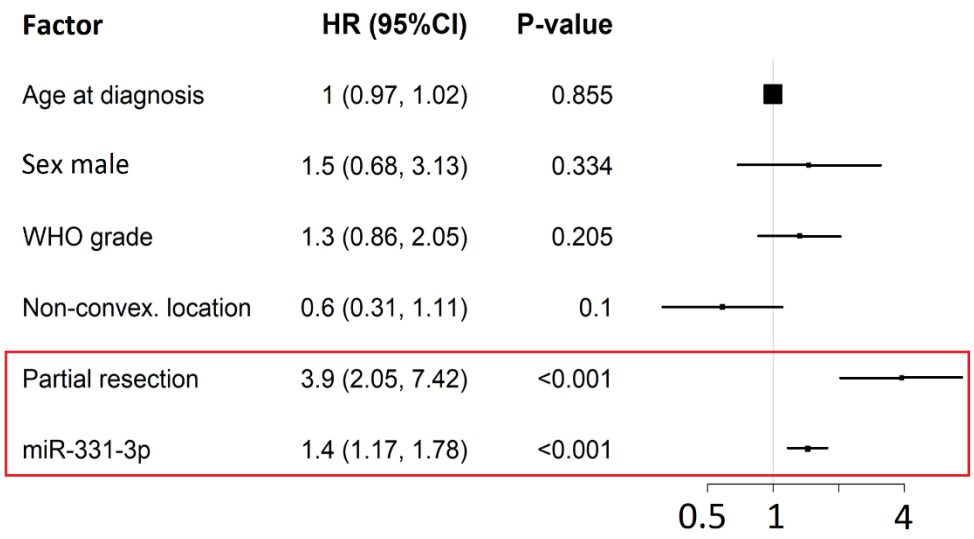

Figure 20. *Final multivariate Cox regression model built with factors selected by stepwise selection with data from validation phase for 161 patients with complete records. Characteristics from the Cox regression model are visualized as forest plot with a hazard ratio (HR) and respective 95% confidential intervals (CI).*

4.2. Aim 2: longRNA profiling

The purpose of this aim was to identify meningioma patients at high risk of recurrence using mRNAs and lncRNAs as biomarkers. The data will be accepted for publication at Neurosurgery (Oxford Academic; IF: 4.65) after few revisions according to the reviewers and the article is attached as Appendix 2. This part of the thesis is also focused on transcriptomic signatures of WHO grade, sex, and developmental origin of meningiomas. Appropriate potential biomarkers were selected using initial unbiased RNA-seq screening, following the validation phase performed by RT-qPCR on the independent cohort. The whole experimental design and description of particular patient cohorts are described in the following Fig. 21 in detail.

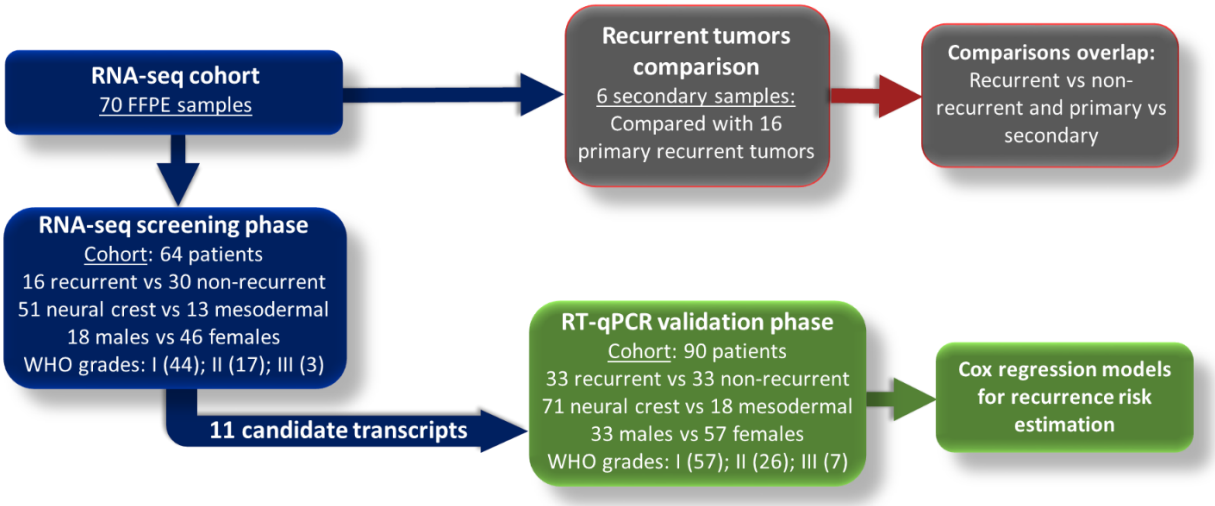

Figure 21. *Schematic overview of the study designed for selection of an appropriate longRNA-based model for recurrence risk estimation. Only patients after at least 5 years' follow-up were considered non-recurrent. Other patients are not included in the analysis of recurrence but are included in other comparisons.*

Transcripts of coding and non-coding genes exhibiting differential expression with respect to tumor recurrence (primary recurrent vs. non-recurrent and secondary vs. primary recurrent), sex (male vs. female), histogenesis (neural crest vs. mesodermal origin), or histopathological grade (WHO grade I vs. grades II and III) were studied and aligned separately. Only differentially expressed transcripts with log2 fold change > 2 or < -2 and adjusted p-value (q-value) < 0.05 were analyzed further in respective comparison. The differentially expressed RNAs considered to be most prognostically relevant were validated in an independent cohort.

RNA-seq screening phase

We identified 69 mRNAs and 108 lncRNAs that were differentially expressed in primary tumors of recurrent and non-recurrent patients. Many identified transcripts were deregulated also among WHO grades or between different developmental origins (Fig. 22A). Only one transcript was also deregulated comparing males and females (S100B). Because of such interesting overlap, this coding transcript was selected for further validation. Three other mRNAs were selected for further validation, due to their biological relevance and high distinguishing potential between recurrent and non-recurrent samples (low q-value and high absolute log2 fold change). That set included HEPACAM2, TDRD1, and ISLR2. HEPACAM2 and TDRD1 are independently deregulated between recurrent and non-recurrent patients, however ISLR2 is also deregulated between WHO grade III and I tumors. Closely related lnc-

GOLGA6A-1 reported similar features and was also selected for further validation. Among other deregulated lncRNAs, oncogenic transcript CCAT2 and completely biologically undescribed transcripts lnc-MAST4-5 and lnc-FAT1-3 were selected for RT-qPCR validation.

Most of the corresponding genes lie on chromosomes 1-8 (Fig. 22B), but there were also five X-chromosomal lncRNAs and one X-chromosomal mRNA (XPNPEP2). Based on functional annotation clustering, the coding genes were divided into ten clusters representing various biological functions and roles (Fig. 22C). Interestingly, developmental genes, immunoglobulin-like and ATP-binding genes were also differentially expressed in tumors of different histogenetic origin.

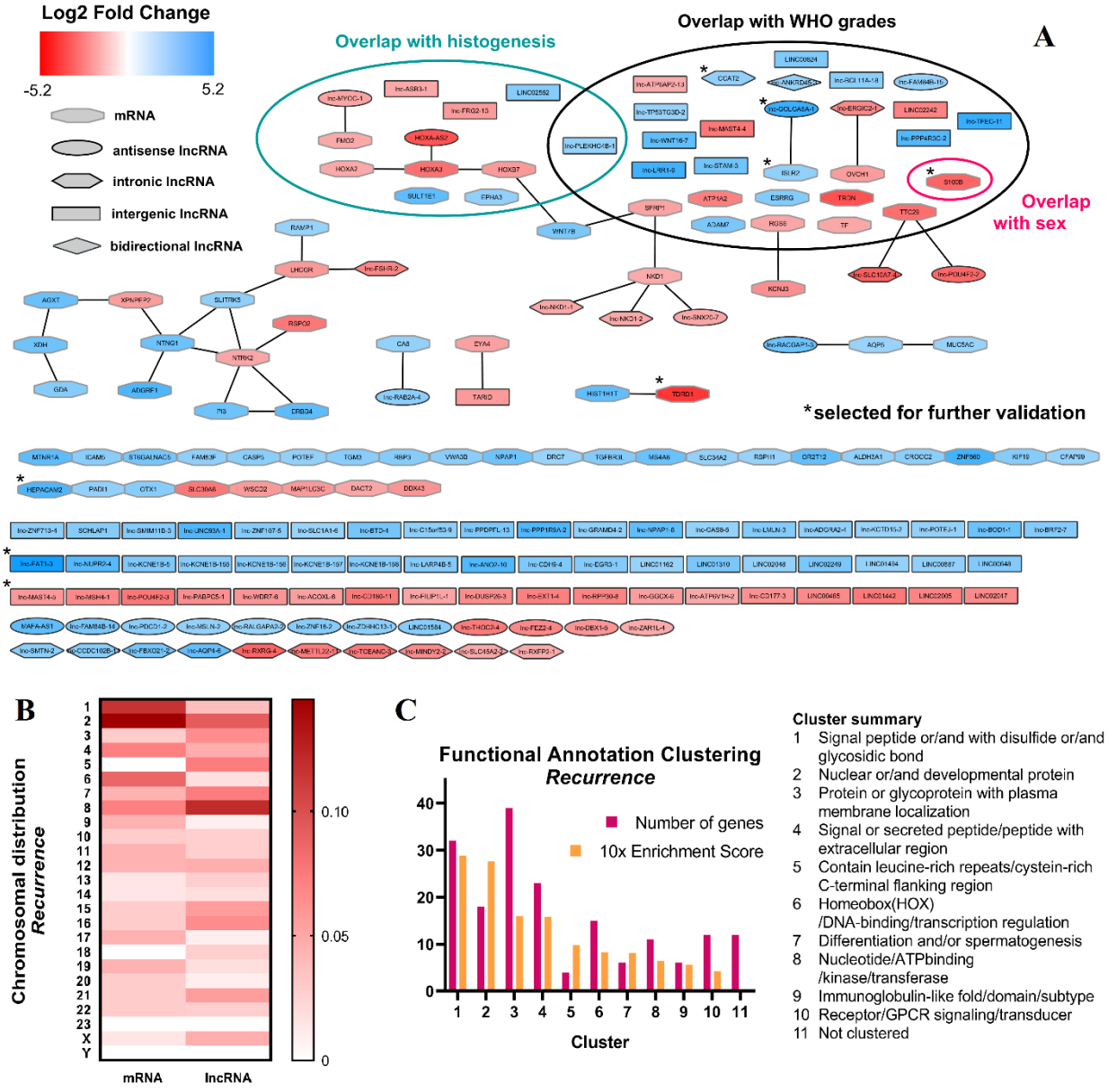

Figure 22. *Differentially expressed genes among primary tumors in recurrent and non-recurrent patients. Transcripts upregulated in recurrent patients are shown in blue: (A) Network showing the fold changes, overlaps, transcript types, and connections of differentially expressed transcripts (B) Chromosomal distribution of differentially expressed transcripts. (C) Overview of functional annotation clustering of mRNAs in which the biological significance of each cluster is quantified using enrichment scores.*

Pathway analysis yielded no statistically significant results, but there were a few of the significantly differentially expressed mRNAs belonging to common pathways. The pathway with the greatest number of mRNAs exhibiting differential expression between recurrent and non-recurrent patients (EPHA3, TF, WNT7B, and SFRP1) was the angiogenesis pathway; the Wnt signaling (NKD1, WNT7B, SFRP1) and purine metabolism pathways (XDH, GDA) had also multiple differentially expressed RNAs. However, only the angiogenesis and Wnt signaling pathways were associated with transcripts exhibiting differential expression in other comparisons. Pathways including at least 2 genes differentially expressed between recurrent and non-recurrent patients are shown in Fig. 23.

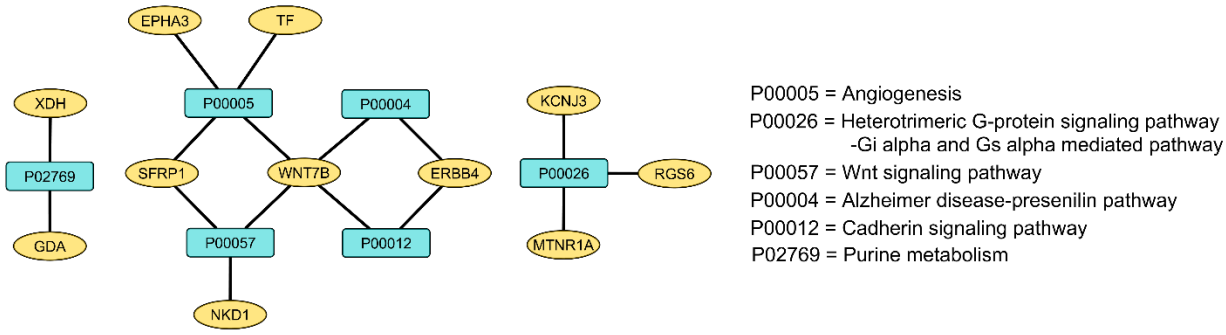

Figure 23. *Differentially expressed genes (yellow nodes) belonging to certain pathways according to PANTHER Enrichment Test (PANTHER version 15). Only the pathways with at least 2 genes deregulated between recurrent and non-recurrent patients are showed.*

Additionally, a transcriptomic signature of meningioma developmental origin was discovered. There were 79 mRNAs and 76 lncRNAs exhibiting differential expression between mesodermal lesions and those arising from the neural crest, most of which were closely connected. For instance, there were 45 connections between these mRNAs and lncRNAs based on their chromosomal coordinates (Fig. 24). The only significantly up-regulated group of RNAs in mesodermal tumors were homeobox-related transcripts; the majority of the remaining transcripts were down-regulated. However, a few non-homeobox-related transcripts (4 mRNAs

and 11 lncRNAs) were up-regulated in mesodermal tumors. Chromosomes 1, 7, and 17 had the greatest numbers of mapped transcripts exhibiting differential expression with respect to histogenesis; in addition, there were 3 differentially expressed X-chromosomal mRNAs. Functionally, these transcripts were linked to angiogenesis, blood coagulation, neural and general development, and 4 were associated with Wnt signaling. All identified groups of deregulated transcripts are summarized in the following Fig. 24.

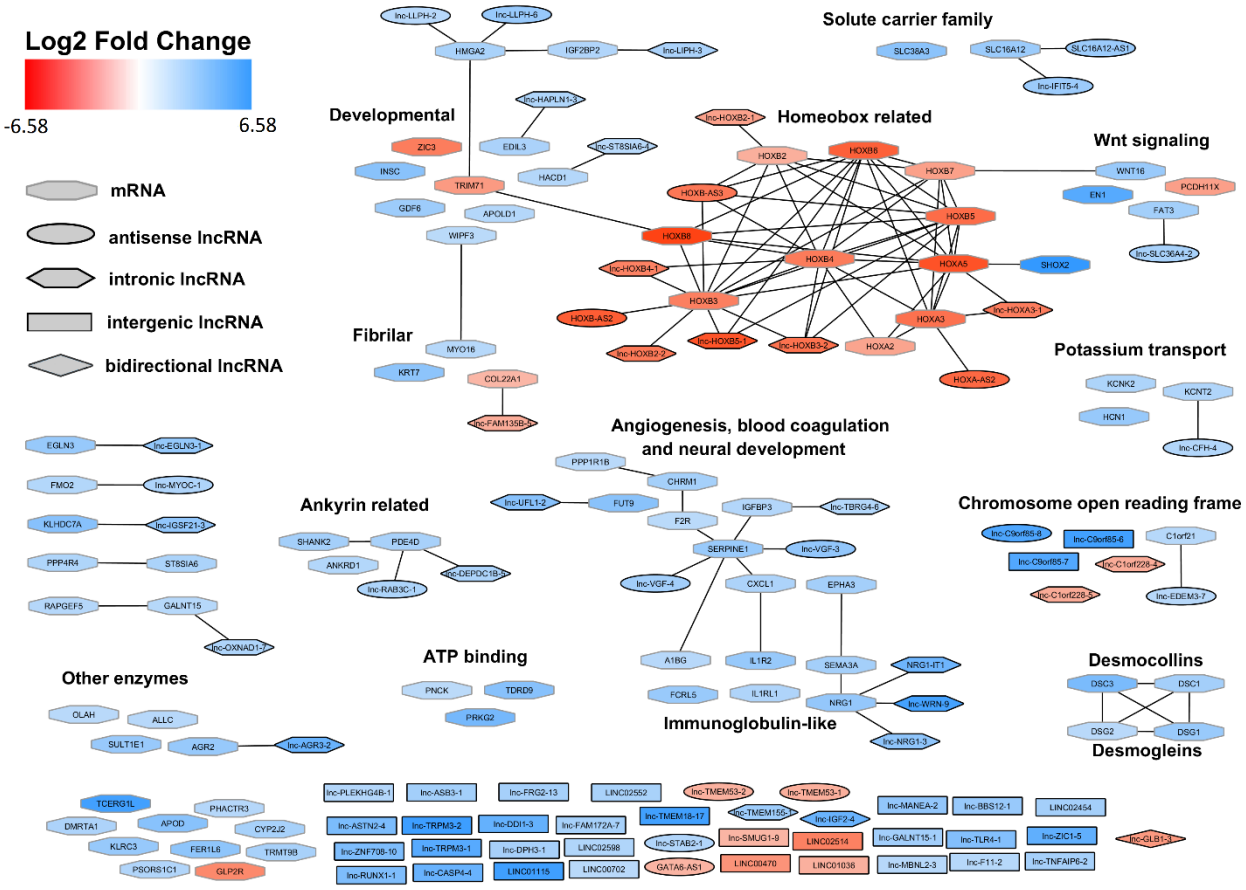

Figure 24. *Differentially expressed mRNAs and lncRNAs among tumors arising from the neural crest and mesodermal cells showing their fold changes, common biological roles, transcript types, and connections. Transcripts upregulated in neural crest tumors are shown in blue.*

There were 59 non-coding and 12 coding transcripts that were expressed differentially in males and females. As expected, most of these transcripts were localized to the Y chromosome. However, two autosomal coding genes, S100B and NTM, were also identified. Both of them are associated with neural development, and especially with neurite outgrowth. S100B exhibited differential expression with respect to WHO grade and tumor recurrence. In addition, seven autosomal and 5 X-chromosomal lncRNAs were differentially expressed between males

and females. Of these lncRNAs, the autosomal lnc-PXDN-3 and the Y-chromosomal lnc-BPY2C-4 intergenic transcripts are also differentially expressed with respect to WHO grades. Interestingly, the intergenic X-chromosomal lnc-TGIF2LX-1 transcript was expressed more strongly in males than in females ($q < 0.001$).

Transcriptomic differences among clinically relevant histopathological subgroups were also investigated. The WHO grade II and WHO grade III groups were merged because of the low number of WHO grade III tumors, involving only three patients, and compared to the WHO grade I group in our analyses. The only one WHO grade III-specific transcript, CPE, was selected for further validation. The CPE is neural-specific carboxypeptidase down-regulated in WHO grade III tumors ($q < 0.001$). In total, 58 mRNAs and 98 lncRNAs were deregulated between WHO grade II+III and WHO grade I. The functional annotation clustering showed 11 common functional patterns of deregulated mRNAs (Fig. 25). Interestingly, there are also genes involved in homeobox and DNA binding and metal ions binding and transport, similarly as in previous comparisons. AMH, ECEL1, and CCAT2 were selected for further validation. AMH is a coding transcript for the Antimüllerian hormone involved in the gonadotropin-releasing hormone receptor pathway. AMH was down-regulated in the WHO grade I group ($q < 0.001$). Two other genes from this pathway were also deregulated (NOS1 up-regulated and PITX1 down-regulated in WHO grade I). Moreover, neural-specific endopeptidase ECEL1 ($q = 0.004$), up-regulated in WHO grade I, and previously described CCAT2 ($q < 0.001$), down-regulated in WHO grade I tumors were selected for further validation as well.

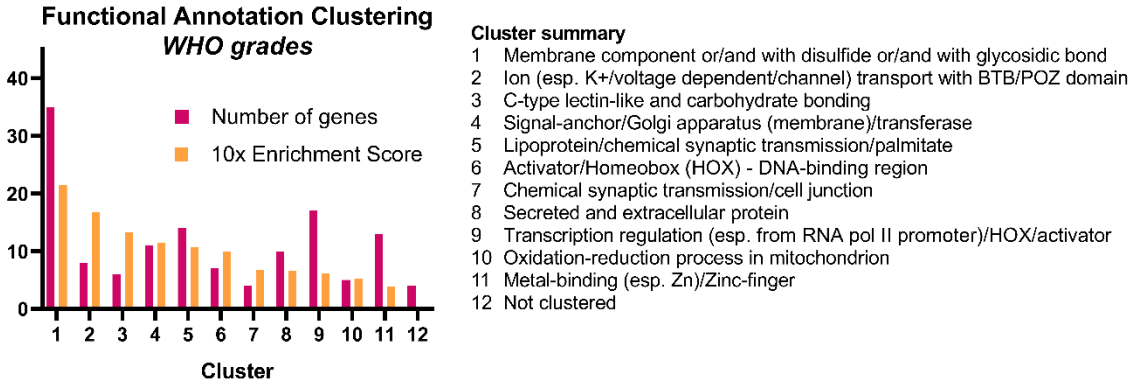

Figure 25. *Overview of functional annotation clustering of mRNAs, differentially expressed between high grades (WHO grade II+III) and low grade (WHO grade I), in which the biological significance of each cluster is quantified using enrichment scores.*

Recurrent tumors comparison

Furthermore, samples of recurrent patients were compared with their following tumors (not paired-matched analysis). Twenty mRNAs and twelve lncRNAs showed differential expression between primary and secondary recurrent tumors. Deregulated mRNAs showed overlap only with WHO grades (MT1E and SCN7A). However, lnc-GOLGA6A-1 is down-regulated in secondary tumors ($q = 0.036$) and deregulated also in other comparisons. Additionally, lnc-ASB3-1 is up-regulated in secondary tumors ($q = 0.015$) and deregulated in recurrent patients in comparison with non-recurrent patients and mesodermal tumors in comparison with tumors arising from the neural crest. In general, there is the lowest overall transcriptomic difference between primary and secondary tumors from recurrent patients in comparison with all other investigated groups.

RT-qPCR validation phase

Eleven transcripts, exhibiting low q-value and high fold change in certain comparisons, were selected for this experimental phase. HEPACAM2, TDRD1, lnc-FAT1-3, and lnc-MAST4-5 were selected for their exclusive expression differences between recurrent and non-recurrent samples. ISLR2, lnc-GOLGA6A-1, and CCAT2 exhibited differential expression among recurrent and non-recurrent patients and WHO grades. AMH, ECEL1, and CPE showed distinguishing potential between particular WHO grades within the RNA-seq data. S100B was deregulated according to the recurrence status, WHO grade, and sex. All those markers were measured with RT-qPCR on an independent cohort of 90 patients using GAPDH mRNA as a normalizator. Measurement of HEPACAM2, TDRD1 and lnc-FAT1-3 did not provide efficient RT-qPCR data, even trying 3 different probe sets for each of them, thus these transcripts were not analyzed further. Two transcripts exhibited a high number of samples with no amplification during RT-qPCR, thus they were analyzed from the qualitative point of view. Those are S100B with 28 RT-qPCR negative samples (31.1%) and lnc-MAST4-5 with 34 samples without RT-qPCR amplification (37.8%).

Differential expression of the remaining 8 transcripts, exhibiting RT-qPCR positivity, were analyzed among all comparisons previously studied within the RNA-seq experiment. ISLR2, lnc-GOLGA6A-1, and AMH were up-regulated in recurrent patients and males. Surprisingly, S100B did not show any significant quantitative changes among investigated subgroups. Also, none of the presumed markers proved differential expression among WHO grades. Only lnc-MAST4-5 was down-regulated in WHO grade II and III tumors, but this feature was not

identified in the RNA-seq experiment. This transcript was also quantitatively down-regulated in neural crest tumors. All differences are summarized in the following Fig. 26.

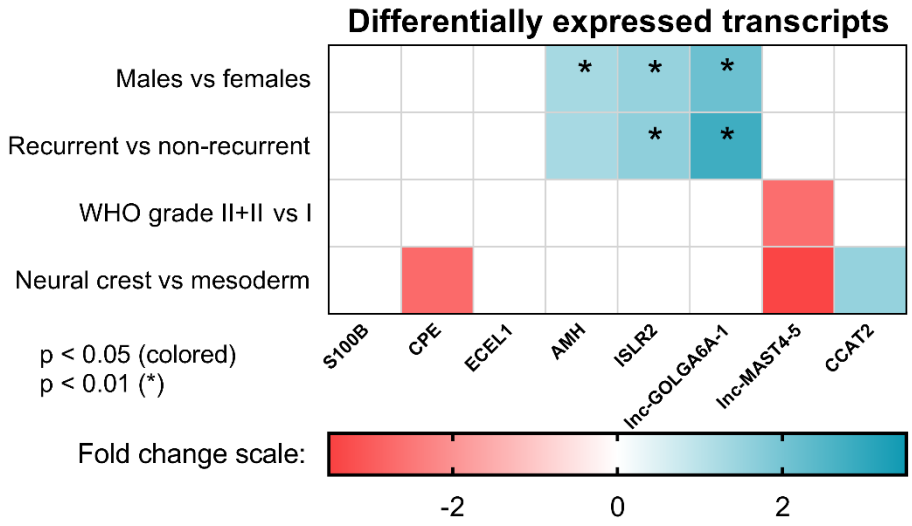

Figure 26. *Overview of significantly deregulated transcripts, where the fold change is calculated from ΔΔCt values in all comparisons on the level of significance p < 0.05.*

Qualitative analysis showed that S100B exhibits more frequent RT-qPCR positivity in females (78.9%) than males (51.5%). According to Pearson's test, this difference is statistically significant (p = 0.013). Additionally, lnc-MAST4-5 exhibited statistically significant qualitatively reduced expression in groups with unfavorable prognosis, except the group of neural crest developmental origin (Fig. 27).

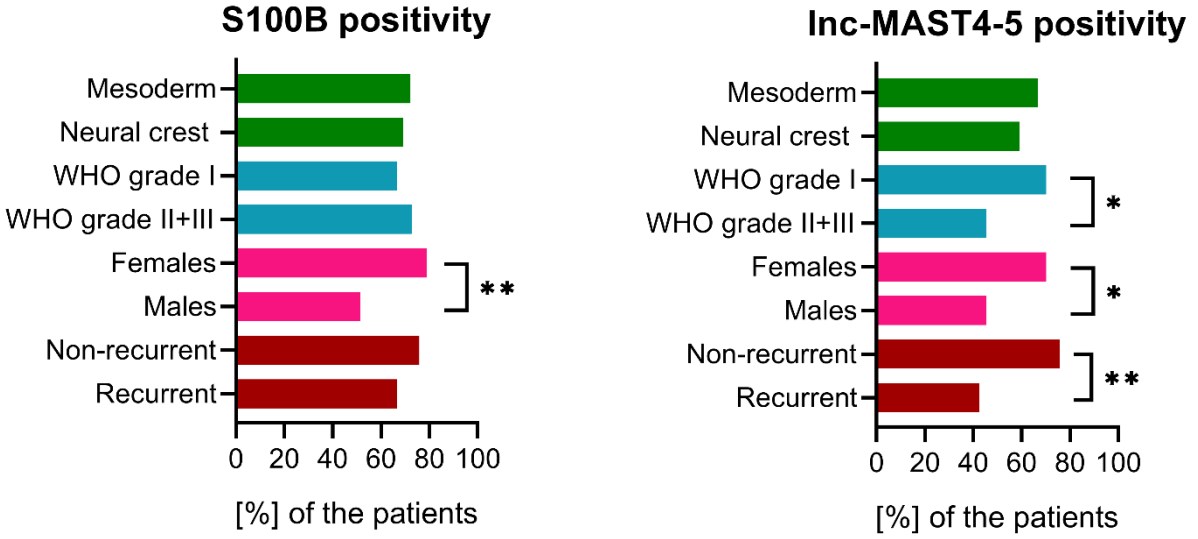

Figure 27. *Significant differences in the proportion of S100B and lnc-MAST4-5 RT-qPCR positive samples among selected groups (* p ≤ 0.05, ** p ≤ 0.01).*

Univariate Cox regression models of TTR were created for all 8 validated transcripts. Adjusting clinical factors (age at diagnosis, extent of surgical resection, tumor localization, sex, and WHO grade) were included and fixed in each model. ISLR2, lnc-GOLGA6A-1, and AMH significantly influenced TTR survival. Interestingly, expression patterns of those three transcripts were correlated across the entire RT-qPCR cohort (the correlation coefficient r varied from 0.72 to 0.85) with high significance ($p < 0.001$). Nevertheless, the extent of surgical resection was the most important contributor to the estimated recurrence risk in all the adjusted univariate models. Only the models with the validated transcript as a significant factor for recurrent risk estimation are shown in the following Tab. 5.

Table 5. *Univariate models for recurrence risk prediction for each measured transcript; significant factors are marked with bold. Hazard ratio (HR) is reflecting one unit of ΔCt increase with respective 95% confidential intervals (CI).*

Factor	HR	1/HR	95% Cl range		p-value
ISLR2 – based model					
Age at diagnosis	1.0	1.0	0.98	1.03	0.747
WHO grade II+III	2.4	0.4	1.12	5.19	0.025
Sex (Male)	0.6	1.6	0.29	1.40	0.261
Partial resection	6.3	0.2	2.18	18.45	0.001
Tumor location (convexity)	1.9	0.5	0.71	5.23	0.200
ISLR2	0.6	1.7	0.38	0.86	0.007
AMH – based model					
Age at diagnosis	1.0	1.0	0.98	1.04	0.656
WHO grade II+III	3.0	0.3	1.29	6.90	0.011
Sex (Male)	0.6	1.6	0.28	1.39	0.246
Partial resection	5.8	0.2	1.82	18.23	0.003
Tumor location (convexity)	2.5	0.4	0.87	7.33	0.089
AMH	0.4	2.5	0.20	0.82	0.012
Lnc-GOLGA6A-1 – based model					
Age at diagnosis	1.0	1.0	0.98	1.03	0.751
WHO grade II+III	2.3	0.4	1.08	5.06	0.031
Sex (Male)	0.6	1.7	0.27	1.30	0.190
Partial resection	6.6	0.2	2.19	19.76	0.001
Tumor location (convexity)	2.3	0.4	0.82	6.24	0.115
Lnc-GOLGA6A-1	0.7	1.4	0.59	0.87	0.001

The final multivariate model was created by stepwise selection using the Bayesian information criterion and featured lnc-GOLGA6A-1 as the sole significant recurrence risk factor, with 1/HR = 1.31 and $p = 0.002$. A model in which the clinical factors were fixed was identical to the adjusted univariate model for lnc-GOLGA6A-1 in the Tab. 5. Thus, TTR

survival was analyzed separately for patients expressing lnc-GOLGA6A-1 at low and high levels. The influence of the categorized lnc-GOLGA6A-1 marker on TTR was studied by estimating an optimal cut-off value for GOLGA6A-1 with respect to TTR using the maximally selected rank statistics method implemented in the survminer R package (ver. 0.4.8). In this case, the TTR survival values for subgroups of patients with higher expression of lnc-GOLGA6A-1 ($\Delta Ct \leq 2.34$) and lower expression ($\Delta Ct > 2.34$) were estimated by the Kaplan-Meier method and compared using the log-rank test. Meningioma patients whose expression of lnc-GOLGA6A-1 was below the cut-off ($\Delta Ct > 2.34$) had significantly longer TTR survival ($p = 0.001$; Fig. 28).

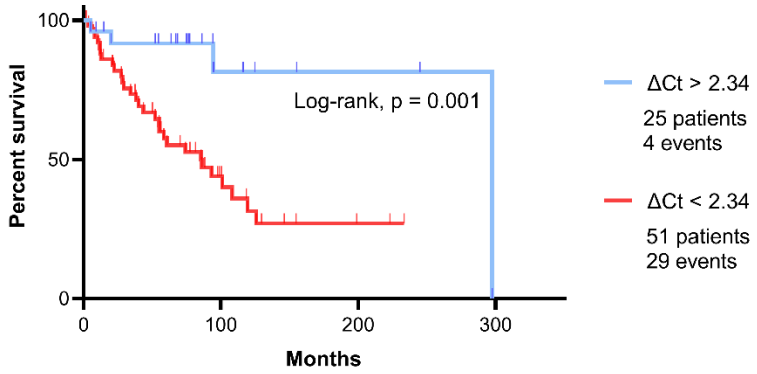

Figure 28. *Time-to-recurrence (TTR) survival analysis for patients expressing lnc-GOLGA6A-1 at low (ΔCt > 2.34) and high levels (ΔCt ≤ 2.34).*

4.3. Aim 3: MEG3 profiling

Identification of the clinically relevant features of MEG3 in meningioma is the main objective of this aim. The data has not been published yet. For this purpose, transcriptomic data from the Aim 2 were analyzed. MEG3 was not differentially expressed among studied parameters (changes according to WHO grade, sex, recurrence, and developmental origin of the tumor). Thus, splicing variants (isoforms) of MEG3 were differentially analyzed with respect to mentioned subgroups. This analysis revealed 27 annotated MEG3 isoforms according to the GRCh38.p13 file from the Ensembl database. Differential analysis of those isoforms showed significant deregulation of some isoforms among studied subgroups. Nineteen isoforms were deregulated in at least one comparison at the level of significance $q < 0.05$. MEG3 isoforms were most frequently deregulated among WHO grades, but those changes were quantitatively weak. Only one isoform was deregulated between recurrent and non-recurrent patients. This transcript (MEG3-016) was up-regulated in recurrent patients and also in the

subgroup of mesodermal tumors. This isoform contains 9 exons and the final length is 1,726 nt. The 5-6 exon junction provides the unique sequence contained only in this isoform. This region can be used for the specific detection of MEG3-016. The results of the analysis of splicing variants are summarized in the Fig. 29.

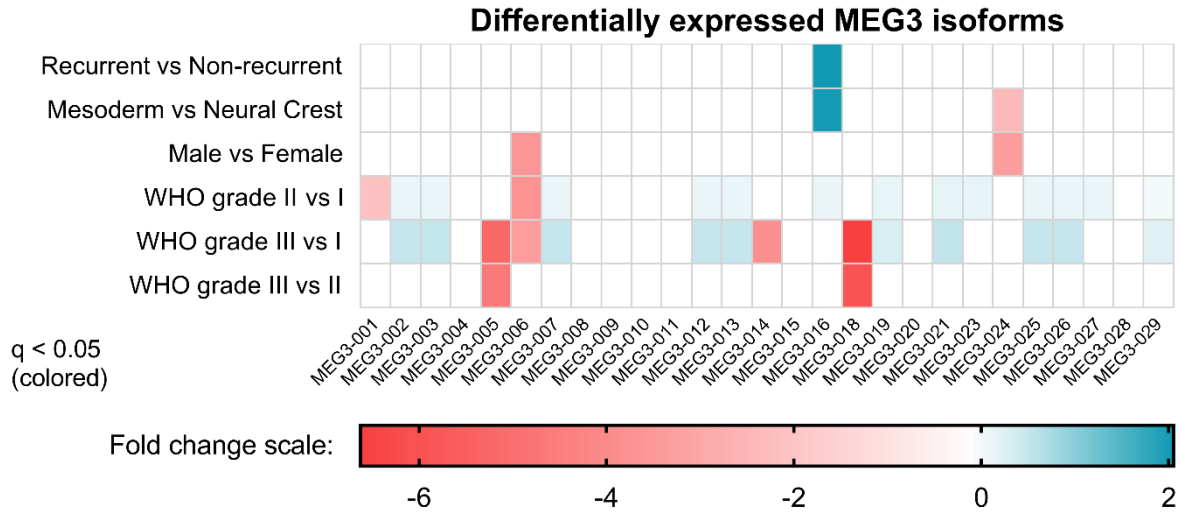

Figure 29. *Overview of significantly deregulated transcripts, where the fold change is calculated from RNA-seq data in all comparisons on the level of significance q < 0.05.*

Subcellular localization and tissue distribution of MEG3 were studied. For that purpose, RISH was performed for 123 samples on TMA. Image analyses were performed for 82 samples in doublets with efficient MEG3 signal and sufficient preparation quality. In the remaining 41 samples, no or poorly evaluable signal was detected. In higher size categories (> 15 px), clusters of MEG3 gene transcripts were supposed to be formed. The amount and distribution of the signal were correlated with recurrence and TTR. For the analysis of the size categories, 5% of samples with the smallest number of signals and samples containing less than 3 analyzed ROIs were excluded. This cohort included 73 samples from 60 patients, thus also secondary tumor samples were analyzed with respect to recurrence, but only the primary recurrent samples were used for Cox models of TTR. Nevertheless, recurrence status with 5 years' follow-up was set up only for 58 patients/samples. Only the highest quality images were selected for the analysis of the signal distribution between nuclei and surroundings (non-nuclei) because this analysis was performed manually. This set included 64 samples from 55 patients and recurrence status with 5 years' follow-up was set up for 49 patients/samples. Again, the secondary samples were excluded from TTR analyses. Overview of the RISH study with representative images is summarized in the following Fig. 30.

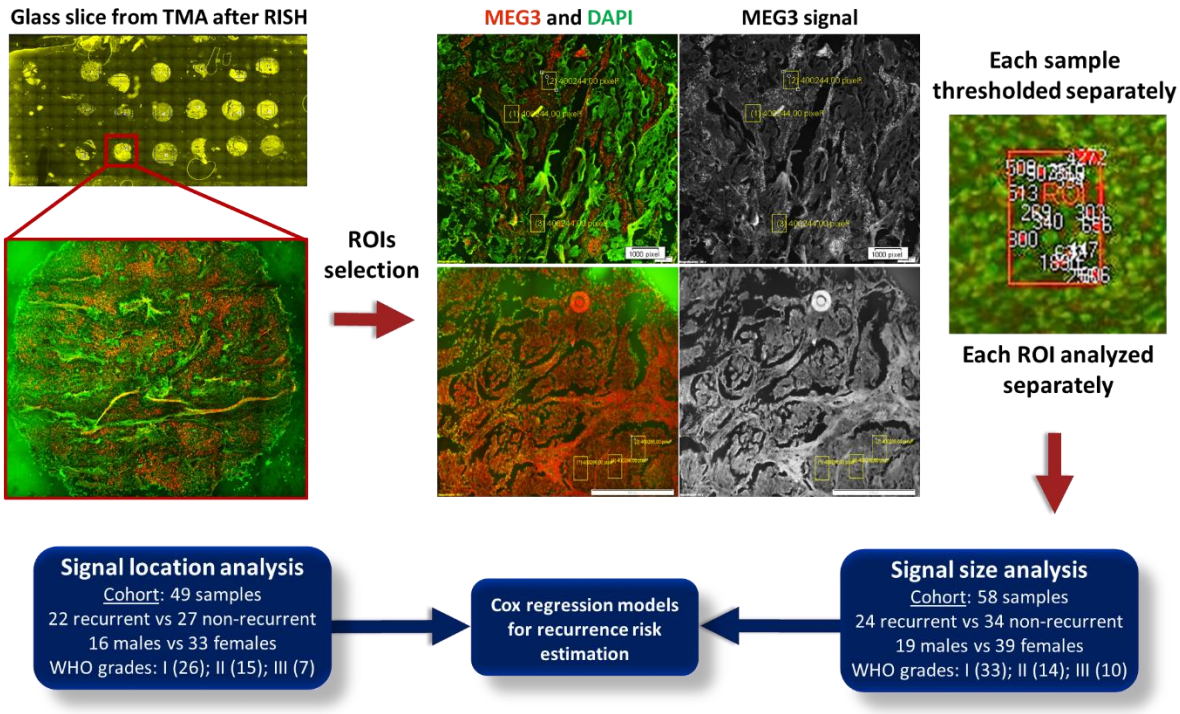

Figure 30. *Schematic overview of the study designed for selection of appropriate MEG3 feature for recurrence risk estimation according to the RISH image data. DAPI is shown in green for better visibility of the red MEG3 signal. Only patients after at least 5 years' follow-up were considered non-recurrent. Signal location analysis differentiates between nuclear and non-nuclear localization of MEG3 transcript and Signal size analysis shows the proportion among single signals and MEG3 clusters of various sizes.*

Most of the signals were distributed in single transcripts (> 60%), clusters of various sizes (> 15 px) were less frequent (Fig. 31A). Importantly, the distribution of single transcripts and their clusters correlated significantly with recurrence status in all size categories up to 250 px. The proportion of single transcripts (1 – 15 px) was the most significant. Samples from recurrent patients exhibited a higher proportion of single transcripts than their non-recurrent counterparts ($p < 0.001$). On the other hand, the proportion of the clusters (15 – 250 px) was significantly lower in recurrent patients (Fig. 31A-B). This phenomenon was typical for the following size categories; 15 – 30 px ($p = 0.032$), 30 – 60 px ($p = 0.020$), 60 – 100 px ($p < 0.001$) and 100 – 250 px ($p = 0.008$). The differences in the proportion of single signals and clusters had also the same trends after dividing only into two categories (Fig. 31B); > 15 px and < 15 px. Samples with a signal percentage < 15 px greater than 72.7% were more likely to come from recurrent patients ($p < 0.001$). The cut-off of 72.7% was set up according to TTR. The Cox model of TTR also showed a significantly higher probability of recurrence in patients with a higher proportion

of single transcripts than this cut-off value (HR = 5.2; p = 0.002). According to the survival analysis, the TTR differs significantly for groups of patients with a lower or higher proportion of individual transcripts in the size category 1 - 15 px (p < 0.001; Fig. 31C).

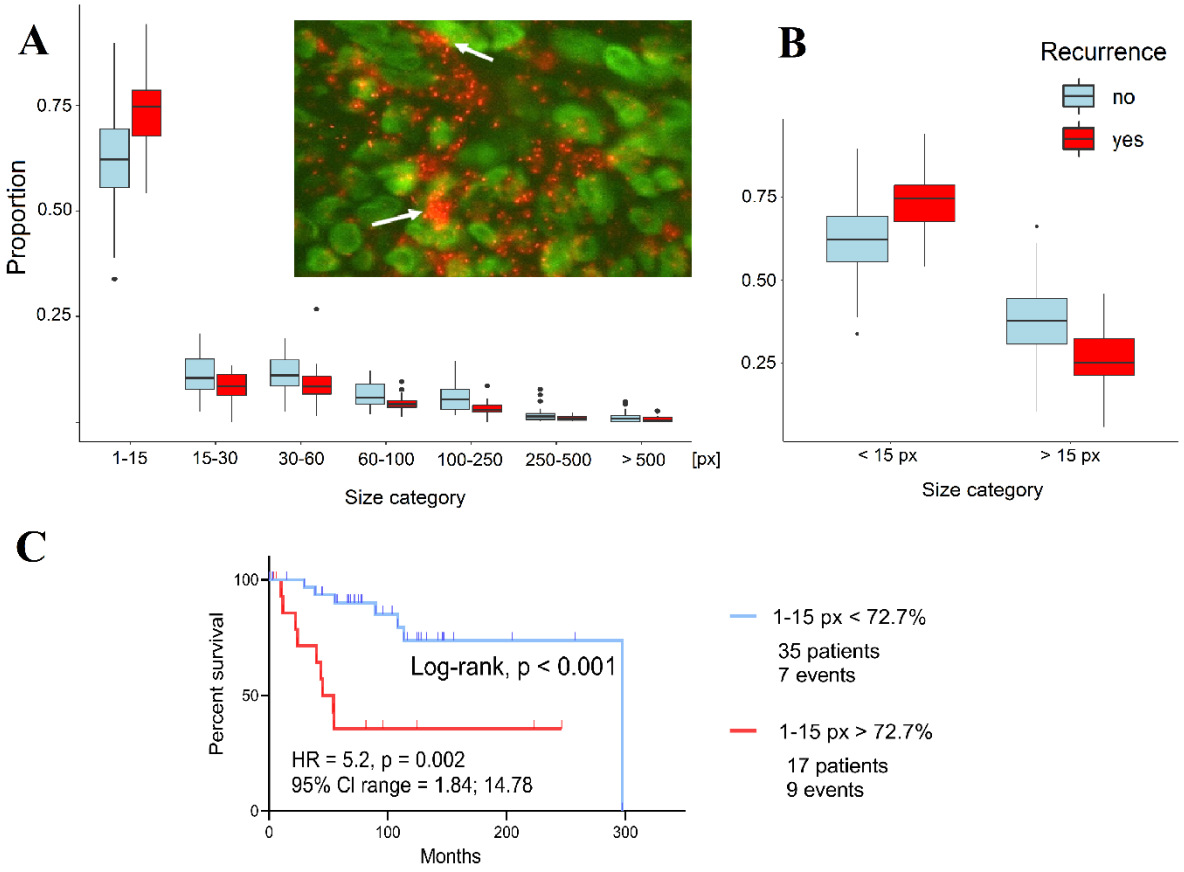

Figure 31. *Signal size analysis of MEG3 transcript in meningioma tissue: (A) Proportion of points in individual categories within the data set expressed as boxplots. MEG3 clusters (> 15 px) are marked with white arrows in the representative image. MEG3 signal is shown in red and nuclei in green. (B) The second boxplot shows the same data, but the size is divided only into two categories; single MEG3 transcripts (< 15 px) and MEG3 clusters (> 15 px). (C) Time-to-recurrence (TTR) survival analysis for patients with the low proportion of single transcripts (< 72.7%) and the high proportion of single transcripts (> 72.7%). Characteristics from the Log-rank test and Cox regression model are showed; p-value, hazard ratio (HR), and respective 95% confidential intervals (CI).*

Regarding the signal location analysis, Cox regression models showed a significant correlation between TTR and the nuclear location of the MEG3 signal. Only the signals from the single transcripts were included in the analysis, because of discrepancy during the

estimation of the exact location of clusters, which often exhibited strong over-illuminated signals (Fig. 32A). A 10% increase in the proportion of signal in the nucleus significantly increases the probability of early recurrence according to the univariate Cox regression model (HR = 1.47; p = 0.003; Fig. 32B). As previously described, the influence of the categorized parameter on TTR was again studied by estimating an optimal cut-off value for the proportion of the signal within the nuclei with respect to TTR using the maximally selected rank statistics method. The resulted cut-off value was a 64% representation of the single signals of MEG3 in the nuclei. The Cox model of TTR showed a significantly higher probability of recurrence in patients with a higher proportion of single transcripts in the nuclei than this cut-off value (HR = 4.7; p = 0.009). According to the survival analysis, the TTR differs significantly in groups of patients with a lower or higher proportion of individual transcripts in the nuclei (p = 0.004; Fig. 32D).

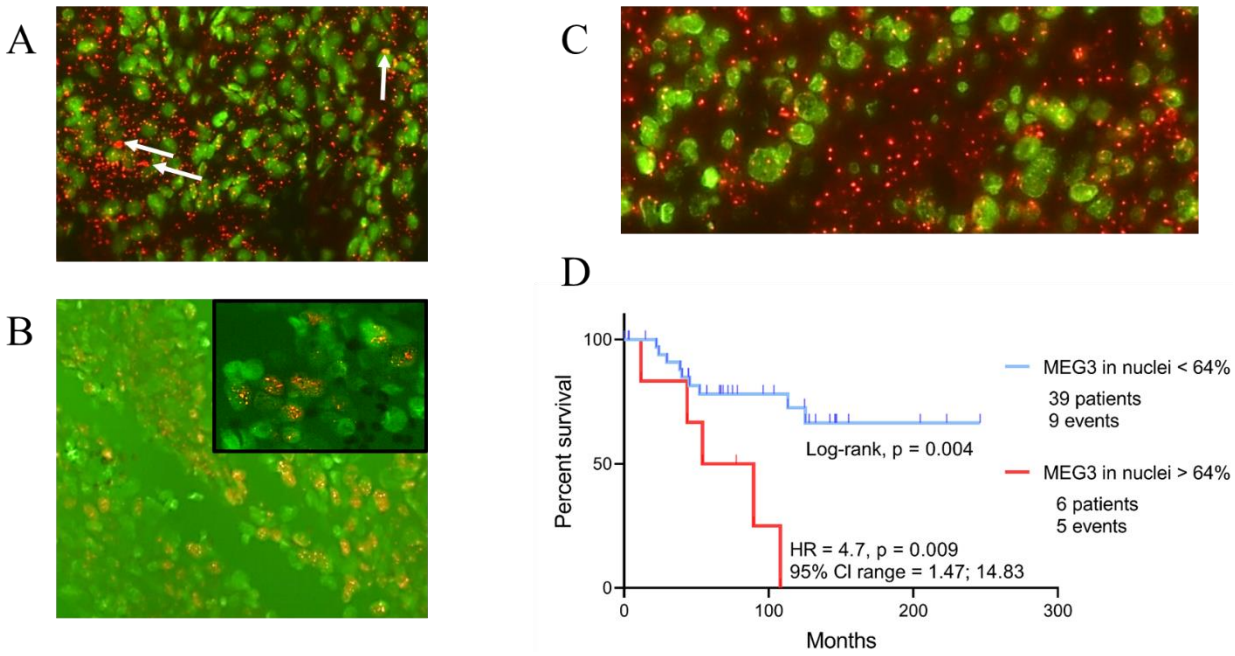

Figure 32. *Signal location analysis of MEG3 transcript in meningioma tissue: (A) MEG3 signal distribution both inside and outside the nuclei. MEG3 signal is shown in red and nuclei in green channels. Location was determined only for the single transcripts, clusters with questionable locations are shown by white arrows. (B) Recurrent tumor tissue with strong nuclear accumulation of MEG3. (C) Tissue with a higher proportion of MEG3 localized outside of the nuclei. (D) Time-to-recurrence (TTR) survival analysis for patients with low (< 64%) and high (> 64%) proportion of single transcripts in the nuclei. Characteristics from the Log-rank test and Cox regression model are showed; p-value, hazard ratio (HR), and respective 95% confidential intervals (CI).*

5. Discussion

Despite the fact that histopathological features and Simpson grade (SG) evaluation are routinely used prognostic markers, WHO grade I meningiomas may recur even after adequate total resection, whereas the WHO grade II and III tumors may not [12]. This calls into question the value of histology in predicting their recurrence. It has recently emerged that epigenetics-based classifications predict meningiomas' biological behavior more accurately than morphology-based taxonomies. For example, DNA methylation profiling was shown to identify WHO grade I meningiomas at high risk of recurrence as well as those with a low tendency to recur despite having morphological features of WHO grade II lesions [45]. Also, abnormalities in genomic DNA have been already included in routine prognostication of other brain tumors. Most of the investigated abnormalities include the mutational status of coding loci in DNA, such as IDH1 status in glioblastomas [99]. These aspects have been recently investigated also in meningioma. For instance, Hedgehog activation, including oncogenic SMO and SUFU mutations, as well as TRAF7 mutations, exhibit elevated risk of recurrence in WHO grade I meningiomas. PI3K activating mutations shorten the TTR too [100]. On the other hand, KLF4 mutations were associated with a low recurrence rate and longer progression-free survival. Nevertheless, a further multivariate Cox regression model identified only the Hedgehog activation as an independent negative risk factor for meningioma recurrence (HR = 2.7; p = 0.046) among all others studied mutations [100]. The main intention of this thesis was to find the biomarkers of meningioma recurrence on the level of non-coding RNAs. Currently, there is no other unbiased study properly addressing this issue. A link between aberrant miRNA expression and meningioma recurrence has so far been identified in only three studies. However, none of these miRNAs overlap with the set of 49 deregulated miRNAs identified during the screening phase of the presented thesis [48] [75] [101]. All those studies were performed on the Chinese population and only one study included proper screening not using predesigned panel [48]. During our miRNA study, potential markers of recurrence were screened with an unbiased microarray method. The final validation set of markers included miR-15a-5p, miR-146a-5p, and miR-331-3p. Cox multivariate model with stepwise selection identified the predictive miR-331-3p-based model as the most effective. The validation cohort included the patients from previous experimental phases and was expanded by 75 patients, which were not previously included. Thus, the validation phase is not independent and represents a potential limitation. This approach was selected because of lack of the samples from recurrent patients.

Both miR-15a-5p and miR-331-3p are tumor suppressors playing the role in various cancers and cancer-related signaling pathways. According to TarBase v7.0, those miRNAs are also significantly related to viral infections, protein and fatty acids processing, and hormone-mediated oocyte development. Thus, it was found that miR-15a-5p and miR-331-3p influence both mitosis and meiosis [102]. Which proteins are crucial targets of these miRNAs in meningiomas remains unclear, yet there are some most probable relations. For instance, it has been found that EGF signaling, HRAS, hypoxia, and angiogenesis are involved in the progression of benign meningiomas [18]. EGFR and RASL10B are the direct targets of miR-331-3p and angiogenesis is strongly regulated by miR-15 [103]. Regarding mentioned fatty acids metabolism, meningiomas with proposed unfavorable prognosis exhibit the higher expression of fatty acid synthase and brain fatty acid-binding proteins. Those molecules are associated with higher aggressiveness of tumors because they allow the acceleration of metabolism in cancer cells by increasing cellular fatty acid uptake, processing, and transfer [104]. This suggests that miR-331-3p in particular, which plays such an important role in the meningioma prognostication, may largely suppress the described oncogenic properties and pathways in meningioma.

The second most effective predictive model was identified as the one involving miR-146a-5p. Interestingly, miR-146a-5p is not only an effective prognostic biomarker, but also an ideal candidate for a predictive marker and therapeutic target. MiR-146a acts as a tumor suppressor in gastric cancer cells and metastases [105], and complete suppression of its expression in C57BL/6 mice leads to the development of myeloid sarcoma and lymphoma [106]. Studies using glioma cell lines have reported that combined treatment with gamma-linolenic acid (GLA) and ionizing irradiation leads to overexpression of miR-146a (Fig. 33) [107]. Because surgical resection in combination with irradiation is the standard therapy for recurrent meningiomas, it would be beneficial to determine whether GLA and radiotherapy would have a similar positive therapeutic effect on miR-146a-5p expression in meningiomas. Decreased expression of miR-146b leads to increased expression of the NF-κB gene causing increased production of IL-6, which activates STAT3 [108]. STAT3, which exhibited overexpression in meningiomas with a worse prognosis, is indirectly affected by miR-146b, which decreases expression of NF-κB leading to down-regulation of IL-6 production (Fig. 33). In addition, a strong activating phosphorylation signal of STAT3 has been observed predominantly in recurrent tumors [109]. Although suppression of IL-6 by miR-146a leading to decreased STAT3 expression has not yet been demonstrated in meningiomas, current knowledge on the relationship between STAT3 and miR-146 suggests potential therapeutic use of miR-146a as a

targeted treatment for these tumors. Combination therapy with GLA and radiation may be an effective strategy to increase the expression of this miRNA, thus inactivating the JAK/STAT signaling pathway (Fig. 33), which could lead to a reduced risk of recurrence in meningioma.

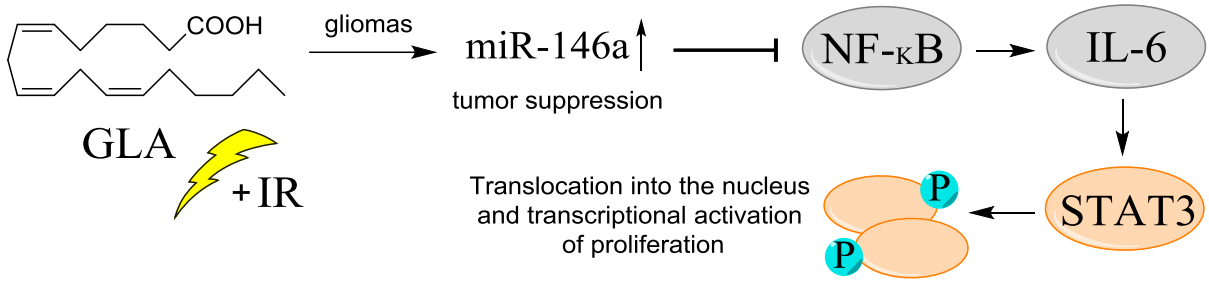

Figure 33. *The proposed mechanism of the treatment with gamma-linolenic acid (GLA) in combination with ionizing radiation (IR) leading to the overexpression of the miR-146 family, which targets NF-κB, important for recruiting the cytokines. Interleukin-6 (IL-6) is the crucial cytokine for activation of the JAK/STAT signaling. Dimerized and phosphorylated (P) STAT3 acts as an oncogenic transcription factor.*

Besides miRNA profiling, long RNA profiling was ensured by RNA-seq. The differences among various clinical subgroups of meningiomas were investigated. Also here we focused mainly on meningioma recurrence. Only three markers showed significant deregulation between recurrent and non-recurrent tumors and proved their prognostic features in adjusted Cox regression models of TTR. Those are ISLR2, lnc-GOLGA6A-1, and AMH. The expression of those three oncogenic transcripts mutually correlates among the whole RT-qPCR validation cohort ($p < 0.001$). Here, we have found a clear explanation for this phenomenon. ISLR2 and lnc-GOLGA6A-1 have a synergic oncogenic effect, and both may play important roles in neural and brain tumor development. It was observed in neuroblastomas that ALK mutation and MYCN amplification were both associated with elevated lnc-GOLGA61-1 and ISLR2 levels [110]. Mutual upregulation of both ISLR2 and lnc-GOLGA61-1 can be caused by the fact that those transcripts are mapped to the same locus and are both controlled by the regulatory sequence GH15J074130, according to the interaction analysis from GeneCards [111] and Ensembl [91] databases (Fig. 34). Additionally, ISLR2, lnc-GOLGA6A-1, and AMH are regulated by many common transcription factors including KLF4 (Fig. 34). Noteworthy, KLF4 was previously reported to carry activating mutations in meningiomas [3].

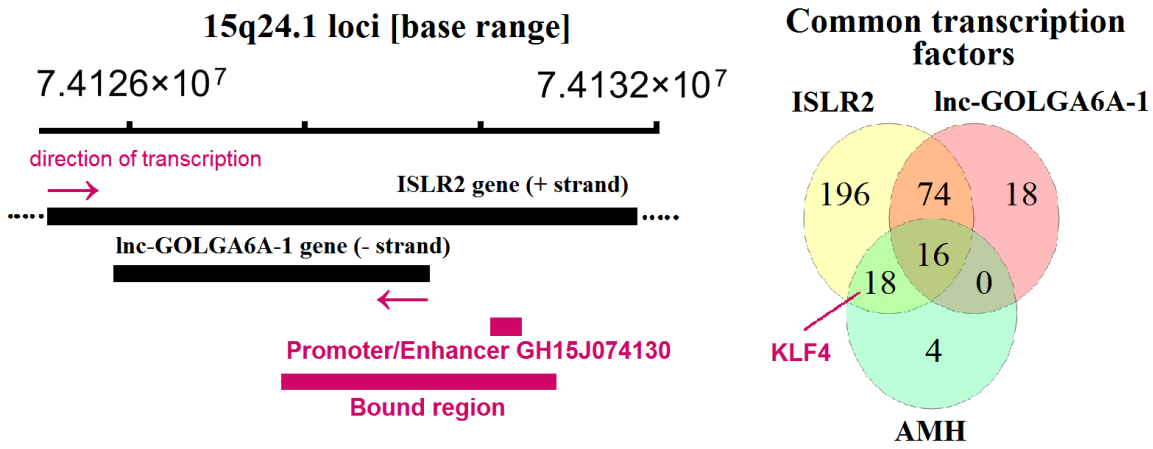

Figure 34. *Proposed explanation of transcriptional correlation and regulation of the expression of ISLR2, AMH, and lnc-GOLGA6A-1. ISLR2 and lnc-GOLGA6A-1 share the genomic loci and regulatory sequence GH15J074130. ISLR2, AMH, and lnc-GOLGA6A-1 expression are mostly regulated by the common transcription factors. KLF4, often mutated in meningiomas, also transcriptionally regulates ISLR2 and AMH expression.*

Despite the strong prognostic significance of those three transcripts, only lnc-GOLGA6A-1 was determined by the stepwise selection as the most significant factor for recurrence risk estimation in the multivariate Cox regression model of TTR. Although the exact function of this lncRNA is currently unknown, there is considerable evidence for its oncogenic properties in brain tumors. Besides bioinformatics investigation from the previously mentioned neuroblastoma study [110], lnc-GOLGA6A-1 promoter methylation was also associated with longer OS in patients with IDH1-wild-type glioblastomas [99]. In any case, it would be beneficial to determine the exact role of lnc-GOLGA6A-1 in brain tumors and utilize it in personalized medicine.

Probably because of partly degraded RNA within the FFPE samples, some of the transcripts were completely undetectable by RT-qPCR (HEPACAM2, TDRD1, and lnc-FAT1-3). Two transcripts often exhibited RT-qPCR negativity, thus the qualitative categorization to positivity and negativity of those RNAs was correlated with investigated clinical aspects. According to RNA-seq data, downregulated S100B within the prognostically unfavorable groups (males, recurrent patients, WHO grade II+III) showed only a lower proportion of RT-qPCR positive samples from males within the validation cohort. S100B serum level was previously associated with poor outcomes in patients after meningioma resection [112]. However, its expression is also affected by brain injury and a course of surgery [112], which may introduce bias when comparing results across different patient cohorts. On the other hand,

qualitative categorization showed lnc-MAST4-5 as significantly downregulated in the prognostically unfavorable groups (males, recurrent patients, WHO grade II+III). This potential prognostic biomarker with very low basal expression within both of our cohorts should be validated in the future using non-FFPE samples with higher RNA quality – either fresh-frozen tissue or samples that have undergone RNase inactivation.

Furthermore, the functional aspects of deregulated genes have been studied during Aim 2 of this thesis. Here we identified coding genes, and potentially related non-coding genes, involved in ATP and metal binding, general and neural development, Homeobox domain, Wnt signaling, angiogenesis, and immunoglobulin-like fold as crucial for meningioma development and aggressiveness. Similar molecular patterns were previously reported and especially the importance of Wnt signaling in meningioma is often mentioned [22] [26] [113]. Interestingly, the importance of Wnt signaling and angiogenesis was also reported in canine meningiomas [25]. Additionally, this is the first study to examine differences in expression profiles between meningiomas of different histogenetic origins. Here, we found out that especially developmental and homeobox-related genes are deregulated between mesodermal and neural crest meningiomas. Expression of homeobox-related genes, including the lncRNA HOXA-AS2, which was also deregulated between the mesoderm and neural crest within our data set, was associated with specific clinical outcomes in meningioma [113]. Moreover, hypermethylation of homeobox-related genes was observed in more aggressive and malignant meningiomas, but this phenomenon did not have efficient prognostic power [26].

As an example of the link between our miRNA and lncRNA data, the connection between CCAT2, prognostically unfavorable according to our RNA-seq data, and the prognostically favorable miRNAs according to Aim 1, was identified. CCAT2 is a known non-coding oncogenic transcript associated with a worse prognosis in many malignancies. It is crucial in carcinogenesis and influences the cell cycle as well as RNA biogenesis and degradation [114]. Most of its effects on signaling pathways are exerted via miRNAs. For example, it blocks the maturation and nuclear export of the tumor suppressor miR-145 [115]. Interestingly, miR-146a/b and miR-15a can be similarly inhibited and were identified as the tumor suppressors in meningioma. Thus, the regulation between CCAT2 and miR-146a-5p can be crucial in meningioma development and pathogenesis.

Additionally, we also conducted a detailed investigation of the lncRNA MEG3 in meningioma and found out that its isoforms and localization within the tumor cells change as a function of the risk of recurrence. MEG3 is expressed in arachnoid cells, which are likely to give rise to meningiomas. On the other hand, MEG3 is not expressed in most human

meningiomas, respectively human meningioma cell lines such as IOMM-Lee or CH157-MN. Functionally, MEG3 suppresses DNA synthesis and stimulates p53. Loss of MEG3 expression, as well as deletion of MEG3 gene copies, is more commonly observed in higher-grade meningiomas [116]. This is consistent with our observation that MEG3 gene expression was often difficult to detect in tumor cells. However, the overall expression of MEG3 is not significantly changed among defined clinically relevant patient subgroups according to our RNA-seq data. Nevertheless, the distribution of various isoforms is changed among studied subgroups. Most importantly, the MEG3-016 isoform was significantly up-regulated in recurrent tumors ($q < 0.001$). The human MEG3 gene contains ten exons, which can produce 27 splicing variants / isoforms [91]. Individual splicing variants differ in their ability to stimulate the p53 pathway. Tumor tissue expresses different isoforms than healthy tissue and has a different splicing mechanism [117]. Thus, it is in accordance with previous investigations, that resolution among individual MEG3 isoforms could be clinically beneficial. For instance, splicing variant analysis in breast cancer recently revealed 25 alternative exons, functionally related to EMT, which can serve as accurate biomarkers for the identification of aggressive behavior of triple-negative breast cancer [118].

In addition to splicing variant analysis, we performed a single-molecule resolution RISH for MEG3. LncRNAs are most often detected by RT-qPCR, but we used a single-molecule RNAscope method that is considered very accurate and specific [119]. The RT-qPCR method is not able to distinguish cell types, their individual populations in the tissue, and the location of the transcripts. Thanks to the RISH method, histological and morphological information can be combined with the localization and expression of lncRNA. According to Tripathi et al., understanding the localization and expression of lncRNA may be useful in developing more effective therapeutic approaches [120]. Because different lncRNAs can exhibit various cellular localization and clustering patterns [97], we hypothesized, that this feature can be potentially used in disease prognostication. This study showed that the size and the location of a signal from MEG3 transcripts are associated with meningioma recurrence. Univariate Cox regression models revealed that 10% share increase of nuclear MEG3 fraction in size category 1 – 15 px significantly shorten the TTR ($p = 0.003$). Also, 10% share increase of the signals in size category 1 – 15 px (single transcripts) is associated with shorter TTR ($p = 0.025$). Thus, the increased share of single transcripts and decreased share of MEG3 clusters of various size categories are associated with recurrence. According to our knowledge, this is the first study to examine the localization and cluster formation as the disease prognostic biomarker.

6. Conclusion

Meningiomas belong to common tumors of the central nervous system. A common issue in these cancers is their recurrence even in benign forms within 5 to 10 years, which cannot be accurately estimated. This suggests an existence of key regulators that affect their biological behavior independently on WHO grade. The presented thesis provides evidence that coding and non-coding RNAs might play such a regulatory role. Significant differential expression of mRNAs, miRNA, and lncRNAs was observed between recurrent and non-recurrent tumors of differing WHO grades. The most effective miRNA-based predictive model was selected including the miR-331-3p expression, the extent of tumor resection, and its localization as significant predictors of meningioma recurrence. These findings might lead to improvement of postoperative care by optimization of follow-up surveillance. Moreover, identification of the patients that might benefit from early irradiation and gamma-linolenic acid administration has been shown to result in upregulation of miR-146a-5p, the second most important factor for recurrence risk estimation identified in our study. However, this effect must be proven in meningiomas yet. The expression of the lnc-GOLGA61-1 was also found to be a more reliable predictor of meningioma recurrence than well-known predictors including WHO grades and the extent of tumor resection. Furthermore, transcripts encoding developmental and homeobox-related genes were differentially expressed in lesions with different proposed histogenesis, providing the first evidence of transcriptomic differences between meningiomas with different developmental origins. Further analysis of the biological processes associated with these differentially expressed transcripts may reveal pathways that could be targeted by innovative therapies. Additionally, important features of lncRNA MEG3 were identified to estimate the risk of recurrence. One of these is the splicing mechanism leading to the higher elevation of the MEG-016 isoform; however, this phenomenon has to be further validated using RT-qPCR. Also, a decreased pattern of cluster formation and nuclear localization of MEG3 transcripts are associated with a higher risk of recurrence. This is the first evidence of lncRNA localization pattern in disease prognostication.

7. List of abbreviations

3’UTR	Untranslated Region at the 3’ termini
ALK	Anaplastic Lymphoma receptor tyrosine Kinase
AMH	Anti-Mullerian Hormone
AMPK	AMP-activated, alpha 2 catalytic subunit, protein Kinase
ANRIL	Antisense Noncoding RNA in the INK4 Locus
AR / ER / PR	Androgen / Estrogen / Progesterone Receptors
ATP	Adenosine Triphosphate
BBB	Blood-Brain Barrier
CAF-1	Chromatin Assembly Factor 1
cAMP	cyclic Adenosine Monophosphate
CCAT2	Colon Cancer Associated Transcript 2
CCNB1	Cyclin B1 coding gene
CDC2	Cell Division Control protein 2
CDH1	Cadherin 1 coding gene
CDKN2A/B	Cyclin-Dependent Kinase inhibitor 2A or 2B
cDNA	complementary Deoxyribonucleic Acid
cheRNA	chromatin-enriched Ribonucleic Acid
circRNA	circularized Ribonucleic Acid
CNA	Copy Number Alteration
CPE	Carboxypeptidase E
CSC	Cancer Stem Cells
CSF	Cerebrospinal Fluid
Ct	Cycle-threshold
CT	Computed Tomography
Cy3	Cyanine 3 (tetramethylindo(di)-carbocyanines)
DAPI	4′,6-Diamidino-2-Phenylindole
DEPC	Diethylpyrocarbonate
DGCR8	DiGeorge syndrome Critical Region 8
DICER	Double-stranded RNA-specific Endoribonuclease

DLK1	Delta Like Non-Canonical Notch Ligand 1
DREAM complex	Dimerization partner, RB-like, E2F and Multi-vulval class B complex
ECEL1	Endothelin-Converting Enzyme-Like 1
EGFR	Epidermal Growth Factor Receptor
EMA	Epithelial Membrane Antigen
EMT	Epithelial-Mesenchymal Transition
EPHA3	Ephrin Type-A Receptor 3
eRNA	enhancer Ribonucleic Acid
EXP5	Exportin-5
FAM	Fluorescein Amidite
FFPE	Formalin-Fixed Paraffin-Embedded
FOXM1	Forkhead Box M1
GDA	Guanine Deaminase
GLA	Gamma-Linolenic Acid
GREM2	Gremlin 2 coding gene
HDL	High-Density Lipoprotein
HEPACAM2	HEPACAM family member 2
HIPK3	Homeodomain Interacting Protein Kinase 3
hnRNP A1	heterogeneous nuclear Ribonucleoprotein A1
HOTAIR	HOX (homeobox) antisense intergenic RNA
HOTAIRM1	HOX antisense intergenic RNA myeloid 1
HOTTIP	HOXA Transcript at the Distal Tip
HR	Hazard Ratio
HULC	Hepatocellular Carcinoma Up-regulated Long Non-Coding RNA
ICRs	Imprinted Control Regions
IDH1	Isocitrate Dehydrogenase (NADP(+)) 1
IF	Intensity of Fluorescence
IG-DMR	Intergenic Differentially Methylated Region
IGF2BP1	Insulin-like Growth Factor 2 Binding Protein 1 coding gene
IHC	Immunohistochemistry

IL-6	Interleukin 6
IMTM	Institute of Molecular and Translational Medicine
ISLR2	Immunoglobulin Superfamily containing Leucine Rich Repeat 2
JAK/STAT	Janus Kinases/Signal Transducer and activator of Transcription proteins
JARID2	Jumonji And AT-Rich Interaction Domain containing 2
KLF4	Kruppel Like Factor 4
LEPR	Leptin Receptor
lncRNA	long non-coding Ribonucleic Acid
MALAT1	Metastasis-Associated Lung Adenocarcinoma Transcript 1
mascRNAs	MALAT1‑associated small cytoplasmic Ribonucleic Acids
MDM2	Mouse Double Minute 2
MEG3	Maternally Expressed Gene 3
miRNA	micro Ribonucleic Acid
mRNA	messenger Ribonucleic Acid
MT1E	Metallothionein 1E
mTOR	mechanistic Target Of Rapamycin
MYCN	N-myc proto-oncogene
ND1000	NanoDrop 1000 spectrophotometer
NDRG2	N-Myc Downstream-Regulated Gene 2
NF2	Neurofibromatosis type 2
NF-κB	Nuclear Factor Kappa B
NGS	Next Generation Sequencing
NOS1	Nitric Oxide Synthase 1
NTM	Neurotrimin coding gene
OS	Overall Survival
PCNA	Proliferating Cell Nuclear Antigen
PDCD1	Programmed Cell Death 1 coding gene
PGDS	Prostaglandin D Synthase
PIK3CA	Phosphatidylinositol-4,5-bisphosphate 3-Kinase Catalytic subunit Alpha
piRNA	PIWI-interacting Ribonucleic Acid

PITX1	Pituitary homeobox 1
PRC1/2	Protein Regulator of Cytokinesis 1 or 2
PTEN	Phosphatase and Tensin homolog
PTTG1	Pituitary Tumor-Transforming Gene 1
QKI	Quaking alternative splicing factor
RASL10B	RAS-Like family 10-member B
Rb	Retinoblastoma protein
RECAMO	Research Centre for Applied Molecular Oncology
RFS	Recurrence-Free Survival
RIN	RNA Integrity Number
RISC	RNA-Induced Silencing Complex
RISH	RNA *In Situ* Hybridization
RNAi	RNA interference
RNA-seq	RNA/transcriptomic sequencing
RNPs	Ribonucleoproteins
ROI	Region Of Interest
rRNA	ribosomal RNA
RT-qPCR	Reverse Transcriptase quantitative Polymerase Chain Reaction
S100B	S100 calcium-binding protein B
scaRNA	Small Cajal body-specific RNA
SCN7A	Sodium voltage-gated Channel Alpha subunit 7
SFRP1	Secreted Frizzled Related Protein 1
SG	Simpson grade
SMARCE1	SWI/SNF-related Matrix-associated Actin-dependent Regulator of Chromatin subfamily E member 1
SMO	Smoothened, frizzled class receptor
sncRNAs	small non-coding RNAs
snRNA / snoRNA	small nuclear / small nucleolar RNAs
SSTR2A	Somatostatin Receptor type 2A
SUFU	Suppressor of Fused homolog
SWI/SNF	SWItch/Sucrose Non-Fermentable (chromatin remodeling complexes)

TDRD1	Tudor Domain containing 1 coding gene
TERC	Telomerase RNA Component
TERT	Telomerase Reverse Transcriptase
TF	Transferrin coding gene
TIMP3	Tissue Inhibitor of Metalloproteinase 3
TMA	Tissue Microarray
TNF-α	Tumor Necrosis Factor Alpha
TRAF7	Tumor necrosis factor Receptor-associated Factor 7
Tsix	XIST Antisense RNA
TTR	Time-to-recurrence
WHO	World Health Organization
Wnt	Wingless-type family members and signaling
WNT7B	Wnt family member 7B
XDH	Xanthine Dehydrogenase
Xist	X inactive specific transcript
XPNPEP2	X-Prolyl Aminopeptidase (Aminopeptidase P) 2
ZEB1/2	Zinc finger E-box Binding homeobox 1 or 2

8. Bibliography

Publications in peer-reviewed journals

H. Slavík, V. Balik, F. Zavadil Kokáš, R. Slavkovský, A. Řehulková, J. Vrbková, T. Lausová, J. Ehrman, S. Gurská, I. Überall, M. Hajdúch, J. Srovnal. Transcriptomic Profiling Revealed Lnc-GOLGA6A-1 as a Novel Prognostic Biomarker of Meningioma Recurrence. *Revisions from Neurosurgery*. **2021**, : - . *IF: 4.65* (Appendix 2)

N. Kudlová, **H. Slavík**, P. Dušková, T. Fürst, J. Srovnal, J. Bártek, M. Mistrík, M. Hajdúch. An efficient, non-invasive approach to in-vivo sampling of hair follicles: Design and applications in monitoring DNA damage and aging. *Accepted in Aging.* **2021.** : - . *IF: 5.68*

H. Slavík, V. Balik, J. Vrbková, A. Řehulková, M. Vaverka, L. Hrabálek, M. Vidlařová, S. Gurská, M. Hajdúch, J. Srovnal. Identification of Meningioma Patients at High Risk of Tumor Recurrence Using MicroRNA Profiling. *Neurosurgery*. **2020**, 87: 1055–1063. *IF: 4.85* (Appendix 1)

T. Oždian, D. Holub, Z. Macečková, L. Varanasi, G. Rylová, J. Řehulka, J. Václavková, **H. Slavík**, P. Moudrý, P. Znojek, J. Stanková, J. B. de Sanctis, M. Hajdúch, P. Džubák. Proteomic Profiling Reveals DNA Damage, Nucleolar and Ribosomal Stress Are the Main Responses to Oxaliplatin Treatment in Cancer Cells. *Journal of Proteomics*. **2017**, 162: 73-85. *IF: 3.54*

M. Ghothim, J. Srovnal, L. Bébarová, J. Tesaříková, P. Skalický, D. Klos, A. Prokopová, M. Vahalíková, **H. Slavík**, J. Vrbková, Č. Neoral, R. Havlík, M. Hajdúch, M. Loveček. Determination of CEA, EGFR and hTERT Expression in Peritoneal Lavage in Patients with Pancreatic Adenocarcinoma Using RT - PCR Method. *Rozhledy v chirurgii / Perspectives in Surgery*. **2015**, 94: 464-469. *Peer-reviewed Czech article* (Appendix 3)

Active participation in conferences with published abstracts

H. Slavík, A. Řehulková, F. Zavadil Kokáš, R. Slavkovský, V. Balik, J. Srovnal, H. Štefanová, B. Blumová, M. Hajdúch. Transcriptomic profiling in meningiomas for understanding of pathophysiology and biomarkers discovery. *XV. Diagnostic, Predictive and Experimental Oncology Days*. Olomouc (Czech Rep.), November 25-27 **2019**. ISBN 978-80-270-6977-4.

H. Slavik, A. Rehulkova, P. Stejskal, K. Staffova, J. Srovnal, M. Hajduch. Analysis of circulating biomarker stability in different blood preservation tubes. *4th ACTC*. Corfu (Greece), October 2-5 **2019**.

H. Slavík, V. Balik, J. Srovnal, T. Lausová, J. Vrbková, A. Řehulková, S. Gurská, M. Hajdúch. Predikce rekurence meningeomů za využití miRNA profilování. *10. pražské mezioborové onkologické kolokvium: Prague Onco Journal*. Prague (Czech Rep.), January 23-25 **2019**. ISBN 978-80-87339-36-7.

H. Slavík, P. Dušková, M. Mistrík, T. Furst, J. Srovnal, M. Hajdúch. Utilization of murine hair follicles for biomarker studies in ionizing radiation response model. *XIV. Diagnostic, Predictive and Experimental Oncology Days*. Olomouc (Czech Rep.), November 19-21 **2018**. ISBN 978-80-270-5084-0.

H. Slavík, M. Mistrík, P. Dušková, T. Fürst, J. Srovnal, M. Hajdúch. Hair follicles as a minimally invasive resource of epithelial cells in mouse studies of ionizing radiation. *AACR annual meeting 2018.* Chicago (IL; USA), April 14-18 **2018**. ISSN 0197-016X.

H. Slavík, J. Srovnal, T. Lausová, J. Vrbková, V. Balik, M. Hajdúch. MiRNA profilování u meningeomů. *9. pražské mezioborové onkologické kolokvium: Prague Onco Journal*. Prague (Czech Rep.), January 24- 26 **2018**. ISBN 978-80-87339-36-7.

H. Slavík, J. Srovnal, T. Lausová, J. Vrbková, V. Balik, M. Hajdúch. MiRNA profiling in recurrent and non-recurrent meningeomas. *XIII. Diagnostic, Predictive and Experimental Oncology Days*. Olomouc (Czech Rep.), November 28-30 **2017**. ISBN 978-80-270-2795-8.

H. Slavík, J. Srovnal, T. Lausová, J. Vrbková, V. Balik, M. Hajdúch. MiRNA profiling in meningeomas. *XXII. Biologické dni*. Smolenice (Slovakia), October 23-25 **2017**. ISBN 978-80-270-2809-2

H. Slavík, P. Švarcová, P. Dušková, E. Veselá, M. Mistrík, J. Srovnal, J. Drábek, M. Hajdúch. Detekce biomarkerů ionizujícího záření v myších chlupových folikulech. *8. pražské mezioborové onkologické kolokvium: Prague Onco Journal*. Prague (Czech Rep.), January 25-27 **2017**. ISBN 978-80-87339-26-8.

H. Slavík, P. Švarcová, P. Dušková, E. Veselá, M. Mistrík, J. Srovnal, J. Drábek, M. Hajdúch. Detection of ionizing radiation biomarkers in mouse hair follicles. *XII. Diagnostic, Predictive and Experimental Oncology Days*. Olomouc (Czech Rep.), November 30 - December 1 **2016**. ISBN 978-80-270-0464-5.

H. Slavík, P. Dušková, P. Švarcová, J. Drábek, M. Mistrík, J. Srovnal. Utilization of RNA from hair follicles in forensic science. *The 5th International Conference on Forensic Genetics: Forensica 2016 – Conference Proceedings*. Olomouc (Czech Rep.), May 23-25 **2016**. ISBN 978-80-263-1045-7.

H. Slavík, P. Vojta, J. Volejníková, J. Srovnal, M. Špenerová, V. Mihál, P. Džubák, M. Hajdúch. Vliv léčby prednisolonem na transkriptomové profily u dětí s akutní lymfoblastickou leukémií. XL. *Brněnské onkologické dny a XXX. Konference pro nelékařské zdravotnické pracovníky: Klinická onkologie*. Brno (Czech Rep.), April 27- 29 **2016**. ISSN 1802-5307.

H. Slavík, P. Vojta, J. Volejníková. Vliv léčby prednisonem na transkriptomovou mapu u dětí s akutní lymfoblastickou leukémií. *7. pražské mezioborové onkologické kolokvium: Prague Onco Journal*. Prague (Czech Rep.), January 25-27 **2016**. ISSN 1804-2252.

H. Slavík, J. Srovnal, Z. Bačová, R. Slavkovský. Possibilities of detection of miRNAs in the samples of exhaled breath condensates. *XI. Diagnostic, Predictive and Experimental Oncology Days*. Olomouc (Czech Rep.), December 2-3 **2015**. ISBN 978-80-260-8368-9.

H. Slavík, P. Dušková, L. Ewerlingová, K. Burdová, J. Drábek, M. Mistrík. Vliv rentgenového záření na genovou expresi v lidských chlupových folikulech. *X. Diagnostic, Predictive and Experimantal Oncology Days*. Olomouc (Czech Rep.), December 2-3 **2014**.

9. References

1. Prayson R (2009) Meningiomas. In: Pathology of meningiomas, 1 ed.. Springer, London, pp. 31-43

2. Ohnishi Y, Iwatsuki K, Morii E, Kobayashi M, Hori Y, Moriwaki T, Ishihara M, Yoshimura K, Umegaki M, Yoshimine T (2011) Histopathological study of spinal meningioma originating from the arachnoid villi. Brain Tumor Pathology 28:77-81. doi: 10.1007/s10014-010-0003-3

3. Suppiah S, Nassiri F, Bi W, Dunn I, Hanemann C, Horbinski C, Hashizume R, James C, Mawrin C, Noushmehr H, Perry A, Sahm F, Sloan A, Wen P, Aldape K, Zadeh G (2019) Molecular and translational advances in meningiomas. Neuro-oncology 21:4-17. doi: 10.1093/neuonc/noy178

4. Shivapathasundram G, Wickremesekera A, Tan S, Itinteang T (2018) Tumour stem cells in meningioma: A review. Journal of Clinical Neuroscience 47:66-71. doi: 10.1016/j.jocn.2017.10.059

5. JOHN J. K (1986) Presidential Address: The Histopathology of Meningiomas. A Reflection of Origins and Expected Behavior?. Journal of Neuropathology and Experimental Neurology 45:95-96

6. Kalamarides M, Stemmer-rachamimov A, Niwa-kawakita M, Chareyre F, Taranchon E, Han Z, Martinelli C, Lusis E, Hegedus B, Gutmann D, Giovannini M (2011) Identification of a progenitor cell of origin capable of generating diverse meningioma histological subtypes. Oncogene 30:2333-2344. doi: 10.1038/onc.2010.609

7. Dasgupta K, Jeong J (2019) Developmental biology of the meninges. Genesis 57:1-12. doi: 10.1002/dvg.23288

8. Schulten H, Hussein D (2019) Array expression meta-analysis of cancer stem cell genes identifies upregulation of PODXL especially in DCC low expression meningiomas. PloS one 14:1-20. doi: 10.1371/journal.pone.0215452

9. Goldbrunner R, Minniti G, Preusser M, Jenkinson M, Sallabanda K, Houdart E, von Deimling A, Stavrinou P, Lefranc F, Lund-johansen M, Moyal E, Brandsma D, Henriksson R, Soffietti R, Weller M (2016) EANO guidelines for the diagnosis and treatment of meningiomas. The Lancet Oncology 17:383-391. doi: 10.1016/S1470-2045(16)30321-7

10. Louis D, Perry A, Reifenberger G, Figarella-branger D, Cavenee W, Ohgaki H, Wiestler O, Kleihues P, Ellison D (2016) The 2016 World Health Organization Classification of Tumors of the Central Nervous System: a summary. Acta neuropathologica 131:803-820. doi: 10.1007/s00401-016-1545-1

11. Rogers L, Barani I, Chamberlain M, Kaley T, Mcdermott M, Raizer J, Schiff D, Weber D, Wen P, Vogelbaum M (2015) Meningiomas: knowledge base, treatment outcomes, and uncertainties. A RANO review. Journal of Neurosurgery 122:4-23. doi: 10.3171/2014.7.jns131644

12. Bi W, Abedalthagafi M, Horowitz P, Agarwalla P, Mei Y, Aizer A, Brewster R, Dunn G, Al-mefty O, Alexander B, Santagata S, Beroukhim R, Dunn I (2016) Genomic landscape of intracranial meningiomas. Journal of Neurosurgery 125:525-535. doi: 10.3171/2015.6.JNS15591

13. Brastianos P, Galanis E, Butowski N, Chan J, Dunn I, Goldbrunner R, Herold-mende C, Ippen F, Mawrin C, Mcdermott M, Sloan A, Snyder J, Tabatabai G, Tatagiba M, Tonn J, Wen P, Aldape K, Nassiri F, Zadeh G, Jenkinson M, Raleigh D (2019) Advances in multidisciplinary therapy for meningiomas. Neuro-oncology 21:18-31. doi: 10.1093/neuonc/noy136

14. Simpson D (1957) The recurrence of intracranial meningiomas after surgical treatment. J Neurol Neurosurg Psychiatry 20:22-39. doi: 10.1136/jnnp.20.1.22

15. Fathi A, Roelcke U (2013) Meningioma. CURRENT NEUROLOGY AND NEUROSCIENCE REPORTS 13:1-8. doi: 10.1007/s11910-013-0337-4

16. Maclean J, Fersht N, Short S (2014) Controversies in Radiotherapy for Meningioma. Clinical Oncology 26:51-64. doi: 10.1016/j.clon.2013.10.001

17. BARNHOLTZ-SLOAN J, KRUCHKO C (2007) Meningiomas: causes and risk factors. Neurosurg Focus 23:1-8. doi: https://doi.org/10.3171/FOC-07/10/E2

18. Zhang B, Martinez-lage M, Xiang C, Tosi U, Gungor B, Zhu Y, Roccograndi L, Zhang L, Dahmane N (2019) Transcriptome signatures associated with meningioma progression. Acta Neuropathologica Communications 7:1-13. doi: 10.1186/s40478-019-0690-x

19. James M, Han S, Polizzano C, Gusella J, Ramesh V, Plotkin S, Stemmer-rachamimov A, Manning B (2009) NF2/merlin is a novel negative regulator of mTOR complex 1, and activation of mTORC1 is associated with meningioma and schwannoma growth. Molecular and Cellular Biology 29:4250 - 4261. doi: 10.1128/MCB.01581-08

20. Pereira B, Oba-shinjo S, de Almeida A, Marie S (2019) Molecular alterations in meningiomas: Literature review. Clinical Neurology and Neurosurgery 176:89-96. doi: 10.1016/j.clineuro.2018.12.004

21. Coy S, Rashid R, Stemmer-rachamimov A, Santagata S (2020) An update on the CNS manifestations of neurofibromatosis type 2. Acta Neuropathologica 139:643-665. doi: 10.1007/s00401-019-02029-5

22. Vasudevan H, Braunstein S, Phillips J, Pekmezci M, Tomlin B, Wu A, Reis G, Magill S, Zhang J, Feng F, Nicholaides T, Chang S, Sneed P, Mcdermott M, Berger M, Perry A, Raleigh D (2018) Comprehensive Molecular Profiling Identifies FOXM1 as a Key

Transcription Factor for Meningioma Proliferation. Cell Reports 22:3672-3683. doi: 10.1016/j.celrep.2018.03.013

23. Li T, Ren J, Ma J, Wu J, Zhang R, Yuan H, Han X (2019) LINC00702/miR-4652-3p/ZEB1 axis promotes the progression of malignant meningioma through activating Wnt/β-catenin pathway. Biomedicine 113:108718-108718. doi: 10.1016/j.biopha.2019.108718

24. Zhang Y, Yu R, Li Q, Li Y, Xuan T, Cao S, Zheng J (2020) SNHG1/miR-556-5p/TCF12 feedback loop enhances the tumorigenesis of meningioma through Wnt signaling pathway. Journal of Cellular Biochemistry 121:1880 - 1889. doi: 10.1002/jcb.29423

25. Grenier J, Foureman P, Sloma E, Miller A (2017) RNA-seq transcriptome analysis of formalin fixed, paraffin-embedded canine meningioma. PloS one 12:e0187150. doi: 10.1371/journal.pone.0187150

26. Olar A, Wani K, Wilson C, Zadeh G, Demonte F, Jones D, Pfister S, Sulman E, Aldape K (2017) Global epigenetic profiling identifies methylation subgroups associated with recurrence-free survival in meningioma. Acta Neuropathologica: Pathology and Mechanisms of Neurological Disease 133:431-444. doi: 10.1007/s00401-017-1678-x

27. Papaioannou M, Djuric U, Kao J, Karimi S, Zadeh G, Aldape K, Diamandis P (2019) Proteomic analysis of meningiomas reveals clinically-distinct molecular patterns. Neuro-oncology 21:1028–1038. doi: 10.1093/neuonc/noz084

28. Dennis L, Mcguire V, Drangsholt M, Koepsell T (1993) Epidemiology of intracranial meningioma. Cancer 72:639-48. doi: 10.1002/1097-0142(19930801)72:3639::aid-cncr28207203043.0.co;2-p

29. Harter P, Braun Y, Plate K (2017) Classification of meningiomas-advances and controversies. Chinese clinical oncology 6:S2. doi: 10.21037/cco.2017.05.02

30. Boulagnon-rombi C, Fleury C, Fichel C, Bressenot A, Lefour S, Gauchotte G (2017) Immunohistochemical approach to the differential diagnosis of meningiomas and their mimics. Journal of Neuropathology and Experimental Neurology 76:289 - 298. doi: 10.1093/jnen/nlx008

31. Liu N, Song S, Jiang J, Wang T, Yan C (2020) The prognostic role of Ki-67/MIB-1 in meningioma A systematic review with meta-analysis. MEDICINE 99:e18644. doi: 10.1097/MD.0000000000018644

32. Corniola M, Lemée J, Meling T (2020) Histological transformation in recurrent WHO grade I meningiomas. Scientific Reports 10:1-7. doi: 10.1038/s41598-020-68177-x

33. Bi W, Greenwald N, Mei Y, Al-mefty O, Dunn I, Wala J, Gibson W, Agarwalla P, Schumacher S, Beroukhim R, Chevalier A, Abedalthagafi M, Santagata S, Horowitz P, Esaulova E, Artyomov M, Dunn G, Ducar M, Thorner A, Van Hummelen P, Stemmer-rachamimov A (2017) Genomic landscape of high-grade meningiomas. npj Genomic Medicine 2:525-535. doi: 10.1038/s41525-017-0014-7

34. Splavski B, Hadzic E, Bagic I, Vrtaric V, Splavski J (2017) Simple Tumor Localization Scale for Estimating Management Outcome of Intracranial Meningioma. World Neurosurgery 104:876-882. doi: 10.1016/j.wneu.2017.05.039

35. (2002) Brain Science Foundation. https://www.brainsciencefoundation.org/brain-tumor-resources/meningioma/locations/. 2021-01-28

36. Anil N, Prasad V (2008) Recurrence and Outcome in Skull Base Meningiomas: Do They Differ from Other Intracranial Meningiomas?. Skull Base: An Interdisciplinary Approach 18:243-244

37. Voß K, Spille D, Sauerland C, Suero Molina E, Brokinkel C, Paulus W, Stummer W, Holling M, Jeibmann A, Brokinkel B (2017) The Simpson grading in meningioma surgery: does the tumor location influence the prognostic value?. Journal of Neuro-Oncology 133:641-651. doi: 10.1007/s11060-017-2481-1

38. Maguire L, Thomas A, Goldstein A (2015) Tumors of the Neural Crest: Common Themes in Development and Cancer. DEVELOPMENTAL DYNAMICS 244:311-322. doi: 10.1002/dvdy.24226

39. Jiang X, Iseki S, Maxson R, Sucov H, Morriss-kay G (2002) Tissue origins and interactions in the mammalian skull vault. Developmental biology 241:106-16. doi: 10.1006/dbio.2001.0487

40. Balik V (2019) Histological Structure of the Major Dural Sinus Walls in the Posterior Cranial Fossa: A Factor that Might Matter in Dural Sinus Surgery. World neurosurgery 128:431-432. doi: 10.1016/j.wneu.2019.05.158

41. Mendez-maldonado K, Vega-lopez G, Aybar M, Velasco I (2020) Neurogenesis From Neural Crest Cells: Molecular Mechanisms in the Formation of Cranial Nerves and Ganglia. FRONTIERS IN CELL AND DEVELOPMENTAL BIOLOGY 8:1-26. doi: 10.3389/fcell.2020.00635

42. Ostrom Q, Gittleman H, Liao P, Rouse C, Chen Y, Dowling J, Wolinsky Y, Kruchko C, Barnholtz-sloan J (2014) CBTRUS statistical report: primary brain and central nervous system tumors diagnosed in the United States in 2007-2011. Neuro-oncology 16:iv1-63. doi: 10.1093/neuonc/nou223

43. Clark V, Erson-omay E, Caglayan A, Sencar L, Serin A, Ceyhun E, Atik A, Bayri Y, Bai H, Kolb L, Hebert R, Omay S, Yilmaz S, Mishra-gorur K, Choi M, Overton J, Yin J, Holland E, Mane S, State M (2013) Genomic Analysis of Non-NF2 Meningiomas Reveals Mutations in TRAF7, KLF4, AKT1, and SMO. Science 339:1077-1080. doi: 10.1126/science.1233009

44. Portet S, Banor T, Bousquet J, Simonneau A, Flores M, Ingrand P, Milin S, Karayan-tapon L, Bataille B (2020) New Insights into Expression of Hormonal Receptors by Meningiomas. World Neurosurgery 140:e87. doi: 10.1016/j.wneu.2020.04.168

45. Sahm F, Schrimpf D, Stichel D, Dtw J, Hielscher T, Schefzyk S, Okonechnikov K, Koelsche C, Reuss D, Capper D, Sturm D, Wirsching H, Berghoff A, Baumgarten P, Kratz A, Huang K, Wefers A, Hovestadt V, Sill M, Ellis H, Kurian K, Okuducu A, Jungk C, Drueschler K, Schick M, Bewerunge-hudler M, Mawrin C, Seiz-rosenhagen M, Ketter R, Simon M, Westphal M, Lamszus K, Becker A, Koch A, Schittenhelm J, Rushing E, Collins V, Brehmer S, Chavez L, Platten M, Hänggi D, Unterberg A, Paulus W, Wick W, Pfister S, Mittelbronn M, Preusser M, Herold-mende C, Weller M (2017) DNA methylation-based classification and grading system for meningioma: a multicentre, retrospective analysis. The Lancet. Oncology 18:682-694. doi: 10.1016/S1470-2045(17)30155-9

46. Yuzawa S, Mohri H, Tsuda M, Tanaka S, Nishihara H, Wang L, Kimura T, Terasaka S, Houkin K, Sato N, Yamaguchi S, Tanino M, Kobayashi H (2016) Clinical impact of targeted amplicon sequencing for meningioma as a practical clinical-sequencing system. Modern Pathology 29:708 - 716. doi: 10.1038/modpathol.2016.81

47. Smith M, Wallace A, Bennett C, Hasselblatt M, Elert-dobkowska E, Evans L, Hickey W, Bauer D, Lee A, Hevner R, Beetz C, Kilday J, Newman W, Evans D (2014) Germline SMARCE1 mutations predispose to both spinal and cranial clear cell meningiomas. The Journal of pathology 234:436-40. doi: 10.1002/path.4427

48. Zhi F, Li B, Xue L, Deng D, Xu Y, Yang Y, Shao N, Peng Y, Lan Q (2016) A serum 6-miRNA panel as a novel non-invasive biomarker for meningioma. Scientific Reports 6:1-10. doi: 10.1038/srep32067

49. Korhonen K, Salminen T, Raitanen J, Auvinen A, Isola J, Haapasalo H (2006) Female predominance in meningiomas can not be explained by differences in progesterone, estrogen, or androgen receptor expression. Journal of neuro-oncology 80:1-7. doi: 10.1007/s11060-006-9146-9

50. Apra C, Roblot P, Alkhayri A, Le Guérinel C, Polivka M, Chauvet D (2020) Female gender and exogenous progesterone exposition as risk factors for spheno-orbital meningiomas. Journal of Neuro-Oncology 149:95-101. doi: 10.1007/s11060-020-03576-8

51. Peyre M, Gaillard S, de Marcellus C, Giry M, Bielle F, Villa C, Boch A, Loiseau H, Baussart B, Cazabat L, Raffin-sanson M, Sanson M, Kalamarides M (2018) Progestin-associated shift of meningioma mutational landscape. ANNALS OF ONCOLOGY 29:681-686. doi: 10.1093/annonc/mdx763

52. Shen L, Lin D, Cheng L, Tu S, Wu H, Xu W, Pan Y, Wang X, Zhang J, Shao A (2020) Is DNA Methylation a Ray of Sunshine in Predicting Meningioma Prognosis?. FRONTIERS IN ONCOLOGY 10:1-13. doi: 10.3389/fonc.2020.01323

53. Johnson N, Conneely K (2019) The role of DNA methylation and hydroxymethylation in immunosenescence. Ageing Research Reviews 51:11-23. doi: 10.1016/j.arr.2019.01.011

54. Loewenstern J, Rutland J, Gill C, Pain M, Bederson J, Shrivastava R, Arib H, Sebra R, Umphlett M, Kinoshita Y, Mcbride R, Donovan M, Fowkes M (2019) Comparative

genomic analysis of driver mutations in matched primary and recurrent meningiomas. Oncotarget 10:3506 - 3517

55. Schmidt M, Mock A, Jungk C, Ull A, Ketter R, Roesch S, Rapp C, Unterberg A, Herold-mende C, Sahm F, Schefzyk S, Urbschat S, Reuss D, Von Deimling A, Warta R, Westphal M, Lamszus K, Simon M, Gousias K, Lahrmann B, Grabe N, Kessler A, Löhr M, Senft C, Beckhove P (2016) Transcriptomic analysis of aggressive meningiomas identifies PTTG1 and LEPR as prognostic biomarkers independent of WHO grade. Oncotarget 7:14551 - 14568. doi: 10.18632/oncotarget.7396

56. Chen W, Vasudevan H, Choudhury A, Pekmezci M, Lucas C, Phillips J, Magill S, Susko M, Braunstein S, Bush N, Boreta L, Nakamura J, Villanueva-meyer J, Sneed P, Perry A, Mcdermott M, Solomon D, Theodosopoulos P, Raleigh D (2021) A Prognostic Gene-Expression Signature and Risk Score for Meningioma Recurrence After Resection. Neurosurgery 88:202-210. doi: 10.1093/neuros/nyaa355

57. Patel A, Oneissi M, Jalali A, Magnotti J, Sebastian S, Gopinath S, Yoshor D, Wan Y, Al-ouran R, Revelli J, Liu Z, Zoghbi H, Klisch T, Plon S, Cardenas M, Xi L, Muzny D, Doddapaneni H, Wheeler D, Heck K, Clay Goodman J, Rao G (2019) Molecular profiling predicts meningioma recurrence and reveals loss of DREAM complex repression in aggressive tumors. PNAS 116:21715 - 21726. doi: 10.1073/pnas.1912858116

58. Quinn J, Chang H (2016) Unique features of long non-coding RNA biogenesis and function. Nature reviews. Genetics 17:47-62. doi: 10.1038/nrg.2015.10

59. Cech T, Steitz J (2014) The Noncoding RNA Revolution—Trashing Old Rules to Forge New Ones. Cell 157:77-94. doi: 10.1016/j.cell.2014.03.008

60. Alles J, Fehlmann T, Fischer U, Backes C, Galata V, Minet M, Hart M, Abu-halima M, Grässer F, Lenhof H, Keller A, Meese E (2019) An estimate of the total number of true human miRNAs. Nucleic acids research 47:3353-3364. doi: 10.1093/nar/gkz097

61. Slabý O, Svoboda M (2012) MikroRNA v onkologii / Ondřej Slabý, Marek Svoboda et al. [pořadatelé], 1.. Galén, Praha

62. Ha M, Kim V (2014) Regulation of microRNA biogenesis. Nature Reviews Molecular Cell Biology 15:509-524. doi: 10.1038/nrm3838

63. Jonas S, Izaurralde E (2015) Towards a molecular understanding of microRNA-mediated gene silencing. Nature reviews. Genetics 16:421-33. doi: 10.1038/nrg3965

64. Kosaka N, Iguchi H, Ochiya T (2010) Circulating microRNA in body fluid: a new potential biomarker for cancer diagnosis and prognosis. Cancer Science 101:2087-2088. doi: 10.1111/j.1349-7006.2010.01650.x

65. Courts C, Madea B (2010) Micro-RNA – A potential for forensic science?. Forensic Science International 203:106-111. doi: 10.1016/j.forsciint.2010.07.002

66. Wu K, Li L, Li S (2015) Circulating microRNA-21 as a biomarker for the detection of various carcinomas: an updated meta-analysis based on 36 studies. Tumor Biology: Tumor Markers, Tumor Targeting and Translational Cancer Research 36:1973-1981. doi: 10.1007/s13277-014-2803-2

67. Sohel M (2020) Circulating microRNAs as biomarkers in cancer diagnosis. Life Sciences 248:117473. doi: 10.1016/j.lfs.2020.117473

68. Garofalo M, Calore F, Lovat F (2013) Non-Coding RNAs and Cancer. International Journal of Molecular Sciences 14:17085-17110. doi: 10.3390/ijms140817085

69. Kong Y, Ferland-mccollough D, Jackson T, Bushell M (2012) microRNAs in cancer management. Lancet Oncology 13:e249. doi: 10.1016/S1470-2045(12)70073-6

70. Titze-de-almeida R, David C, Titze-de-almeida S (2017) The Race of 10 Synthetic RNAi-Based Drugs to the Pharmaceutical Market. Pharmaceutical Research: An Official Journal of the American Association of Pharmaceutical Scientists 34:1339-1363. doi: 10.1007/s11095-017-2134-2

71. Zhang L, Liao Y, Tang L (2019) MicroRNA-34 family: a potential tumor suppressor and therapeutic candidate in cancer. Journal of Experimental & Clinical Cancer Research 38:1-13. doi: 10.1186/s13046-019-1059-5

72. (2019) MicroRNA based theranostics for brain cancer: basic principles. Journal of Experimental & Clinical Cancer Research 38:1-21. doi: 10.1186/s13046-019-1180-5

73. Kopkova A, Sana J, Machackova T, Vecera M, Radova L, Trachtova K, Slaby O, Vybihal V, Smrcka M, Fadrus P, Kazda T (2019) Cerebrospinal fluid microRNA signatures as diagnostic biomarkers in brain tumors. Cancers 11:1546. doi: 10.3390/cancers11101546

74. Wang L, Chen S, Liu Y, Zhang H, Ren N, Ma R, He Z (2020) The biological and diagnostic roles of MicroRNAs in meningiomas. Reviews in the Neurosciences 31:771-778. doi: 10.1515/revneuro-2020-0023

75. Zhi F, Zhou G, Wang S, Shi Y, Peng Y, Shao N, Guan W, Qu H, Zhang Y, Wang Q, Yang C, Wang R, Wu S, Xia X, Yang Y (2013) A microRNA expression signature predicts meningioma recurrence. International journal of cancer 132:128-36. doi: 10.1002/ijc.27658

76. Volders P, Anckaert J, Verheggen K, Nuytens J, Martens L, Mestdagh P, Vandesompele J (2019) LNCipedia 5: towards a reference set of human long non-coding RNAs. Nucleic acids research 47:D135-D139. doi: 10.1093/nar/gky1031

77. Chen Y, Belmont A (2019) Genome organization around nuclear speckles. Current Opinion in Genetics 55:91-99. doi: 10.1016/j.gde.2019.06.008

78. Rao A, Rajkumar T, Mani S (2017) Perspectives of long non-coding RNAs in cancer. Molecular Biology Reports: An International Journal on Molecular and Cellular Biology 44:203-218. doi: 10.1007/s11033-017-4103-6

79. Zhang H, Jiang L, Sun D, Hou J, Ji Z (2018) CircRNA: a novel type of biomarker for cancer. Breast cancer 25:1-7. doi: 10.1007/s12282-017-0793-9

80. Li Y, Qin L, Guo Z, Liu L, Xu H, Hao P, Su J, Shi Y, He W, Li Y (2006) In silico discovery of human natural antisense transcripts. BMC bioinformatics 7:1-8. doi: 10.1186/1471-2105-7-18

81. Hu W, Alvarez-dominguez J, Lodish H (2012) Regulation of mammalian cell differentiation by long non-coding RNAs. EMBO reports 13:971-83. doi: 10.1038/embor.2012.145

82. Beltran M, Puig I, Álvarez A, Peña R, De Herreros A, Peña C, García J, Bonilla F (2008) A natural antisense transcript regulates Zeb2/Sip1 gene expression during Snail1-induced epithelial-mesenchymal transition. Genes and Development 22:756 - 769. doi: 10.1101/gad.455708

83. Gayen S, Kalantry S (2017) Chromatin-enriched lncRNAs: a novel class of enhancer RNAs. Nature structural 24:556-557. doi: 10.1038/nsmb.3430

84. Sun X, Wang Z, Hall J, Perez-cervantes C, Ruthenburg A, Moskowitz I, Gribskov M, Yang X (2020) Chromatin-enriched RNAs mark active and repressive cis-regulation: An analysis of nuclear RNA-seq. PLoS computational biology 16:e1007119. doi: 10.1371/journal.pcbi.1007119

85. Ghafouri-fard S, Esmaeili M, Taheri M, Samsami M (2020) Highly upregulated in liver cancer (HULC): An update on its role in carcinogenesis. JOURNAL OF CELLULAR PHYSIOLOGY 235:9071-9079. doi: 10.1002/jcp.29765

86. Tang Q, Hann S (2018) HOTAIR: An Oncogenic Long Non-Coding RNA in Human Cancer. Cellular physiology and biochemistry: international journal of experimental cellular physiology, biochemistry, and pharmacology 47:893-913. doi: 10.1159/000490131

87. Mozdarani H, Ezzatizadeh V (2020) The emerging role of the long non-coding RNA HOTAIR in breast cancer development and treatment. Journal of Translational Medicine 18:1-15. doi: 10.1186/s12967-020-02320-0

88. Latowska J, Grabowska A, Zarebska Z, Kuczynski K, Kuczynska B, Rolle K (2020) Non-Coding RNAs in Brain Tumors, the Contribution of lncRNAs, circRNAs, and snoRNAs to Cancer Development-Their Diagnostic and Therapeutic Potential. INTERNATIONAL JOURNAL OF MOLECULAR SCIENCES 21:7001. doi: 10.3390/ijms21197001

89. Xing H, Wang S, Li Q, Ma Y, Sun P (2018) Long noncoding RNA LINC00460 targets miR-539/MMP-9 to promote meningioma progression and metastasis. Biomedicine 105:677-682. doi: 10.1016/j.biopha.2018.06.005

90. Balik V, Srovnal J, Sulla I, Kalita O, Foltanova T, Vaverka M, Hrabalek L, Hajduch M (2013) MEG3: a novel long noncoding potentially tumour-suppressing RNA in meningiomas. Journal of neuro-oncology 112:1-8. doi: 10.1007/s11060-012-1038-6

91. Cunningham F, Achuthan P, Akanni W, Allen J, Amode M, Armean I, Bennett R, Bhai J, Billis K, Boddu S, Cummins C, Davidson C, Dodiya K, Gall A, Girón C, Gil L, Grego T, Haggerty L, Haskell E, Hourlier T, Izuogu O, Janacek S, Juettemann T, Kay M, Laird M, Lavidas I, Liu Z, Loveland J, Marugán J, Maurel T, Mcmahon A, Moore B, Morales J, Mudge J, Nuhn M, Ogeh D, Parker A, Parton A, Patricio M, Schmitt B, Schuilenburg H, Sheppard D, Sparrow H, Stapleton E, Szuba M, Taylor K, Threadgold G, Thormann A, Vullo A, Walts B, Winterbottom A, Zadissa A, Chakiachvili M, Frankish A, Hunt S, Kostadima M, Langridge N, Martin F, Muffato M, Perry E, Ruffier M, Staines D, Trevanion S, Aken B, Yates A, Zerbino D, Flicek P (2019) Ensembl 2019. Nucleic acids research 47:D745-D751. doi: 10.1093/nar/gky1113

92. Benetatos L, Dasoula A, Hatzimichael E, Georgiou I, Syrrou M, Bourantas K (2008) Promoter Hypermethylation of the MEG3 (DLK1/MEG3) Imprinted Gene in Multiple Myeloma. Clinical Lymphoma 8:171-175. doi: 10.3816/CLM.2008.n.021

93. Al-rugeebah A, Alanazi M, Parine N (2019) MEG3: an Oncogenic Long Non-coding RNA in Different Cancers. Pathology oncology research: POR 25:859-874. doi: 10.1007/s12253-019-00614-3

94. Gejman R, Batista D, Zhong Y, Zhou Y, Zhang X, Swearingen B, Stratakis C, Hedley-whyte E, Klibanski A (2008) Selective Loss of MEG3 Expression and Intergenic Differentially Methylated Region Hypermethylation in the MEG3/DLK1 Locus in Human Clinically Nonfunctioning Pituitary Adenomas. The Journal of Clinical Endocrinology 93:4119-4120

95. Galani V, Lampri E, Varouktsi A, Alexiou G, Mitselou A, Kyritsis A (2017) Genetic and epigenetic alterations in meningiomas. Clinical Neurology and Neurosurgery 158:119-125. doi: 10.1016/j.clineuro.2017.05.002

96. Ghafouri-fard S, Taheri M (2019) Maternally expressed gene 3 (MEG3): A tumor suppressor long non coding RNA. Biomedicine 118:1-11. doi: 10.1016/j.biopha.2019.109129

97. Cabili M, Dunagin M, Mcclanahan P, Biaesch A, Padovan-merhar O, Regev A, Rinn J, Raj A (2015) Localization and abundance analysis of human lncRNAs at single-cell and single-molecule resolution. Genome biology 16:20. doi: 10.1186/s13059-015-0586-4

98. Slavik H, Balik V, Vrbkova J, Rehulkova A, Vaverka M, Hrabalek L, Ehrmann J, Vidlarova M, Gurska S, Hajduch M, Srovnal J (2020) Identification of Meningioma Patients at High Risk of Tumor Recurrence Using MicroRNA Profiling. Neurosurgery 87:1055–1063. doi: 10.1093/neuros/nyaa009

99. Mock A, Geisenberger C, Orlik C, Warta R, Schwager C, Jungk C, Dutruel C, Geiselhart L, Weichenhan D, Zucknick M, Nied A, Friauf S, Exner J, Capper D, Hartmann C, Lahrmann B, Grabe N, Debus J, von Deimling A, Popanda O, Plass C, Unterberg A, Abdollahi A, Schmezer P, Herold-mende C (2016) LOC283731 promoter hypermethylation prognosticates survival after radiochemotherapy in IDH1 wild-type

glioblastoma patients. International Journal Of Cancer 139:424-425. doi: 10.1002/ijc.30069

100. Youngblood M, Miyagishima D, Jin L, Gupte T, Li C, Duran D, Montejo J, Zhao A, Sheth A, Tyrtova E, Özduman K, Iacoangeli F, Peyre M, Boetto J, Pease M, Avşar T, Huttner A, Bilguvar K, Kilic T, Pamir M, Amankulor N, Kalamarides M, Erson-omay E, Günel M, Moliterno J (2020) Associations of Meningioma Molecular Subgroup and Tumor Recurrence. Neuro-oncology noaa226:1-12. doi: 10.1093/neuonc/noaa226

101. Wang M, Deng X, Ying Q, Jin T, Li M, Liang C (2015) MicroRNA-224 targets ERG2 and contributes to malignant progressions of meningioma. Biochemical and Biophysical Research Communications 460:354 - 361. doi: 10.1016/j.bbrc.2015.03.038

102. Vlachos I, Zagganas K, Paraskevopoulou M, Georgakilas G, Karagkouni D, Vergoulis T, Dalamagas T, Hatzigeorgiou A (2015) DIANA-miRPath v3.0: deciphering microRNA function with experimental support. Nucleic acids research 43:W460-6. doi: 10.1093/nar/gkv403

103. Zheng X, Chopp M, Lu Y, Buller B, Jiang F (2013) MiR-15b and miR-152 reduce glioma cell invasion and angiogenesis via NRP-2 and MMP-3. Cancer Letters 329:146-154. doi: 10.1016/j.canlet.2012.10.026

104. Jiang J, Lin C, Liu N, Zhang Z, Sun Y, Fang X, Qi J (2013) The expression of fatty acid metabolism-associated proteins is correlated with the prognosis of meningiomas. APMIS: acta pathologica, microbiologica, et immunologica Scandinavica 121:997-1003. doi: 10.1111/apm.12135

105. Hou Z, Yin H, Chen C, Dai X, Li X, Liu B, Fang X (2012) microRNA-146a targets the L1 cell adhesion molecule and suppresses the metastatic potential of gastric cancer. Molecular Medicine Reports 6:501 - 506. doi: 10.3892/mmr.2012.946

106. Zhao J, Rao D, Boldin M, Taganov K, O'connell R, Baltimore D (2011) NF-kappaB dysregulation in microRNA-146a-deficient mice drives the development of myeloid malignancies. Proceedings of the National Academy of Sciences of the United States of America 108:9184-9. doi: 10.1073/pnas.1105398108

107. Antal O, Hackler Jr L, Shen J, Mán I, Hideghéty K, Kitajka K, Puskás L (2014) Combination of unsaturated fatty acids and ionizing radiation on human glioma cells: cellular, biochemical and gene expression analysis. Lipids in Health 13:1-15. doi: 10.1186/1476-511X-13-142

108. Xiang M, Walker S, Yeh J, Liu S, Kroll Y, Frank D, Birkbak N, Richardson A, Vafaizadeh V, Groner B, Boldin M, Taganov K (2014) STAT3 induction of miR-146b forms a feedback loop to inhibit the NF-κB to IL-6 signaling axis and STAT3-driven cancer phenotypes. Science Signaling 7:ra11. doi: 10.1126/scisignal.2004497

109. Johnson M, O'connell M, Walter K (2017) STAT3 activation and risk of recurrence in meningiomas. Oncology Letters 13:2432-2436. doi: 10.3892/ol.2017.5736

110. Rombaut D, Chiu H, Decaesteker B, Everaert C, Yigit N, Peltier A, Janoueix-lerosey I, Bartenhagen C, Fischer M, Roberts S, D'haene N, Speleman F, Denecker G, Sumazin P, Vandesompele J, Lefever S, Mestdagh P (2019) Integrative analysis identifies lincRNAs up- and downstream of neuroblastoma driver genes. Scientific reports 9:5685. doi: 10.1038/s41598-019-42107-y

111. Stelzer G, Rosen N, Plaschkes I, Zimmerman S, Twik M, Fishilevich S, Iny Stein T, Nudel R, Rappaport N, Safran M, Lancet D, Lieder I, Mazor Y, Kaplan S, Dahary D, Warshawsky D, Guan-golan Y, Kohn A (2016) The GeneCards suite: From gene data mining to disease genome sequence analyses. Current Protocols in Bioinformatics 54:1.30.1 - 1.30.33. doi: 10.1002/cpbi.5

112. Stranjalis G, Korfias S, Psachoulia C, Boviatsis E, Kouyialis A, Protopappa D, Sakas D (2005) Serum S-100B as an indicator of early postoperative deterioration after meningioma surgery. Clinical chemistry 51:202-7. doi: 10.1373/clinchem.2004.039719

113. Collord G, Tarpey P, Kurbatova N, Martincorena I, Moran S, Castro M, Nagy T, Bignell G, Maura F, Berna J, Sanders M, Noorani I, Watts C, Leipnitz E, Kirsch M, Schackert G, Pearson D, Devadass A, Ram Z, Allinson K, Zakaria R, Syed K, Dunn J, Esteller M, Behjati S, Brazma A, Santarius T, Mcdermott U (2018) An integrated genomic analysis of anaplastic meningioma identifies prognostic molecular signatures. Scientific Reports 8:1-13. doi: 10.1038/s41598-018-31659-0

114. Huang B, Yu M, Guan R, Liu D, Hou B (2020) A Comprehensive Exploration of the lncRNA CCAT2: A Pan-Cancer Analysis Based on 33 Cancer Types and 13285 Cases. Disease markers 2020:5354702. doi: 10.1155/2020/5354702

115. Yu Y, Nangia-makker P, Farhana L, Majumdar A (2017) A novel mechanism of lncRNA and miRNA interaction: CCAT2 regulates miR-145 expression by suppressing its maturation process in colon cancer cells. Molecular cancer 16:155. doi: 10.1186/s12943-017-0725-5

116. Zhang X, Gejman R, Mahta A, Zhong Y, Rice K, Zhou Y, Cheunsuchon P, Klibanski A, Louis D (2010) Maternally expressed gene 3, an imprinted noncoding RNA gene, is associated with meningioma pathogenesis and progression. Cancer Research 70:2350 - 2358. doi: 10.1158/0008-5472.CAN-09-3885

117. Zhang X, Rice K, Wang Y, Chen W, Zhong Y, Nakayama Y, Zhou Y, Klibanski A (2010) Maternally Expressed Gene 3 (MEG3) Noncoding Ribonucleic Acid: Isoform Structure, Expression, and Functions. Endocrinology 151:939-940

118. Villemin J, Lorenzi C, Cabrillac M, Oldfield A, Ritchie W, Luco R (2021) A cell-to-patient machine learning transfer approach uncovers novel basal-like breast cancer prognostic markers amongst alternative splice variants. BMC biology 19:1-19. doi: 10.1186/s12915-021-01002-7

119. Wang F, Flanagan J, Su N, Wang L, Bui S, Nielson A, Wu X, Vo H, Ma X, Luo Y (2012) RNAscope: A novel in situ RNA analysis platform for formalin-fixed, paraffin-embedded tissues. Journal of Molecular Diagnostics 14:22 - 29. doi: 10.1016/j.jmoldx.2011.08.002

120. Tripathi M, Zacheaus C, Doxtater K, Keramatnia F, Yallapu M, Jaggi M, Chauhan S, Gao C (2018) Z probe, an efficient tool for characterizing long non-coding RNA in FFPE tissues. Non-coding RNA 4:1-10. doi: 10.3390/ncrna4030020

10. Appendixes

Full text publications related to the thesis.

Appendix 1

H. Slavík, V. Balik, J. Vrbková, A. Řehulková, M. Vaverka, L. Hrabálek, M. Vidlařová, S. Gurská, M. Hajdúch, J. Srovnal. Identification of Meningioma Patients at High Risk of Tumor Recurrence Using MicroRNA Profiling. *Neurosurgery*. **2020**, 87: 1055–1063.

Appendix 2

H. Slavík, V. Balik, F. Zavadil Kokáš, R. Slavkovský, A. Řehulková, J. Vrbková, T. Lausová, J. Ehrman, S. Gurská, I. Überall, M. Hajdúch, J. Srovnal. Transcriptomic Profiling Revealed Lnc-GOLGA6A-1 as a Novel Prognostic Biomarker of Meningioma Recurrence.

Appendix 3

M. Ghothim, J. Srovnal, L. Bébarová, J. Tesaříková, P. Skalický, D. Klos, A. Prokopová, M. Vahalíková, H. Slavík, J. Vrbková, Č. Neoral, R. Havlík, M. Hajdúch, M. Loveček. Determination of CEA, EGFR and hTERT Expression in Peritoneal Lavage in Patients with Pancreatic Adenocarcinoma Using RT - PCR Method. *Rozhledy v chirurgii / Perspectives in Surgery*. **2015**, 94: 464-469.

APPENDIX 1

Hanus Slavik, MSc[‡*]
Vladimir Balik, MD, PhD[‡§*]
Jana Vrbkova, PhD[‡]
Alona Rehulkova, MD[‡]
Miroslav Vaverka, MD, PhD[§]
Lumir Hrabalek, MD, PhD[§]
Jiri Ehrmann, MD, PhD[‡¶]
Monika Vidlarova, MSc[‡]
Sona Gurska, PhD[‡]
Marian Hajduch, MD, PhD[‡]
Josef Srovnal, MD, PhD[‡]

[‡]Laboratory of Experimental Medicine, Institute of Molecular and Translational Medicine, Faculty of Medicine and Dentistry, Palacky University and University Hospital Olomouc, Czech Republic; [§]Department of Neurosurgery, Faculty of Medicine and Dentistry, Palacky University and University Hospital Olomouc, Czech Republic; [¶]Institute of Clinical and Molecular Pathology, Faculty of Medicine and Dentistry, Palacky University and University Hospital Olomouc, Czech Republic, Czech Republic

[*]Hanus Slavik and Vladimir Balik contributed equally to this work.

Correspondence:
Josef Srovnal, MD, PhD,
Institute of Molecular and Translational Medicine,
Faculty of Medicine and Dentistry,
University Hospital Olomouc,
Palacky University Olomouc,
Hnevotinska 5,
779 00 Olomouc, Czech Republic.
Email: josef.srovnal@upol.cz

Received, June 6, 2019.
Accepted, December 15, 2019.
Published Online, March 3, 2020.

Identification of Meningioma Patients at High Risk of Tumor Recurrence Using MicroRNA Profiling

BACKGROUND: Meningioma growth rates are highly variable, even within benign subgroups, with some remaining stable, whereas others grow rapidly.
OBJECTIVE: To identify molecular-genetic markers for more accurate prediction of meningioma recurrence and better-targeted therapy.
METHODS: Microarrays identified microRNA (miRNA) expression in primary and recurrent meningiomas of all World Health Organization (WHO) grades. Those found to be deregulated were further validated by quantitative real-time polymerase chain reaction in a cohort of 172 patients. Statistical analysis of the resulting dataset revealed predictors of meningioma recurrence.
RESULTS: Adjusted and nonadjusted models of time to relapse identified the most significant prognosticators to be miR-15a-5p, miR-146a-5p, and miR-331-3p. The final validation phase proved the crucial significance of miR-146a-5p and miR-331-3p, and clinical factors such as type of resection (total or partial) and WHO grade in some selected models. Following stepwise selection in a multivariate model on an expanded cohort, the most predictive model was identified to be that which included lower miR-331-3p expression (hazard ratio [HR] 1.44; $P < .001$) and partial tumor resection (HR 3.90; $P < .001$). Moreover, in the subgroup of total resections, both miRNAs remained prognosticators in univariate models adjusted to the clinical factors.
CONCLUSION: The proposed models might enable more accurate prediction of time to meningioma recurrence and thus determine optimal postoperative management. Moreover, combining this model with current knowledge of molecular processes underpinning recurrence could permit the identification of distinct meningioma subtypes and enable better-targeted therapies.

KEY WORDS: Meningioma, miRNA, Prognosis, Recurrence

Neurosurgery 87:1055–1063, 2020 DOI:10.1093/neuros/nyaa009 www.neurosurgery-online.com

Among CBTRUS (Central Brain Tumor Registry of the United States) specific histology groupings, meningiomas are the most frequently reported primary intracranial tumors with the annual incidence rate of 8.33 per 100 000 population,[1] accounting for about 23.8% and 46.8% of all intracranial neoplasms in males and females, respectively.[1,2] Their recurrence cannot be predicted reliably based on histopathology itself, because even benign lesions can include tumors with distinct biological behavior and oncogenic drivers, as

ABBREVIATIONS: AEG-1, astrocyte-elevated gene-1; **AKT,** protein kinase B; **CBTRUS,** Central Brain Tumor Registry of the United States; **CI,** confidence interval; **FFPE,** formalin-fixed paraffin-embedded; **GLA,** gamma-linolenic acid; **HR,** hazard ratio; **HER2,** tyrosine-protein kinase erbB-2; **MRR$^+$,** meningiomas with evidence of radiographic recurrence up to 8 years after surgery; **MRR$^-$,** meningiomas without evidence of radiographic recurrence up to 8 years after surgery; **miRNA,** microRNA; **NRP-2,** neuropilin-2; **NF-κB,** nuclear factor kappa B; **PI3K/AKT,** phosphoinositide-3-kinase/AKT; **PTEN,** phosphatase and tensin homolog; **qPCR,** quantitative polymerase chain reaction; **STAT3,** signal transducer and activator of transcription 3; **TTR,** time to relapse; **VEGF,** vascular endothelial growth factor; **WHO,** World Health Organization

Supplemental digital content is available for this article at www.neurosurgery-online.com.

demonstrated in both mesenchymal (fibroblastic) and epithelial (meningothelial) lineages of benign meningiomas.[3,4] Recurrence within 5 and 10 yr after gross total resection of World Health Organization (WHO) grade I meningiomas occurs in 12% and 19% of all cases, respectively,[5,6] whereas 5- and 10-yr recurrence rates of subtotally resected benign lesions range from 37% to 60%, and 55% to 100%, respectively.[6] This suggests that there might be key regulators with a significant effect on meningioma biology irrespective of their histopathological degree, the identification of which would allow a more accurate prediction of their behavior. The expression of miRNAs was recently proposed as just such a predictor. These noncoding small RNAs can act as oncogenes or tumor suppressors in various tumors.[4,7] A recent study[4] identified sets of miRNAs that were also deregulated in benign and high-grade meningiomas. Although a few miRNA signatures have been suggested to predict meningioma recurrence, no mutual miRNA sequences have been reported so far.[7-9] The present study was therefore conducted to shed light on these inconsistencies and extend our knowledge of the relationship between miRNA expression and meningioma recurrence.

METHODS

Patients' Description

The study was approved by the Institutional Research Ethics Committee. Of 302 patients who underwent meningioma surgery between 1990 and 2012, only 172 from whom sufficient tissue for miRNA analysis and comprehensive clinical data were available were selected. All patients signed their informed consent. Imaging/clinical follow-up were performed at 3 and 12 mo after surgery, and approximately every 24 to 72 mo thereafter if no recurrence/regrowth was detected. When meningioma recurrence/regrowth was found, additional follow-ups were scheduled. Recurrence, after total or gross total (Simpson grades I, II, and III) and incomplete (Simpson grade >III) resection, has been defined as the reappearance of any new lesion in which meningioma tissue had previously been removed, or when any remnants of tumor after primary surgery were noticed on the follow-up imaging to have grown. If significant tumor growth was noted at follow-up or meningioma became symptomatic, patients were reoperated on or underwent radiation therapy when indicated. Because of overall follow-up of the whole cohort, the 8-yr limit was used as an adequate cutoff time for recurrence for simple 2-sample analyses. This cutoff time is for descriptive purposes only and has no influence on the main results of the study.

miRNA Expression Analysis

Briefly, in the screening phase, formalin-fixed paraffin-embedded (FFPE) tumor samples were obtained from 38 patients for microarray analysis following RNA purification. Of these, 11 had primary samples of meningiomas with evidence of radiographic recurrence up to 8 yr after surgery (MRR^+); 15 had meningiomas without evidence of radiographic recurrence within the same time period (MRR^-); and 12 had meningiomas without radiological recurrence within the follow-up of <8 yr. Moreover, paired-matched primary and recurrent samples from 10 MRR^+ patients were also analyzed. In the training phase, 59 previously unanalyzed samples were assembled for quantitative polymerase chain reaction (qPCR) analyses (20 MRR^+ [primary samples], 25 MRR^-, and 14 meningiomas without radiological recurrence within the follow-up of <8 yr). Finally, the validation phase included all 172 patients, including cohorts from the screening and training phases, the total comprising 37 with MRR^+ (primary samples), 59 with MRR^-, and 76 with meningiomas without radiological recurrence within the follow-up of <8 yr (Table 1 and Figure 1). For detailed information about RNA purification (QIAGEN, Hilden, Germany), miRNA array, and TaqMan assay (Applied Biosystems, Foster City, California), see **Text**, **Supplemental Digital Content 1**.

Statistical Methods

Statistical analyses were performed with R (R Foundation for Statistical Computing, Vienna, Austria) and Bioconductor. Wilcoxon exact one-sample tests and Cox regression analysis were applied to the microarray data to identify differentially expressed miRNAs and miRNAs with a significant time-to-relapse (TTR) effect. Univariate adjusted and nonadjusted Cox regression models were selected for qPCR data following the building of a full multivariate model and consequent stepwise selection method, which provided factors for the final multivariate model. Each prognostic factor was characterized by HR (hazard ratio) and *P* value. For more information, see **Text**, **Supplemental Digital Content 1**.

RESULTS

Screening Phase

The microarray analysis revealed 49 miRNAs with their expression strongly dependent on TTR in meningiomas at various risks of recurrence (Figure 2A), according to the Cox regression model of TTR. Only mature miRNA with higher abundance (intensity of fluorescence >5) were analyzed in all microarray experiments. Decreasing gene expression as risk of recurrence increases is typical for most miRNAs. Only 12 miRNAs increased expression following recurrence; among them were members of the miR-320 family showing the highest HR values. Seven highly abundant and biologically relevant miRNAs were subsequently selected for further validation by qPCR. That set included hsa-miR-15a-5p, hsa-miR-19b-3p, hsa-miR-30e-5p, hsa-miR-107, hsa-miR-146a-5p, hsa-miR-320c, and hsa-miR-331-3p; their characteristics are shown in **Figure**, **Supplemental Digital Content 2**. Additionally, 4 miRNAs that exhibited stable expression and did not correlate with recurrence status or other clinical characteristics were selected for qPCR normalization (let-7b-5p, miR-324-5p, miR-181b-5p, and miR-1281) (**Figure**, **Supplemental Digital Content 3**).

Paired Analysis

A total of 41 mature miRNAs exhibited differential expression in paired-matched primary and recurrent MRR^+ samples (Figure 2B). Most of these were expressed less strongly in the recurrent samples, with only about 13 of them expressing more strongly in recurrent samples. Interestingly, the sample pairs formed 2 main clusters according to differentially expressed miRNAs, with some miRNAs changing their level of expression in opposite ways. One of these clusters contained only patients

TABLE 1. The Clinical-Pathological Characteristics of Meningioma Patients Included in the Data Set at All Phases of the Study

Cohort	n	Screening phase				Training phase				Validation phase			
		38				59				172			
		MRR^-	MRR^+	*P* value	Total[a]	MRR^-	MRR^+	*P* value	Total[a]	MRR^-	MRR^+	*P* value	Total[a]
Female/male	n (%)	13/2 (86.7/13.3)	7/4 (63.6/36.4)	.348	28/10 (73.7/26.3)	21/4 (84.0/16.0)	10/10 (50.0/50.0)	.034	40/19 (67.8/32.2)	47/12 (79.7/20.3)	19/18 (51.4/48.6)	.007	115/57 (66.9-33.1)
Age (yr)	Median (IQR)	54 (43-61)	53 (45-61)	.812	54 (43-64)	51 (43-61)	48 (41-61)	.912	50 (43-60)	56 (45-62)	52 (42-64)	.596	56 (45-65)
WHO grade I/II/III	n (%)	9/2/3 (64.3/14.3/ 21.4)	3/5/3 (27.3/45.5/ 27.3)	.128	14/12/11 (37.8/32.4/ 29.7)	24/1/0 (96.0/4.0/ 0.0)	16/4/0 (80.0/20.0/ 0.0)	.155	51/8/0 (86.4/13.6/ 0.0)	51/3/4 (87.9/5.2/ 6.9)	21/11/4 (58.3/30.6/ 11.1)	.001	125/31/14 (73.5/18.2/ 8.2)
Convexity/skull base meningioma	n (%)	6/9 (40.0/60.0)	7/4 (63.6/36.4)	.427	17/21 (44.7/55.3)	8/17 (32.0/68.0)	8/12 (40.0/60.0)	.807	23/36 (39.0/61.0)	20/39 (33.9/66.1)	18/19 (48.6/51.4)	.221	72/100 (41.9/58.1)
Simpson grade I-III/>III	n (%)	12/3 (80.0/20.0)	8/3 (72.7/27.3)	1	30/7 (81.1/18.9)	21/2 (91.3/8.7)	9/11 (45.0/55.0)	.003	40/17 (70.2/29.8)	47/8 (85.5/14.5)	20/17 (54.1/45.9)	.002	127/39 (76.5/23.5)
Add-on radiotherapy (yes/no)	n (%)	4/11 (26.7/73.3)	6/5 (54.5/45.5)	.228	13/25 (34.2/65.8)	3/22 (12.0/88.0)	12/8 (60.0-40.0)	.002	15/44 (25.4/74.6)	10/49 (16.9/83.1)	22/15 (59.5/40.5)	<.001	36/136 (20.9/79.1)
Follow-up (mo)	Median (IQR)	149.3 (113.7-198.1)	99.8 (87.6-123.4)	.005	100.9 (66.8-144.7)	161.2 (124.4-202.2)	138.3 (102.3-191.8)	.233	124.4 (85.5-181.5)	146.2 (124.5-202.6)	120.0 (87.3-173.4)	.004	95.7 (65.8-145.7)
Time to relapse[b]	%	–	–	–	64.5 ± 8.8	–	–	–	61.3 ± 6.9	–	–	–	72.5 ± 4.0

IQR, interquartile range (first quartile through third quartile); MRR^+, patients with meningiomas with evidence of radiographic recurrence up to 8 yr after surgery; MRR^-, patients with meningiomas without evidence of radiographic recurrence up to 8 yr after surgery; WHO, World Health Organization.

[a]Including patients with follow-up <8 yr without recurrence.

[b]Kaplan-Meier estimate of survival at the time of 8 yr after surgery: 8-yr survival ± standard error.

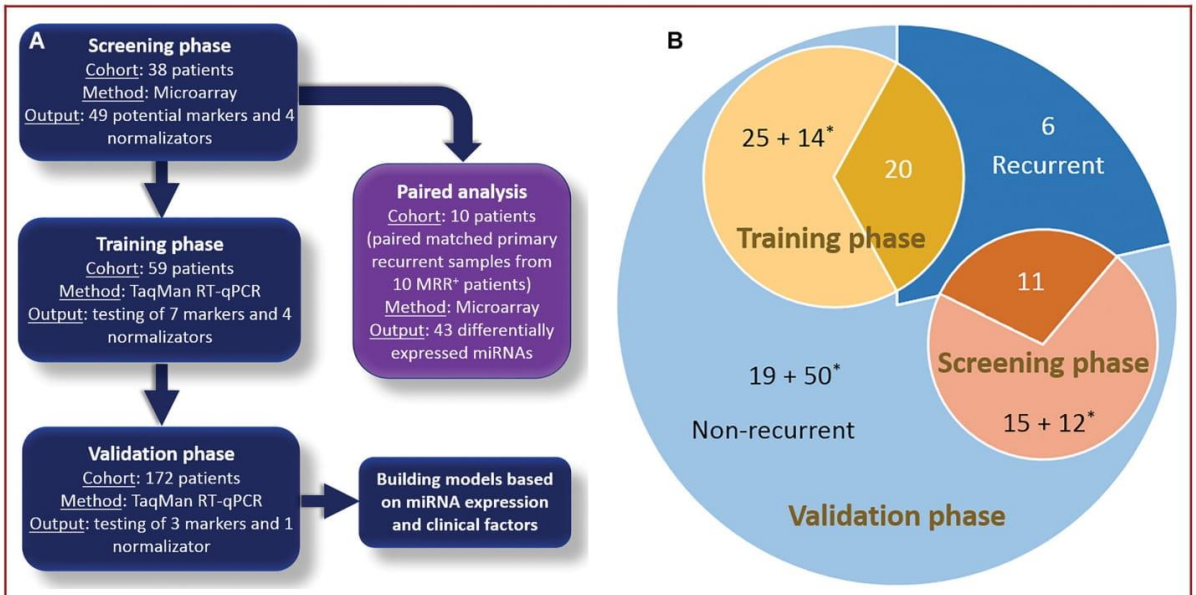

FIGURE 1. *Overview of the present study.* **A**, *Design of the study (screening phase, training phase, validation phase, and separately performed paired analyses).* **B**, *Description of the patient's cohort in each phase. MRR+, primary samples of meningiomas with evidence of radiographic recurrence up to 8 yr after surgery; *follow-up <8 yr.*

with convexity meningiomas and who were generally older and presented with higher histopathological WHO grades at diagnosis. Only 2 miRNAs, miR-193b-3p and miR-27a-3p, exhibited deregulation between paired-matched primary and recurrent samples of MRR+ and also showed dependence on TTR within the screening phase. These were not chosen for further validation of relapse prediction. Interestingly, miR-30c-5p was deregulated in recurrent samples of MRR+, whereas the expression of the closely related miR-30e-5p, miR-30b-5p, and miR-30a-5p was found to be dependent on TTR in the screening phase, which indicates that miR-30 is significantly involved in meningioma pathogenesis; it was therefore also selected for further validation.

Training Phase

The expression of candidate miRNAs was normalized against miR-181, which exhibited the most stable basal expression over all samples within the qPCR data (**Figure**, **Supplemental Digital Content 4**). A univariate analysis confirmed the differences in some of the miRNA's expression in primary samples of MRR+ observed in microarray experiments. The following miRNAs exhibited significant dependence on TTR within the samples using adjusted or nonadjusted models in their expression: hsa-miR-15a-5p, hsa-miR-146a-5p, and hsa-miR-331-3p (Table 2). Nonadjusted models used only certain miRNAs as prognostic factors, whereas the adjusted model also included clinical factors such as age, sex, WHO grade, tumor location, and type of resection. All 3 miRNAs were selected for final validation on the extended cohort.

Validation Phase

The 3 miRNAs selected in the training phase were tested in 172 patients, including cohorts from the screening and training phases. The final model was developed using the complete set of ΔCt values for the cohort that had a realistically unbalanced ratio of MRR+ and MRR− patients. Adjusting clinical factors were included in the Cox regression model for the final analysis of TTR in patients. Univariate analyses once again confirmed the miR-331-3p as the most promising prognostic factor. In the analysis of each marker separately, miR-331 gave the highest HR and the lowest *P* value among other miRNA-based univariate models. This analysis was also performed on the total resection subgroup in order to exclude the influence of such a strong prognostic factor that probably has no molecular background. Notably, this analysis produced similar results. Moreover, miR-15a was not a statistically significant candidate in the present models. Investigating the influence of clinical adjusting factors, the type of resection had the strongest prognostic value in all models. However, WHO grade in the subgroup of patients with a total resection was the strongest prognostic factor within the miR-146a- and miR-15a-based models. The results from the univariate Cox regression models are summarized in Table 3. The multivariate model was built in order to test whether miRNA represents real additional value in meningioma recurrence prognostication. The stepwise selection method with fixed clinical adjusting factors

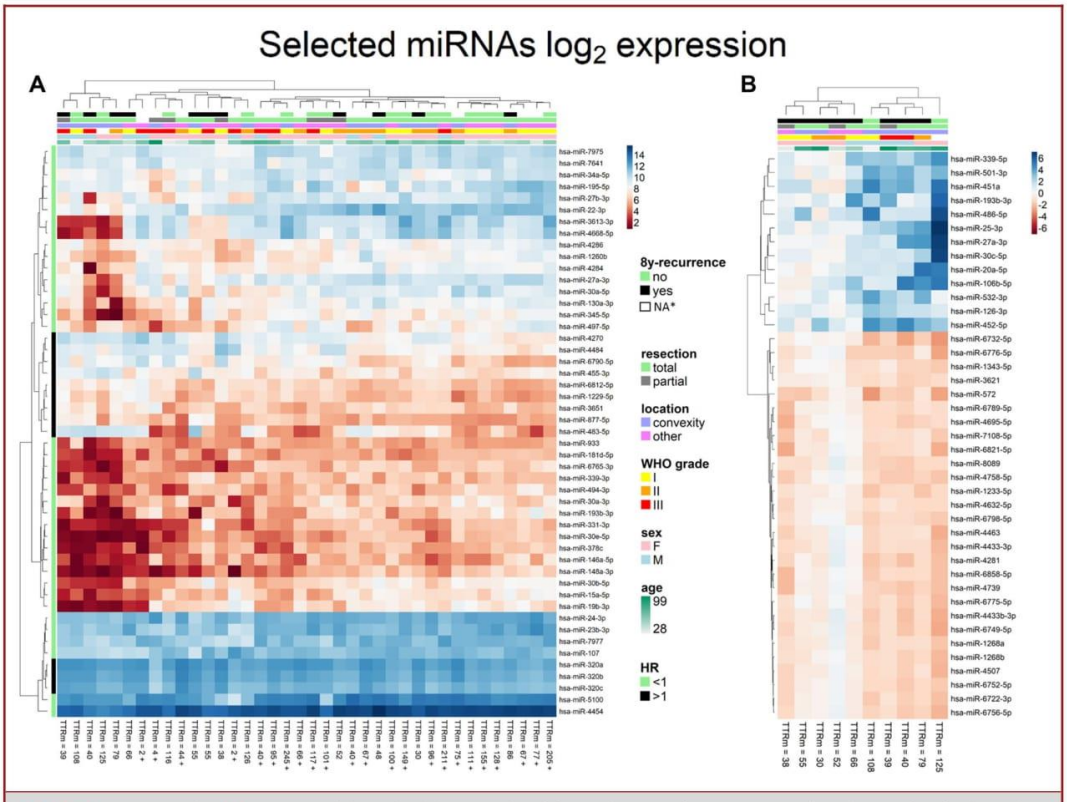

FIGURE 2. *Microarray data.* **A**, *Unsupervised hierarchical clustering of 49 differentially expressed miRNAs in MRR$^+$ and MRR$^-$ based on logarithmic values (log_2) of miRNA's expression compared to recurrence in 8 yr of follow-up, sex, histopathological grade, type of resection, tumor location, and age at diagnosis. Hazard ratio (HR) is also marked for each miRNA.* **B**, *Differentially expressed miRNAs between primary and recurrent samples of MRR$^+$ from paired analyses. TTRm, time to relapse in months; + censored if there is no event during follow-up period; ∗ no evidence of radiographic recurrence, but follow-up <8 yr.*

was used to select the most important prognostic factors in the multivariate model. The only significant ($P < .001$) candidate identified by the model was miR-331-3p, the extent of resection being the only other significant clinical factor, other factors having only supportive functions. The final model is shown in Figure 3. Among all tested models, WHO grades and miR-146a-5p also appeared to be predictors. The question remains, whether balanced cohorts in terms of Simpson grades in the validation phase would lead to similar results, or would alternatively confirm the role of the extent of tumor resection as a predictor of recurrence.

DISCUSSION

miRNA Profile and Meningioma Recurrence

A link between aberrant miRNA expression and meningioma recurrence has so far been identified in only 3 studies.[7-9] However, none of the miRNAs overlaps with the set of 49 deregulated miRNAs identified during the screening phase of the present study. This discrepancy might stem from differences in sample size or cohort homogeneity.[8] For example, in contrast to the present study, the other cited studies[7-9] included Asian cohorts comprising various numbers of patients ranging from 103 to 230 and a mixture of recurrent and nonrecurrent tumors (see **Table**, **Supplemental Digital Content 5**). Other differences between the approaches exist in the methodology, study design, and sample type. For example, only one study performed miRNA-profiling analysis incorporating all 3 phases,[7] whereas the screening phase was omitted in the other 2 studies[8,9]; moreover, one of them selected only one candidate miRNA for analysis without utilizing screening and training dataset.[9] These factors combined might have led to the eventual selection of different miRNAs. Regarding tissue samples, one of the cited studies prospectively analyzed circulating miRNAs from

TABLE 2. Univariate Adjusted and Nonadjusted Cox Regression Models of Time to Relapse From Training Phase for Each Measured miRNA

	Nonadjusted model					Adjusted model				
Factor	**HR**	**1/HR**	**95% CI range**		***P* value**	**HR**	**1/HR**	**95% CI range**		***P* value**
miR-107	1.25	0.80	0.86	1.80	.240	0.94	1.06	0.63	1.41	.761
miR-331-3p	1.76	0.57	1.14	2.70	.010	1.57	0.64	0.93	2.65	.090
miR-15a-5p	1.15	0.87	0.97	1.35	.103	1.25	0.80	1.01	1.55	.038
miR-19b-3p	1.27	0.79	0.90	1.78	.175	1.25	0.80	0.88	1.77	.214
miR-30e-5p	1.11	0.90	0.89	1.38	.357	1.21	0.83	0.90	1.64	.209
miR-320c	1.23	0.81	0.79	1.92	.364	0.89	1.12	0.49	1.62	.710
miR-146a-5p	1.55	0.65	1.13	2.13	.007	1.42	0.70	1.00	2.02	.053

Significant miRNAs in at least one model are marked in bold.

TABLE 3. Univariate Adjusted Cox Regression Models of Time to Relapse From Validation Phase for Each Measured miRNA

	All patients					Patients after total resection					
Factor	**HR**	**1/HR**	**95% CI range**		***P* value**	**Factor**	**HR**	**1/HR**	**95% CI range**		***P* value**
miR-146a-5p based model											
Age at diagnosis	0.99	1.01	0.97	1.01	.436	Age at diagnosis	1.01	0.99	0.98	1.04	.709
Sex: male	1.68	0.59	0.84	3.37	.142	Sex: male	1.15	0.87	0.47	2.82	.759
WHO grade	1.63	0.61	1.07	2.50	.024	**WHO grade**	1.86	0.54	1.06	3.24	.029
Nonconvex. location	0.63	1.60	0.33	1.18	.148	Nonconvex. location	0.54	1.85	0.23	1.25	.150
Partial resection	3.16	0.32	1.67	6.00	4.24E-04	–	–	–	–	–	–
miR-146a-5p	1.34	0.74	1.10	1.63	.003	**miR-146a-5p**	1.37	0.73	1.07	1.76	.014
miR-15a-5p based model											
Age at diagnosis	0.99	1.01	0.97	1.01	.254	Age at diagnosis	0.99	1.01	0.97	1.02	.656
Sex: male	2.77	0.36	1.45	5.27	.002	Sex: male	1.69	0.59	0.72	3.95	.228
WHO grade	1.37	0.73	0.91	2.08	.132	**WHO grade**	1.85	0.54	1.07	3.18	.027
Nonconvex. location	0.69	1.46	0.37	1.28	.236	Nonconvex. location	0.65	1.55	0.28	1.50	.310
Partial resection	3.67	0.27	1.92	7.02	8.52E-05	–	–	–	–	–	–
miR-15a-5p	0.94	1.06	0.84	1.05	.283	miR-15a-5p	0.96	1.04	0.82	1.11	.573
miR-331-3p based model											
Age at diagnosis	1.00	1.00	0.97	1.02	.827	Age at diagnosis	1.01	0.99	0.98	1.04	.443
Sex: male	1.43	0.70	0.67	3.03	.354	Sex: male	1.12	0.89	0.44	2.87	.811
WHO grade	1.33	0.75	0.86	2.05	.200	WHO grade	1.53	0.65	0.86	2.73	.146
Nonconvex. location	0.58	1.72	0.31	1.10	.095	Nonconvex. location	0.46	2.17	0.19	1.11	.085
Partial resection	3.87	0.26	2.03	7.38	4.11E-05	–	–	–	–	–	–
miR-331-3p	1.45	0.69	1.17	1.79	.001	**miR-331-3p**	1.43	0.70	1.10	1.87	.007

Significant factors are marked in bold.

patients' serum,[7] whereas the others[8,9] used tumor tissue either as snap-frozen or FFPE samples, and collected data retrospectively. Moreover, although quantitative reverse transcription PCR was used in the training and validation phases of all 3 cited studies,[7,8] we used microarrays in our screening phase, which is a more advanced technique, as it targets all miRNAs. However, the differences between our results and those of other studies might also stem from the fact that other gene regulation mechanisms play a more robust role in meningioma recurrence.[10] The previous studies also reported that the upregulation of miR-190a[8] and miR-409-3p[7] and downregulation of miR-29c-3p[8] and miR-219-5p[8] were associated with increased recurrence rates, whereas the effect of miR-224 expression was inconsistent in the different studies. Its downregulation was associated with increased recurrence,[7] whereas Wang et al[9] found the opposite, which they attributed to the activation of the ERG2-BAK-induced apoptosis pathway. Based on the high biological relevance and differential expression profile resulting from the Cox regression model and hierarchical clustering analysis, 7 miRNAs were selected for qPCR validation on an independent cohort, namely miR-15a-5p, miR-19b-3p, miR-30e-5p, miR-107, miR-146a-5p, miR-320c, and miR-331-3p. Following normalization against stably expressed

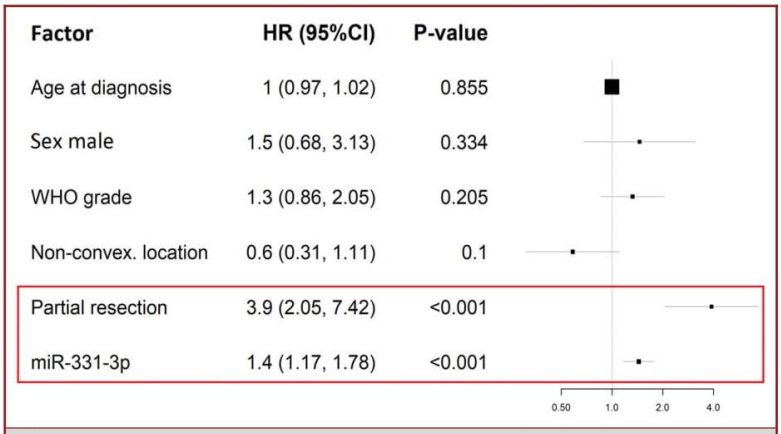

FIGURE 3. *Final multivariate Cox regression model built with factors selected by stepwise selection with data from validation phase for 161 patients with complete records. Characteristics from the Cox regression model are visualized as a forest plot. HR, hazard ratio.*

miR-181, adjusted and nonadjusted models were used to test for effects on the TTR with estimated P values $< .1$. Among the miRNAs, the most significant positive prognostic factors were selected as being miR-15a-5p ($P = .038$), miR-146a-5p ($P = .053$), and miR-331-3p ($P = .09$). Subsequent testing of the 3 miRNAs on an expanded cohort using stepwise selection in the multivariate model identified the most effective predictive model to be the miR-331-3p-based model. The model which incorporated clinical factors identified those patients with a high miR-331-3p expression (HR 1.44; $P < .001$) and total/gross total meningioma resection (HR 3.90; $P < .001$) as cases with a significant influence on TTR. Other clinical factors played only a supportive role.

Having compared various models, the second most effective model was identified to be the one that included miR-146a-5p. In addition to the miRNA, the WHO grades and the extent of tumor resection were also good prognosticators. Factors identified as indicating a low propensity to recur were totally/gross totally removed (HR 3.16; $P < .001$) benign meningiomas (HR 1.63; $P = .024$) with upregulated miR-146a-5p expression (HR 1.34; $P = .003$). In a total/gross total resection subgroup analysis, both miRNAs remained significant predictive factors. Additionally, in the model with miR-146a-5p, the WHO grading system still functioned as a prognosticator.

miR-15a

miR-15 has been reported to suppress tumors in colon[11] and prostate cancer.[12] Following miR-15 transfection of tumor cells, the apoptosis rate increased significantly, probably because of the inhibition of nuclear factor kappa B (NF-κB) that promotes the transcription of antiapoptotic factors, such as Bcl-2 and Bcl-XL.[11] Additionally, miR-15b has been shown to reduce the invasion of glioma cells and angiogenesis by downregulation of neuropilin-2 (NRP-2) that interacts with vascular endothelial growth factor (VEGF), or through deactivation of the mitogen-activated protein kinase kinase (MEK)/extracellular signal-regulated kinase (ERK) signaling pathway signaling pathway.[13] NRP-VEGF interactions have been shown to promote developmental angiogenesis and metastases.[14] Thus, further investigations are warranted in order to verify which of these mechanisms, if any, is applied in meningioma biology. MEK-ERK as a key signaling pathway[15] and a highly expressed VEGF/VEGF receptor[16] have already been found in meningiomas.

miR-146a-5p

miR-146a is known to suppress gastric cancer cell invasion and metastasis,[17] and knocking out its expression in C57BL/6 mice leads to the development of myeloid sarcomas and lymphomas.[18] A study on gliomas[19] found that a combined treatment with gamma-linolenic acid (GLA) and irradiation led to miR-146a overexpression. Because surgical resection supplemented with irradiation is a standard therapy for recurrent meningiomas,[6] it would be desirable to determine whether this combined therapy has a similar beneficial effect on miR-146a-5p expression in meningiomas. The importance of miR-146 in meningioma recurrence is suggested by the existence of a negative feedback loop between signal transducer and activator of transcription 3 (*STAT3*) and NF-κB involving miR-146b,[20] and the fact that *STAT3* expression was significantly higher in recurrent WHO grade I and/or grade II meningiomas than in nonrecurrent ones.[21] *STAT3* targets miR-146b, which reduces IL-6 production by downregulating NF-κB. This is the final step in the negative feedback loop because IL-6 activates *STAT3*.[20] Upon

miR-146b downregulation, its uninhibited target gene NF-κB induces increased IL-6 production followed by *STAT3* activation. Notably, Johnson et al[21] reported that *STAT3* activation was markedly stronger in WHO grade II meningiomas than those of lower grade. High *STAT3* activation was also identified in 2 out of 3 recurrent WHO grade I meningiomas and in none out of 3 nonrecurrent lesions. Additionally, a strong STAT3 phosphorylation/activation signal was observed in 2 out of 4 recurrent WHO grade II meningiomas and one out of 3 nonrecurrent tumors.[21] Although the suppression of IL-6 by miR-146a leading to reduced *STAT3* expression has not yet been demonstrated in meningiomas,[22] these findings highlight the potential therapeutic value of miR-146a in these tumors. Combining GLA with irradiation might be an effective treatment strategy for overexpression of the miRNA, deactivation of the STAT3 pathway, and, thus, reducing the likelihood of meningioma recurrence.

miR-331-3p

The pronounced downregulation of miR-331-3p in glioblastomas suggests its role as tumor suppressor, possibly by upregulating *NRP-2* expression[23] or influencing targets such as receptor tyrosine-protein kinase erbB-2 (*HER2*),[24] deoxyhypusine hydroxylase,[25] phosphatase and tensin homolog/protein kinase B (PTEN/AKT), astrocyte-elevated gene-1 (*AEG-1*),[26] transcription factor *E2F1*,[27] *HER2/PI3K/AKT*,[28] or kallikrein-related peptidase 4.[29] However, which proteins are targets of miR-331-3p in meningiomas remains unclear. Phosphoinositide-3-kinase (PI3K)/AKT, as a key regulator of cell survival in cancers, has already been associated with meningiomas.[30] Moreover, AEG-1-depleted meningioma cells undergo apoptosis via phospho-AKT and Bcl-2 suppression.[31] It is therefore rational to suspect that a negative impact of miR-331-3p deregulation on meningioma might be carried out through these signaling pathways.

miRNA Profile in Paired Analyses

Recent findings regarding the variability of gene mutations being dependent on meningioma localization,[32] along with the observations that some genetic factors found in these tumors are important embryonic stem cell regulators,[33] suggest that meningiomas may derive from early progenitors/cancer stem cells, whereas their histogenetic origin may be site specific. Of note, based on a differential expression of 41 miRNAs in the paired analyses, 2 clusters were created, one of them predominantly comprising convexity meningiomas with 13 miRNAs highly expressed in their recurrent samples. Because miRNAs are involved in the regulation of embryonic stem cell development and signaling,[34] these findings further support the view that biological properties of meningiomas may be derived from site-specific progenitor/cancer stem cells regulated by respective miRNAs. Moreover, as WHO grade II and III meningiomas are significantly more frequent in the younger patients,[35] it seems that a specific expression profile of the 13 miRNAs can recognize recurrent high-grade meningiomas in older subjects as a biologically distinct tumor subgroup. Basically, this may indicate 2 distinct biological mechanisms required for tumor recurrence, with the mechanism observed in older subjects requiring just the upregulation of the miRNAs. However, because of a small cohort in the paired analyses, all this remains speculative and requires further validation.

Limitations of the Study

The main shortcomings of the present study were its retrospectivity, the limited size of the validation phase cohort, and the lack of an external dataset. As the dataset was unbalanced in terms of Simpson grades, the question remains whether such balancing of the cohort would lead to results similar to those of an unbalanced one. Moreover, miRNA expression profiles in the MRR^+ group might be prejudiced by the fact that only some symptomatic patients with meningioma recurrence underwent reoperation, whereas others were irradiated, and those without clinical manifestation and significant tumor growth were left untreated.

CONCLUSION

Our findings indicate that the miRNA-based model can serve as a novel predictor of meningioma recurrence and can thus help in determining an optimal postoperative surveillance regime to identify patients who may benefit from early retreatment. Moreover, combining the model with molecular mechanisms governing meningioma recurrence, such as miRNA targets and associated signaling pathways, might help to identify clinically distinct meningiomas and better target their treatment. Finally, because the literature indicates that no mutual miRNA predictors have yet been identified, a prospective randomized multicenter controlled trial is justified in order to resolve this ongoing discrepancy.

Disclosures

The authors have no personal, financial, or institutional interest in any of the drugs, materials, or devices described in this article. This work was supported by funding from the Ministry of Health of the Czech Republic (15-29021A); Palacký University Olomouc (LF 2019_003); Ministry of Education, Youth and Sports of the Czech Republic (LM2015091); Czech Technology Agency: Center of Competence for Molecular Diagnostics and Personalized Medicine (TE02000058); and European Regional Development Fund (ENOCH CZ.02.1.01/0.0/0.0/16_019/0000868).

REFERENCES

1. Ostrom QT, Gittleman H, Xu J, et al. CBTRUS statistical report: primary brain and other central nervous system tumors diagnosed in the United States in 2009-2013. *Neuro Oncol*. 2016;18(suppl_5):v1-v75.
2. Bondy M, Ligon BL. Epidemiology and etiology of intracranial meningiomas: a review. *J Neurooncol*. 1996;29(3):197-205.
3. Durand A, Champier J, Jouvet A, et al. Expression of c-Myc, neurofibromatosis type 2, somatostatin receptor 2 and erb-B2 in human meningiomas: relation to grades or histotypes. *Clin Neuropathol*. 2008;27(5):334-345.
4. Ludwig N, Kim YJ, Mueller SC, et al. Posttranscriptional deregulation of signaling pathways in meningioma subtypes by differential expression of miRNAs. *Neuro Oncol*. 2015;17(9):1250-1260.

5. Longstreth WT, Jr, Dennis LK, McGuire VM, Drangsholt MT, Koepsell TD. Epidemiology of intracranial meningioma. *Cancer*. 1993;72(3):639-648.
6. Jaaskelainen J. Seemingly complete removal of histologically benign intracranial meningioma: late recurrence rate and factors predicting recurrence in 657 patients. A multivariate analysis. *Surg Neurol*. 1986;26(5):461-469.
7. Zhi F, Shao N, Li B, et al. A serum 6-miRNA panel as a novel non-invasive biomarker for meningioma. *Sci Rep*. 2016;6:32067.
8. Zhi F, Zhou G, Wang S, et al. A microRNA expression signature predicts meningioma recurrence. *Int J Cancer*. 2013;132(1):128-136.
9. Wang M, Deng X, Ying Q, Jin T, Li M, Liang C. MicroRNA-224 targets ERG2 and contributes to malignant progressions of meningioma. *Biochem Biophys Res Commun*. 2015;460(2):354-361.
10. El-Gewely MR, Andreassen M, Walquist M, et al. Differentially expressed microRNAs in meningiomas grades I and II suggest shared biomarkers with malignant tumors, *Cancers (Basel)*. 2016;8(3):E31.
11. Liu L, Wang D, Qiu Y, Dong H, Zhan X. Overexpression of microRNA-15 increases the chemosensitivity of colon cancer cells to 5-fluorouracil and oxaliplatin by inhibiting the nuclear factor-κB signalling pathway and inducing apoptosis. *Exp Ther Med*. 2018;15(3):2655-2660.
12. Zidan HE, Abdul-Maksoud RS, Elsayed WSH, Desoky EAM. Diagnostic and prognostic value of serum miR-15a and miR-16-1 expression among Egyptian patients with prostate cancer. *IUBMB Life*. 2018;70(5):437-444.
13. Zheng X, Chopp M, Lu Y, Buller B, Jiang F. MiR-15b and miR-152 reduce glioma cell invasion and angiogenesis via NRP-2 and MMP-3. *Cancer Lett*. 2013;329(2):146-154.
14. Geretti E, Klagsbrun M. Neuropilins: novel targets for anti-angiogenesis therapies. *Cell Adh Migr*. 2007;1(2):56-61.
15. Johnson MD, O'Connell M, Vito F, Bakos RS. Increased STAT-3 and synchronous activation of Raf-1-MEK-1-MAPK, and phosphatidylinositol 3-Kinase-Akt-mTOR pathways in atypical and anaplastic meningiomas. *J Neurooncol*. 2009;92(2):129-135.
16. Ragel BT, Jensen RL. Aberrant signaling pathways in meningiomas. *J Neurooncol*. 2010;99(3):315-324.
17. Hou Z, Yin H, Chen C, et al. microRNA-146a targets the L1 cell adhesion molecule and suppresses the metastatic potential of gastric cancer. *Mol Med Rep*. 2012;6(3):501-506.
18. Zhao JL, Rao DS, Boldin MP, Taganov KD, O'Connell RM, Baltimore D. Nf-B dysregulation in microRNA-146a-deficient mice drives the development of myeloid malignancies. *Proc Natl Acad Sci USA*. 2011;108(22):9184-9189.
19. Antal O, Hackler L, Jr, Shen J, et al. Combination of unsaturated fatty acids and ionizing radiation on human glioma cells: cellular, biochemical and gene expression analysis. *Lipids Health Dis*. 2014;13:142.
20. Xiang M, Birkbak NJ, Vafaizadeh V, et al. Stat3 induction of mir-146b forms a feedback loop to inhibit the Nf-B to il-6 signaling axis and stat3-driven cancer phenotypes. *Sci Signal*. 2014;7(310):ra11.
21. Johnson M, O'Connell M, Walter K. STAT3 activation and risk of recurrence in meningiomas. *Oncol Lett*. 2017;13(4):2432-2436.
22. Ye EA, Steinle JJ. miR-146a suppresses STAT3/VEGF pathways and reduces apoptosis through IL-6 signaling in primary human retinal microvascular endothelial cells in high glucose conditions. *Vision Res*. 2017;139:15-22.
23. Epis MR, Giles KM, Candy PA, Webster RJ, Leedman PJ. miR-331-3p regulates expression of neuropilin-2 in glioblastoma. *J Neurooncol*. 2014;116(1):67-75.
24. Epis MR, Giles KM, Barker A, Kendrick TS, Leedman PJ. miR-331-3p regulates ERBB-2 expression and androgen receptor signaling in prostate cancer. *J Biol Chem*. 2009;284(37):24696-24704.
25. Epis MR, Giles KM, Kalinowski FC, Barker A, Cohen RJ, Leedman PJ. Regulation of expression of deoxyhypusine hydroxylase (DOHH), the enzyme that catalyzes the activation of eIF5A, by miR-331-3p and miR-642-5p in prostate cancer cells. *J Biol Chem*. 2012;287(42):35251-35259.
26. Chen L, Ma G, Cao X, An X, Liu X. MicroRNA-331 inhibits proliferation and invasion of melanoma cells by targeting astrocyte-elevated gene-1. *Oncol Res*. published online: February 17, 2018 (doi:10.3727/096504018X15186047251584).
27. Guo X, Guo L, Ji J, et al. miRNA-331-3p directly targets E2F1 and induces growth arrest in human gastric cancer. *Biochem Biophys Res Commun*. 2010;398(1):1-6.
28. Zhao D, Sui Y, Zheng X. MiR-331-3p inhibits proliferation and promotes apoptosis by targeting HER2 through the PI3K/Akt and ERK1/2 pathways in colorectal cancer. *Oncol Rep*. 2016;35(2):1075-1082.
29. White NM, Youssef YM, Fendler A, Stephan C, Jung K, Yousef GM. The miRNA-kallikrein axis of interaction: a new dimension in the pathogenesis of prostate cancer. *Biol Chem*. 2012;393(5):379-389.
30. Miller R, Jr, DeCandio ML, Dixon-Mah Y, et al. Molecular targets and treatment of meningioma. *J Neurol Neurosurg*. 2014;1(1):1000101.
31. Park KJ, Yu MO, Song NH, et al. Expression of astrocyte elevated gene-1 (AEG-1) in human meningiomas and its roles in cell proliferation and survival. *J Neurooncol*. 2015;121(1):31-39.
32. Karsy M, Azab MA, Abou-Al-Shaar H, et al. Clinical potential of meningioma genomic insights: a practical review for neurosurgeons. *Neurosurg Focus*. 2018;44(6):E10.
33. Clark VE, Harmancı AS, Bai H, et al. Recurrent somatic mutations in POLR2A define a distinct subset of meningiomas. *Nat Genet*. 2016;48(10):1253-1259.
34. Zhang Z, Zhuang L, Lin CP. Roles of MicroRNAs in establishing and modulating stem cell potential. *Int J Mol Sci*. 2019;20(15):E3643.
35. Ressel A, Fichte S, Brodhun M, Rosahl SK, Gerlach R. WHO grade of intracranial meningiomas differs with respect to patient's age, location, tumor size and peritumoral edema. *J Neurooncol*. 2019;145(2):277-286.

Supplemental digital content *is available for this article at www.neurosurgery-online.com.*

Supplemental Digital Content 1. Text. Detailed description of the RNA extraction procedure, miRNA array, TaqMan qPCR assay, and statistical analyses.

Supplemental Digital Content 2. Figure. miRNA markers selected for further experimental phases according to the screening phase. Characteristics from a univariate Cox regression model of time to relapse are visualized as a forest plot. HR, hazard ratio.

Supplemental Digital Content 3. Figure. miRNA references: stable expression of the 4 miRNAs identified in the screening phase presented as a heat map.

Supplemental Digital Content 4. Figure. miRNA references measured within training phase using qPCR. T-test revealed miR-181b-5p as the molecule with the most stable expression among MRR^+ and MRR^- samples. MRR^+, primary samples of meningiomas with evidence of radiographic recurrence up to 8 years after surgery; MRR^-, primary samples of meningiomas without evidence of radiographic recurrence up to 8 years after surgery.

Supplemental Digital Content 5. Table. Description of the studies reporting a link between aberrant miRNA expression and meningioma recurrence.[7-9]

APPENDIX 2

Neurosurgery

Transcriptomic Profiling Revealed Lnc-GOLGA6A-1 as a Novel Prognostic Biomarker of Meningioma Recurrence

--Manuscript Draft--

Manuscript Number:	
Article Type:	Research-Laboratory
Section/Category:	Tumor
Corresponding Author:	Josef Srovnal, MD, PhD Palacký University, Olomouc Olomouc, Czech Republic CZECH REPUBLIC
Order of Authors:	Hanus Slavik, MSc.
	Vladimir Balik, MD, PhD
	Filip Zavadil Kokas, PhD
	Rastislav Slavkovsky, PhD
	Jana Vrbkova, PhD
	Alona Rehulkova, MD
	Tereza Lausova
	Jiri Ehrmann, MD, Professor
	Sona Gurska, PhD
	Ivo Uberall, PhD
	Marian Hajduch, MD, PhD
	Josef Srovnal, MD, PhD
Manuscript Region of Origin:	CZECH REPUBLIC
Abstract:	Background Meningioma is the most common primary central nervous system neoplasm, accounting for about a third of all brain tumors. As their growth rates and prognosis cannot be accurately estimated, biomarkers that enable prediction of their biological behavior would be clinically beneficial. Objective Identification of coding and non-coding RNAs crucial in meningioma prognostication and pathogenesis. Methods Total RNA was purified from FFPE tumor samples of 64 meningioma patients with distinct clinical characteristics (16 recurrent, 30 non-recurrent with follow-up > 5 years, and 18 with follow-up < 5 years without recurrence). Transcriptomic sequencing was performed using the HiSeq 2500 platform (Illumina) and biological and functional differences between meningiomas of different types were evaluated by analyzing differentially expression of mRNA and lncRNA. The prognostic value of 11 differentially expressed RNAs was then validated in an independent cohort of 90 patients using RT-qPCR. Results In total, 69 mRNAs and 108 lncRNAs exhibited significant differential expression between recurrent and non-recurrent meningiomas. Differential expression was also observed with respect to sex (12 mRNAs and 59 lncRNAs), WHO grade (58 mRNAs

	and 98 lncRNAs), and tumor histogenesis (79 mRNAs and 76 lncRNAs). Lnc-GOLGA6A-1, ISLR2, and AMH showed high prognostic power for predicting meningioma recurrence, while lnc-GOLGA6A-1 was the most significant factor for recurrence risk estimation (1/HR = 1.31; p = 0.002). Conclusion Transcriptomic sequencing revealed specific gene expression signatures of various clinical subtypes of meningioma. Expression of the lnc-GOLGA61-1 transcript was found to be the most reliable predictor of meningioma recurrence.
Suggested Reviewers:	Marc Sindou, MD, professor Hopital Neurologique et Neurochirurgical Pierre Wertheimer marc.sindou@chu-lyon.fr Expert in meningiomas surgery involving major dural sinuses.
	Ryan Ormond, MD, professor University of Colorado Denver University of Colorado Medicine david.ormond@ucdenver.edu Expert in meningiomas genetics.
	Yilin Yang, MD, professor Third Affiliated Hospital of Soochow University: Changzhou First People's Hospital yilinyang.czfph@gmail.com Expert in meningioma genetics.
Opposed Reviewers:	
Additional Information:	
Question	Response
Significance of the Work: Please include a brief statement summarizing the significance of the work and in particular how it differs from and advances existing literature.	Despite their homogeneity, growth rates of meningiomas vary. This suggests the existence of key regulators that affect their biological behavior independently of their WHO grade. The study provides evidence that coding and non-coding RNAs might play such a regulatory role. Significant differential expression of mRNAs and lncRNAs was observed between recurrent and non-recurrent tumors of differing WHO grades. Expression of the lnc-GOLGA61-1 transcript was found to be a more reliable predictor of meningioma recurrence than well-known predictors including WHO grades and the extent of surgical resection. Furthermore, transcripts encoding developmental and homeobox-related genes were differentially expressed in lesions with different proposed histogenesis, providing the first evidence of transcriptomic differences between meningiomas with different developmental origins. Further analysis of the biological processes associated with these differentially expressed transcripts may reveal pathways that could be targeted by innovative therapies.
Compliance with Research Reporting Guidelines: *Neurosurgery* endorses several reporting guidelines and requires authors to submit their research articles in accordance with the appropriate guideline statement(s) and checklist(s). Completed applicable checklists and flow diagrams must be included with submissions. Research articles that must be submitted according to the appropriate reporting guideline(s) include, but are not limited to: randomized trials, systematic reviews, meta-analyses of interventions, meta-	Yes - Submission Adheres to Appropriate Reporting Guideline(s) and Applicable Checklists/Materials Are Included

analyses of observational studies, diagnostic accuracy studies, and observational epidemiological studies (eg, case series, cohort, case-control, and cross-sectional studies). Consult the EQUATOR Network, which maintains a useful, up-to-date list of guidelines as they are published, with links to articles and checklists: http://www.equator-network.org. Please confirm below that information is reported according to the relevant reporting guideline(s) and any required materials are included with the submission:	
Please indicate which reporting guideline(s) the study adheres to (eg, STROBE, PRISMA, CONSORT). as follow-up to "**Compliance with Research Reporting Guidelines**: *Neurosurgery* endorses several reporting guidelines and requires authors to submit their research articles in accordance with the appropriate guideline statement(s) and checklist(s). Completed applicable checklists and flow diagrams must be included with submissions. Research articles that must be submitted according to the appropriate reporting guideline(s) include, but are not limited to: randomized trials, systematic reviews, meta-analyses of interventions, meta-analyses of observational studies, diagnostic accuracy studies, and observational epidemiological studies (eg, case series, cohort, case-control, and cross-sectional studies). Consult the EQUATOR Network, which maintains a useful, up-to-date list of guidelines as they are published, with links to articles and checklists: http://www.equator-network.org. Please confirm below that information is reported according to the relevant reporting guideline(s) and any required materials are included with the submission:"	STROBE
Statistical Analysis:	Yes

For manuscripts that report statistics, the Editor requires that the authors provide evidence of statistical consultation or expertise. If your article includes statistics, has the information reported been evaluated by an expert?		
Funding Information:	Ministerstvo Zdravotnictví Ceské Republiky (15-29021A)	Mr. Josef Srovnal
	Ministerstvo Školství, Mládeže a Tělovýchovy (LM2018132)	Mr. Josef Srovnal
	Univerzita Palackého v Olomouci (LF 2021_019)	Mr. Josef Srovnal
	Technologická Agentura České Republiky (TN01000013)	Marian Hajduch
	European Regional Development Fund (ENOCH CZ.02.1.01/0.0/0.0/16_019/0000868, ACGT CZ.02.1.01/0.0/0.0/16_026/0008448)	Marian Hajduch
	Ministerstvo Zdravotnictví Ceské Republiky (MMCI, 00209805)	Filip Zavadil Kokas

Full title

Transcriptomic Profiling Revealed Lnc-GOLGA6A-1 as a Novel Prognostic Biomarker of Meningioma Recurrence

Running title

Transcriptomic profiling in meningioma

All authors' full names and highest academic degree(s)

Hanus Slavik, MSc[1], Vladimir Balik, MD, PhD[1,2,3], Filip Zavadil Kokas, PhD[4], Rastislav Slavkovsky, PhD[1], Jana Vrbkova, PhD[1], Alona Rehulkova, MD[1], Tereza Lausova, BSc[1], Jiri Ehrmann, MD, PhD[5], Sona Gurska, PhD[1], Ivo Uberall, PhD[5], Marian Hajduch, MD, PhD[1], Josef Srovnal, MD, PhD[1*]

1. Laboratory of Experimental Medicine, Institute of Molecular and Translational Medicine, Faculty of Medicine and Dentistry, Palacky University and University Hospital Olomouc, Czech Republic
2. Department of Neurosurgery, Svet Zdravia Hospital Michalovce, Michalovce, Slovak Republic
3. Department of Neurosurgery, Faculty of Medicine and Dentistry, Palacky University and University Hospital Olomouc, Czech Republic
4. Research Centre for Applied Molecular Oncology, Masaryk Memorial Cancer Institute, Zluty kopec 7, Brno, 656 53, Czech Republic
5. Department of Clinical and Molecular Pathology, Faculty of Medicine and Dentistry, Palacky University and University Hospital Olomouc, Czech Republic

Contributions: Conception and design: HS, JS, VB. Development of methodology: HS, SG, JS, VB. Processing of the samples: TL, HS, AR, IU. Clinical data acquisition and management: VB, JE, IU, JS, JV. Acquisition of experimental data: HS, RS, AR, SG. Analysis and interpretation of data: FZK, JV, HS, JS. Writing, review and revision of the manuscript: VB, HS, FZK, RS, JV, MH. Supervision and funding reinsurance: MH, JS. All authors read and approved the final manuscript.

Details of previous presentation(s)

The authors certify that the present work has not been published previously, nor was considered for publication elsewhere in whole or in part in any language.

Disclosure of funding received for this work

This study was supported by Ministry of Health of the Czech Republic (15-29021A), Ministry of Education, Youth and Sport of the Czech Republic (LM2018132), Palacky University Olomouc (LF 2021_019), Technological Agency of the Czech Republic (TN01000013), European Regional Development Fund (ENOCH CZ.02.1.01/0.0/0.0/16_019/0000868, ACGT CZ.02.1.01/0.0/0.0/16_026/0008448), and by the Ministry of Health, Czech Republic - conceptual development of research organization (MMCI, 00209805).

Conflict of interest:

The authors report no conflict of interest concerning the materials or methods used in this study. The authors have no personal, financial or institutional interest in any of the drugs, materials, or devices described in this article.

Acknowledgements

None.

***Corresponding author**

Josef Srovnal, MD, PhD, Institute of Molecular and Translational Medicine, Faculty of Medicine and Dentistry, Palacky University and University Hospital in Olomouc, Hnevotinska 5, 779 00 Olomouc, Czech Republic, Telephone: +420-58-5632137, Fax: +420-58-5632180, e-mail: josef.srovnal@upol.cz; Web: www.imtm.cz

ABSTRACT

Background

Meningioma is the most common primary central nervous system neoplasm, accounting for about a third of all brain tumors. As their growth rates and prognosis cannot be accurately estimated, biomarkers that enable prediction of their biological behavior would be clinically beneficial.

Objective

Identification of coding and non-coding RNAs crucial in meningioma prognostication and pathogenesis.

Methods

Total RNA was purified from FFPE tumor samples of 64 meningioma patients with distinct clinical characteristics (16 recurrent, 30 non-recurrent with follow-up > 5 years, and 18 with follow-up < 5 years without recurrence). Transcriptomic sequencing was performed using the HiSeq 2500 platform (Illumina) and biological and functional differences between meningiomas of different types were evaluated by analyzing differentially expression of mRNA and lncRNA. The prognostic value of 11 differentially expressed RNAs was then validated in an independent cohort of 90 patients using RT-qPCR.

Results

In total, 69 mRNAs and 108 lncRNAs exhibited significant differential expression between recurrent and non-recurrent meningiomas. Differential expression was also observed with respect to sex (12 mRNAs and 59 lncRNAs), WHO grade (58 mRNAs and 98 lncRNAs), and tumor histogenesis (79 mRNAs and 76 lncRNAs). Lnc-GOLGA6A-1, ISLR2, and AMH showed high prognostic power for predicting meningioma recurrence, while lnc-GOLGA6A-1 was the most significant factor for recurrence risk estimation (1/HR = 1.31; p = 0.002).

Conclusion

Transcriptomic sequencing revealed specific gene expression signatures of various clinical subtypes of meningioma. Expression of the lnc-GOLGA61-1 transcript was found to be the most reliable predictor of meningioma recurrence.

Keywords

Meningioma, recurrence, mRNA, lncRNA, prognosis

Short title

Transcriptomic profiling in meningioma

Abbreviations

FFPE = Formalin-fixed and paraffin-embedded; HR = Hazard ratio; lncRNA = Long non-coding ribonucleic acid; mRNA = Messenger ribonucleic acid; NGS = Next-generation sequencing; RNA-seq = RNA / transcriptomic sequencing; RT-qPCR = Reverse transcription quantitative (real-time) polymerase chain reaction; TTR = Time-to-recurrence; WHO = World Health Organization.

INTRODUCTION

Meningiomas are among the most common intracranial tumors and are believed to arise from the highly metabolically active arachnoid cap cells of the leptomeninges, although this hypothesis has never been proven. According to Kalamarides et al., 2011, meningiomas originate in meningeal precursor cells with high expression of prostaglandin D synthase (PGDS).[1] Many aspects of these tumors are not fully explained, including their hormone dependence, higher incidence in females [2], and the fact that some meningiomas recur even after total resection and despite having benign histopathological features.[3] To help explain these observations, we here report transcriptomic differences between various clinical types of meningioma and simultaneous differential analysis of messenger RNA (mRNA) and long non-coding RNA (lncRNA) transcripts from formalin-fixed and paraffin-embedded (FFPE) tissue samples. Additionally, we use quantitative reverse transcription PCR (RT-qPCR) to validate selected mRNA and long-non-coding RNA (lncRNA) transcripts as potential biomarkers of prognosis in meningioma patients. There is a growing body of evidence that products of the non-coding genome are important in tumor prognosis and biology.[4] However, little is known about the functional and biological significance of lncRNAs.[5] We therefore believe that simultaneous analysis of mRNA and lncRNA can provide clearer biological insight and potentially reveal greater numbers of clinically applicable biomarkers and actionable therapeutic targets than would be possible by analyzing mRNA transcripts alone.

MATERIAL AND METHODS

Patients

The study was approved by the Institutional Research Ethics Committee. Comprehensive clinical-pathological data were mined for the study's participants, all of whom signed informed consent forms. Recurrence after total or gross total (Simpson grade I, II, or III) and incomplete (Simpson grade > III) resection was defined as reappearance of the meningioma or any growth of remaining meningiomal tissue detected during follow-up imaging after primary surgery. Patients with no such events after > 5 years' follow-up were considered non-recurrent. In total, 64 tumor samples were subjected to transcriptomic sequencing (RNA-seq) and 90 samples was used for RT-qPCR validation. Detailed information on the cohorts is provided in Table 1 and Fig. 1A.

RNA purification and quality assessment

Total RNA was purified from FFPE tumor samples in the same way as we reported previously.[6] RNA concentration and quality were assessed using a Nanodrop ND 1000 instrument (Thermo Fisher Scientific) and a Bioanalyzer 2100 using RNA Pico Kit and Chips (Agilent) according to the manufacturer's instructions. Only samples with $DV_{200}(\%) \geq 30$ were selected for the subsequent RNA-seq analysis.

Transcriptomic sequencing by NGS (RNA-seq)

Prepared cDNA libraries (TruSeq Stranded Total RNA Library Prep Kit with Ribo-Zero Gold - Set A, Illumina) were denatured, pooled, and sequenced on a HiSeq 2500 instrument using the Illumina TruSeq SR Cluster Kit v3 - cBot – HS and TruSeq SBS Kit v3 - HS (50-cycles) kits (Supplementary Methods S1).

RT-qPCR validation

Reverse transcription was performed separately prior to qPCR analysis (Supplementary Methods S1). The qPCR analyses were performed on a LightCycler 480 thermal cycler (Roche) using TaqMan Gene Expression Assays (Thermo Fisher Scientific) according to the manufacturer's instructions in 10 µl volumes.

93

94 **Data processing and statistical methods**

95 All sequencing data were processed using the bioinformatics pipeline outlined in Supplementary
96 Methods S1. Connections between mRNAs based on protein homology, co-expression, and
97 interactions were visualized using the free web-tool String version 11.0.[7] Connections between
98 mRNAs and lncRNAs based on their chromosomal coordinates, reflecting potential lncRNA *cis*
99 regulatory targets,[5] are also shown in the presented networks. Gene expression data from the RT-
100 qPCR validation phase were processed using the ΔCt method and further analyzed using univariate
101 and multivariate Cox regression models of time-to-recurrence (TTR) implemented in the R
102 software package (www.r-project.org).

103

104 **RESULTS**

105 Differentially expressed coding and non-coding transcripts with $\log_2$ fold change > 2 or < -2 and
106 adjusted p-value (q-value) < 0.05 were analyzed further. The numbers of differentially expressed
107 transcripts and their overlaps between the studied comparisons are summarized in Fig. 1B, and
108 more detailed information on their expression is presented in Supplementary Results S2. Although
109 Panther pathway analyses[8; 9] yielded no statistically significant results, we considered a pathway
110 to exhibit potential differential activity with respect to a given comparison if at least 2 genes
111 belonging to that pathway were differentially expressed within that comparison (Supplementary
112 Results S2). The differentially expressed RNAs considered to be most prognostically relevant
113 (selected according to q-value and $\log_2$ fold change concerning recurrence and/or WHO grade)
114 were validated in an independent cohort. All transcriptomic data are publicly available at
115 https://www.ncbi.nlm.nih.gov/sra/PRJNA705586 (BioProject ID: PRJNA705586).

116

117 **Recurrence**

118 We identified 69 mRNAs and 108 lncRNAs that were differentially expressed in primary tumors
119 of recurrent and non-recurrent patients (Fig. 2A). Most of the corresponding genes lie on
120 chromosomes 1-8, but there were also five X-chromosomal lncRNAs and one X-chromosomal
121 mRNA (XPNPEP2) (Fig. 2B). Based on functional annotation clustering, the coding genes were
122 divided into ten clusters representing various biological functions and roles (Fig. 2C).
123 Interestingly, developmental genes, immunoglobulin-like and ATP-binding genes were also

differentially expressed in tumors of different histogenetic origin. Pathway analysis indicated that only a few of the significantly differentially expressed mRNAs belong to common pathways. These are the angiogenesis; the Wnt signaling and purine metabolism pathways. However, only the angiogenesis and Wnt signaling pathways were associated with transcripts exhibiting differential expression in other comparisons. Six exceptionally strongly differentially expressed ($q < 0.001$) RNAs were selected for further validation and evaluation of their prognostic value. These are HEPACAM2, lnc-FAT1-3, lnc-MAST4-5, TDRD1, ISLR2, and lnc-GOLGA6A-1.

Histogenesis

We identified 79 mRNAs and 76 lncRNAs exhibiting differential expression between mesodermal lesions and those arising from the neural crest, most of which were closely connected (Fig. 3). The only significantly up-regulated group of RNAs in mesodermal tumors were homeobox-related transcripts; the majority of the remaining transcripts were down-regulated. However, a few non-homeobox-related transcripts (4 mRNAs and 11 lncRNAs) were up-regulated in mesodermal tumors. Chromosomes 1, 7, and 17 had the greatest numbers of mapped transcripts exhibiting differential expression with respect to histogenesis; in addition, there were 3 differentially expressed X-chromosomal mRNAs (Supplementary Fig. S3A). Functionally, these transcripts were linked to angiogenesis, blood coagulation, neural and general development, and 4 were associated with Wnt signaling.

Sex

There were 59 non-coding and 12 coding transcripts that were expressed differentially in males and females (Supplementary Fig. S4 and S5). As expected, most of these transcripts were localized to the Y chromosome. However, two autosomal coding genes, S100B and NTM, were also identified. Both of them are associated with neural development, and especially with neurite outgrowth (Supplementary Fig. S4). S100B also exhibited differential expression with respect to WHO grade and tumor recurrence, and was therefore selected for further validation. In addition, seven autosomal and 5 X-chromosomal lncRNAs were differentially expressed between males and females (Supplementary Fig. S5).

WHO grades

Because of the low number of WHO grade III tumors (3 patients) in our cohort, the WHO grade II (17 patients) and WHO grade III groups were merged and compared to the WHO grade I group (44 patients), as it was performed in recently published genomic [10; 11] and proteomic [12] original studies and reviews [13]. In total, 58 mRNAs and 98 lncRNAs exhibited differential expression with respect to tumor grade (Fig. 1 and Supplementary Results S2). Most of them were mapped to chromosomes 2, 5 and 12 (Supplementary Fig. S3B). Functional annotation clustering revealed 11 common functional patterns among the differentially expressed mRNAs (Fig. 4). Three of the differentially expressed RNAs (AMH, ECEL1 and CCAT2) were selected for further validation. Moreover, CPE was also selected for validation because it was specifically down-regulated in grade III tumors ($q < 0.001$).

RT-qPCR validation of selected hits

S100B exhibited qualitatively different expression between males and females (Pearson's test, $p = 0.013$) but there was no significant quantitative difference. Female samples were found to be S100B-positive more frequently (78.9%) than samples from males (51.5%). Lnc-MAST4-5 exhibited qualitatively reduced expression in groups with unfavorable prognosis (Fig. 5A). Three other validated transcripts also exhibited significantly higher expression in males than in females, namely AMH (Student's t-test, $p = 0.004$), ISLR2 (Student's t-test, $p = 0.003$) and lnc-GOLGA6A-1 (Wilcoxon exact test, $p = 0.008$).

The only validated transcript exhibiting significant qualitative (Pearson's test, $p = 0.036$) and quantitative (Student's t-test, $p = 0.045$) differences in expression between samples of different WHO grades was lnc-MAST4-5 (Fig. 5A and 5B). However, it should be noted that grading of meningiomas is often burdened with high subjective error. This may explain why only lnc-MAST4-5 showed any significant correlation with WHO grades.

Among recurrent patients, ISLR2, lnc-GOLGA6A-1, and AMH were strongly up-regulated and their expression patterns were correlated across the entire cohort (the correlation coefficient r varied from 0.72 to 0.85) with high significance ($p < 0.001$; Fig. 5C). ISLR2 and lnc-GOLGA6A-1 were mapped to the same locus and are both controlled by the regulatory sequence GH15J074130. Additionally, ISLR2, lnc-GOLGA6A-1, and AMH are regulated by many common transcription factors including KLF4 (Fig. 5C). *KLF4* was previously reported to carry activating mutations in meningiomas. [14]

Cox regression models with adjustments for clinical factors revealed ISLR2, lnc-GOLGA6A-1, and AMH all significantly influenced time-to-relapse (TTR) survival (Supplementary Table S6). The final multivariate model was created by stepwise selection and featured lnc-GOLGA6A-1 as the sole significant recurrence risk factor, with 1/HR = 1.31 and p = 0.002. A model in which the clinical factors were fixed was identical to the adjusted univariate model for lnc-GOLGA6A-1 (Supplementary Table S6). The modeling procedure and final models are summarized in Fig. 5D. TTR survival was analyzed separately for patients expressing lnc-GOLGA6A-1 at low and high levels. High expression was determined based on a ΔCt cut-off value computed using the maximally selected rank statistics method implemented in the survminer R package. Meningioma patients whose expression of lnc-GOLGA6A-1 was below the cut-off (ΔCt > 2.34) had significantly longer TTR survival (p = 0.001; Fig. 5E).

DISCUSSION

Despite the considerable diagnostic and therapeutic potential of strategies targeting epigenetic factors, only a few studies have examined the relationship between lncRNA expression and meningioma.[14] The importance of lncRNAs and Wnt signaling in meningiomas was previously highlighted.[15; 16] Another study that applied RNA-seq to FFPE canine samples confirmed that angiogenesis and Wnt signaling are crucial in meningioma formation.[17] Our results confirmed that genes associated with Wnt signaling and angiogenesis are expressed differentially in recurrent and non-recurrent patients.

The eleven transcripts were selected for independent RT-qPCR validation in our study. The selection was based on the high level of deregulation and biologically activity. Three of them (HEPACAM2, TDRD1, and lnc-FAT1-3) were not successfully analyzed, probably because of the limited ability of RT-qPCR methods to accurately quantify the heavily degraded RNA in the archived FFPE samples. Another two potential markers, CCAT2 and S100B, did not exhibit significant differences in expression between primary recurrent and non-recurrent tumors in the RT-qPCR validation cohort. S100B serum level was previously associated with poor outcomes in patients after meningioma resection.[18] However, its expression is also affected by brain injury and the course of surgery, which may introduce bias when comparing results across different patient cohorts.

ISLR2 and lnc-GOLGA61-1 showed similar expression patterns in both the RNA-seq and RT-qPCR validation cohorts; in both cases, their levels were higher in groups with unfavorable prognosis. This phenomenon was previously observed in neuroblastomas, where *ALK* mutation and *MYCN* amplification were both associated with elevated lnc-GOLGA61-1 levels. [19] Also, hypermethylation of the promotor region for lnc-GOLGA61-1 was associated with improved survival of IDH1 wild-type glioblastoma patients. [20] These findings strongly support the importance of lnc-GOLGA61-1 oncogenic features in brain tumors. This lncRNA showed the strongest prognostic power in meningioma recurrence estimation, but its physiological function remains unknown. Available tools for functional and interaction annotation didn't show any record of lnc-GOLGA61-1 [21] but *de novo* mechanistic elucidation of function of identified lncRNAs was not the aim of this study. Interestingly, AMH expression also correlated with that of ISLR2 and lnc-GOLGA61-1 in the RT-qPCR validation cohort; this may indicate that they are regulated by common transcription factors, as we showed (Fig. 5C). Our data also indicate that lnc-MAST4 is down-regulated in patient groups with unfavorable prognosis (Fig. 2A and 5A). However, lnc-MAST4-5 exhibited low basal expression during the RT-qPCR experiments and therefore exhibited significant differences at the qualitative level. This potential prognostic biomarker should be validated in future using non-FFPE samples with higher RNA.

To our knowledge, this is the first study to examine differences in expression profiles between meningiomas of different histogenetic origin. Regional variability in meningeal histogenesis with various meningeal progenitors suggests playing a role in meningioma development and their variable behavior. [1] The precursor is of mesoderm origin at the skull base and neural crest-derived at the convexity. [1] During the early prenatal stage, there is a neural crest-mesodermal interface where the frontal neural crest-derived and parietal mesoderm-derived bones meet. When the telencephalon begins to expand caudally, it carries this borderline with it. [22] The neural crest-derived meninges thus extend from the convexity to the posterior/caudal edge of cerebral hemispheres, whereas the meningeal layers of the posterior cranial fossa (around the brainstem and spinal cord) arise from the mesoderm. [23] Meningiomas localized on the convexity have less favorable prognosis because neural crest-derived cells have a higher capacity for migration, proliferation and differentiation. Tumors arising from the neural crest are therefore more likely to be aggressive and malignant. [24] Consequently, it is unsurprising that developmental and homeobox-related transcripts, which are also involved in ontogenetic development, were

differentially expressed among tumors with different proposed histogenesis in our study (Fig. 3). This together with the high interconnectedness of the differentially expressed genes supports the theory that the ontogenetic origin of the tissue from which a meningioma arises is biologically and clinically relevant.

However, this study is burdened by several limitations resulting from its retrospective nature. Firstly, availability and quality of biological material and a paucity of detailed information, such as loss of patients in follow-up or follow-up period less than 5 years in a significant number of cases, have been reasons for the relatively small numbers of patients in the RNA-seq and RT-qPCR validation cohorts. Secondly, as various tumor locations or the extent of tumor involvement of surrounding structures were not adjusted for in RNA-seq cohort (Supplementary Table S7), prospective analyses are warranted to validate the role of lncRNAs after adjustment of these factors.

The final aspect value to mention is the sex distribution of meningiomas. Non-malignant meningiomas occur more frequently in women (2.3:1). [25] Additionally, WHO grade I meningiomas were significantly more frequent in females[10], whereas WHO grade II and III lesions were observed more frequently in males. [26] The greater frequency of higher-grade lesions in men was reflected in sex-specific differences in DNA methylation profiles. [27] In keeping with these results, our data indicated that the prognostically unfavorable markers ISLR2, lnc-GOLGA61-1, and AMH were expressed more strongly in males while the prognostically favorable S100B was expressed more strongly in females.

CONCLUSION

Profiling of coding and non-coding RNA in meningiomas among clinically relevant subgroups revealed the long non-coding RNA lnc-GOLGA61-1 to be of strong prognostic relevance. Moreover, distinct transcriptomic signatures of meningiomas in male and female patients and signatures associated with different histogenetic origins have been revealed for the first time. Finally, we outlined a possible regulatory role of lnc-GOLGA61-1 and other non-coding RNAs such as lnc-MAST4-5 in meningiomas.

REFERENCES

1. Kalamarides M, Stemmer-rachamimov A, Niwa-kawakita M, et al. Identification of a progenitor cell of origin capable of generating diverse meningioma histological subtypes. *Oncogene*. 2011;30(20):2333-2344. 10.1038/onc.2010.609

2. Korhonen K, Salminen T, Raitanen J, Auvinen A, Isola J, Haapasalo H. Female predominance in meningiomas can not be explained by differences in progesterone, estrogen, or androgen receptor expression. *Journal of neuro-oncology*. 2006;80(1):1-7. 10.1007/s11060-006-9146-9

3. Rogers L, Barani I, Chamberlain M, et al. Meningiomas: knowledge base, treatment outcomes, and uncertainties. A RANO review. *Journal of Neurosurgery*. 2015;122(1):4-23. 10.3171/2014.7.jns131644

4. Rao A, Rajkumar T, Mani S. Perspectives of long non-coding RNAs in cancer. *Molecular Biology Reports: An International Journal on Molecular and Cellular Biology*. 2017;44(2):203-218. 10.1007/s11033-017-4103-6

5. Quinn J, Chang H. Unique features of long non-coding RNA biogenesis and function. *Nature reviews. Genetics*. 2016;17(1):47-62. 10.1038/nrg.2015.10

6. Slavik H, Balik V, Vrbkova J, et al. Identification of Meningioma Patients at High Risk of Tumor Recurrence Using MicroRNA Profiling. *Neurosurgery*. 2020;87(5):1055–1063. 10.1093/neuros/nyaa009

7. Szklarczyk D, Gable A, Lyon D, et al. STRING v11: protein-protein association networks with increased coverage, supporting functional discovery in genome-wide experimental datasets. *Nucleic acids research*. 2019;47(D1):D607-D613. 10.1093/nar/gky1131

8. Thomas P, Campbell M, Kejariwal A, et al. Panther: A Library of Protein Families and Subfamilies Indexed by Function. *Genome Research*. 2003;13(9):2129-2141. 10.1101/gr.772403

9. Thomas P, Kejariwal A, Guo N, et al. Applications for protein sequence-function evolution data: mRNA/protein expression analysis and coding SNP scoring tools. *Nucleic acids research*. 2006;34(Web Server issue):W645-650. 10.1093/nar/gkl229

10. Bi W, Greenwald N, Mei Y, et al. Genomic landscape of high-grade meningiomas. *npj Genomic Medicine*. 2017;2(1):525-535. 10.1038/s41525-017-0014-7

11. Youngblood M, Miyagishima D, Jin L, et al. Associations of Meningioma Molecular Subgroup and Tumor Recurrence. *Neuro-oncology*. 2020;23(5):783-794. 10.1093/neuonc/noaa226

12. Papaioannou M, Djuric U, Kao J, et al. Proteomic analysis of meningiomas reveals clinically-distinct molecular patterns. *Neuro-oncology*. 2019;21(8):1028–1038. 10.1093/neuonc/noz084

13. Galani V, Lampri E, Varouktsi A, Alexiou G, Mitselou A, Kyritsis A. Genetic and epigenetic alterations in meningiomas. *Clinical Neurology and Neurosurgery*. 2017;158(-):119-125. 10.1016/j.clineuro.2017.05.002

14. Suppiah S, Nassiri F, Bi W, et al. Molecular and translational advances in meningiomas. *Neuro-oncology*. 2019;21(S1):4-17. 10.1093/neuonc/noy178

15. Li T, Ren J, Ma J, et al. LINC00702/miR-4652-3p/ZEB1 axis promotes the progression of malignant meningioma through activating Wnt/β-catenin pathway. *Biomedicine*. 2019;113(1):108718-108718. 10.1016/j.biopha.2019.108718

16. Zhang Y, Yu R, Li Q, et al. SNHG1/miR-556-5p/TCF12 feedback loop enhances the tumorigenesis of meningioma through Wnt signaling pathway. *Journal of Cellular Biochemistry*. 2020;121(2):1880-1889. 10.1002/jcb.29423

17. Grenier J, Foureman P, Sloma E, Miller A. RNA-seq transcriptome analysis of formalin fixed, paraffin-embedded canine meningioma. *PloSone*. 2017;12(10):e0187150. 10.1371/journal.pone.0187150

18. Stranjalis G, Korfias S, Psachoulia C, et al. Serum S-100B as an indicator of early postoperative deterioration after meningioma surgery. *Clinical chemistry*. 2005;51(1):202-207. 10.1373/clinchem.2004.039719

19. Rombaut D, Chiu H, Decaesteker B, et al. Integrative analysis identifies lincRNAs up- and downstream of neuroblastoma driver genes. *Scientific reports*. 2019;9(1):5685. 10.1038/s41598-019-42107-y

20. Mock A, Geisenberger C, Orlik C, et al. LOC283731 promoter hypermethylation prognosticates survival after radiochemotherapy in IDH1 wild-type glioblastoma patients. *International Journal Of Cancer*. 2016;139(2):424-425. 10.1002/ijc.30069

21. Chen X, Sun Y, Guan N, et al. Computational models for lncRNA function prediction and functional similarity calculation. *Briefings in functional genomics*. 2019;18(1):58-82. 10.1093/bfgp/ely031

22. Jiang X, Iseki S, Maxson R, Sucov H, Morriss-kay G. Tissue origins and interactions in the mammalian skull vault. *Developmental biology*. 2002;241(1):106-16. 10.1006/dbio.2001.0487

23. Balik V. Histological Structure of the Major Dural Sinus Walls in the Posterior Cranial Fossa: A Factor that Might Matter in Dural Sinus Surgery. *World neurosurgery*. 2019;128(-):431-432. 10.1016/j.wneu.2019.05.158

24. Maguire L, Thomas A, Goldstein A. Tumors of the Neural Crest: Common Themes in Development and Cancer. *DEVELOPMENTAL DYNAMICS*. 2015;244(3):311-322. 10.1002/dvdy.24226

25. Ostrom Q, Gittleman H, Liao P, et al. CBTRUS statistical report: primary brain and central nervous system tumors diagnosed in the United States in 2007-2011. *Neuro-oncology*. 2014;16(4):iv1-63. 10.1093/neuonc/nou223

26. Clark V, Erson-omay E, Caglayan A, et al. Genomic Analysis of Non-NF2 Meningiomas Reveals Mutations in TRAF7, KLF4, AKT1, and SMO. *Science*. 2013;339(6123):1077-1080. 10.1126/science.1233009

27. Sahm F, Schrimpf D, Stichel D, et al. DNA methylation-based classification and grading system for meningioma: a multicentre, retrospective analysis. *The Lancet. Oncology*. 2017;18(5):682-694. 10.1016/S1470-2045(17)30155-9

278

279 **FIGURE LEGENDS**

280 **Figure 1:** Study summary: (A) Overview of the study's workflow and the cohorts of meningioma
281 patients. (B) Venn diagrams of differentially expressed genes with $\log_2$ fold changes > 2 or < -2
282 and adjusted p-values (q-values) < 0.05 within each patient subgroup. Differential expression is
283 analyzed with respect to recurrence (primary recurrent vs. non-recurrent patients), WHO grade
284 (grades II and III vs. grade I), histogenesis (neural crest vs. mesodermal tumors), and sex (male
285 vs. female patients).

Figure 2: Differentially expressed genes among primary tumors in recurrent and non-recurrent patients. Transcripts upregulated in recurrent patients are shown in blue: (A) Network showing the fold changes, overlaps, transcript types, and connections of differentially expressed transcripts (B) Chromosomal distribution of differentially expressed transcripts. (C) Overview of functional annotation clustering of mRNAs in which the biological significance of each cluster is quantified using enrichment scores.

Figure 3: Differentially expressed genes among tumors arising from neural crest and mesodermal cells showing their fold changes, common biological roles, transcript types, and connections. Transcripts upregulated in neural crest tumors are shown in blue.

Figure 4: Differentially expressed genes in tumors of different WHO grades (WHO grade II+III vs. WHO grade I): Overview of functional annotation clustering of mRNAs in which the biological significance of each cluster is quantified with an enrichment score.

Figure 5: RT-qPCR validation of selected transcripts: (A) Differences in the lnc-MAST4-5 positivity percentage in selected sub-groups. (B) Overview of significantly deregulated transcripts. (C) Transcriptional correlation and regulation of the expression of ISLR2, AMH, and lnc-GOLGA6A-1. (D) Stepwise selection using the Bayesian information criterion leading to the final multivariate Cox regression models for estimation of recurrence risk; HR, hazard ratio. (E) Time-to-recurrence (TTR) survival analysis for patients expressing lnc-GOLGA6A-1 at low and high levels. Recurrence is considered as an event.

SUPPLEMENTARY CONTENT LEGENDS

Supplementary Methods S1: Detailed description of procedures used to prepare cDNA libraries for RNA-seq, sequencing setup with basic technical outputs, procedures for preparing cDNA for RT-qPCR, and processing of all obtained data.

310 **Supplementary Results S2:** List of significantly differentially expressed genes from specific
311 analyses including the raw outputs from Panther pathway analyses.

312 **Supplementary Figure S3:** Chromosomal distribution of differentially expressed transcripts: (A)
313 Chromosomal origin of differentially expressed transcripts according to the histogenetic origin of
314 the tumors (neural crest vs. mesoderm). (B) Chromosomal origin of differentially expressed
315 transcripts according to tumor grade (WHO grade II+III vs. WHO grade I).

316 **Supplementary Figure S4:** Unsupervised hierarchical clustering of 12 differentially expressed
317 mRNAs in males and females based on log-transformed (log2) RNA expression data including
318 chromosomal locations and function.

319 **Supplementary Figure S5:** Unsupervised hierarchical clustering of 59 differentially expressed
320 lncRNAs in males and females based on log-transformed (log2) RNA expression data including
321 chromosomal locations.

322 **Supplementary Table S6:** Univariate Cox regression models of time-to-relapse (TTR) data with
323 adjustment for clinical factors for all transcripts examined in the validation cohort. Factors shown
324 in bold were statistically significant ($p < 0.05$). Hazard ratios (HR) are computed based on ΔCt
325 unit change.

326 **Supplementary Table S7:** Relationships between individual clinical factors, expressed as p-valu

Figure 1

Click here to access/download;Figure;Figure 1.tif

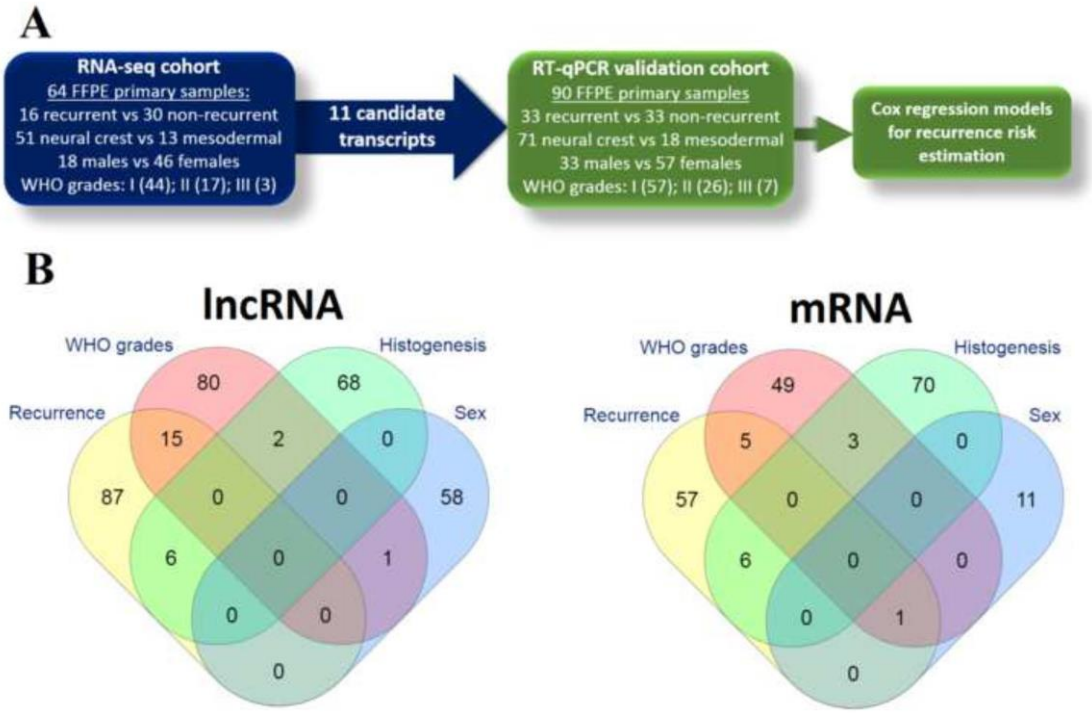

Figure 2

Click here to access/download;Figure;Figure 2.tif

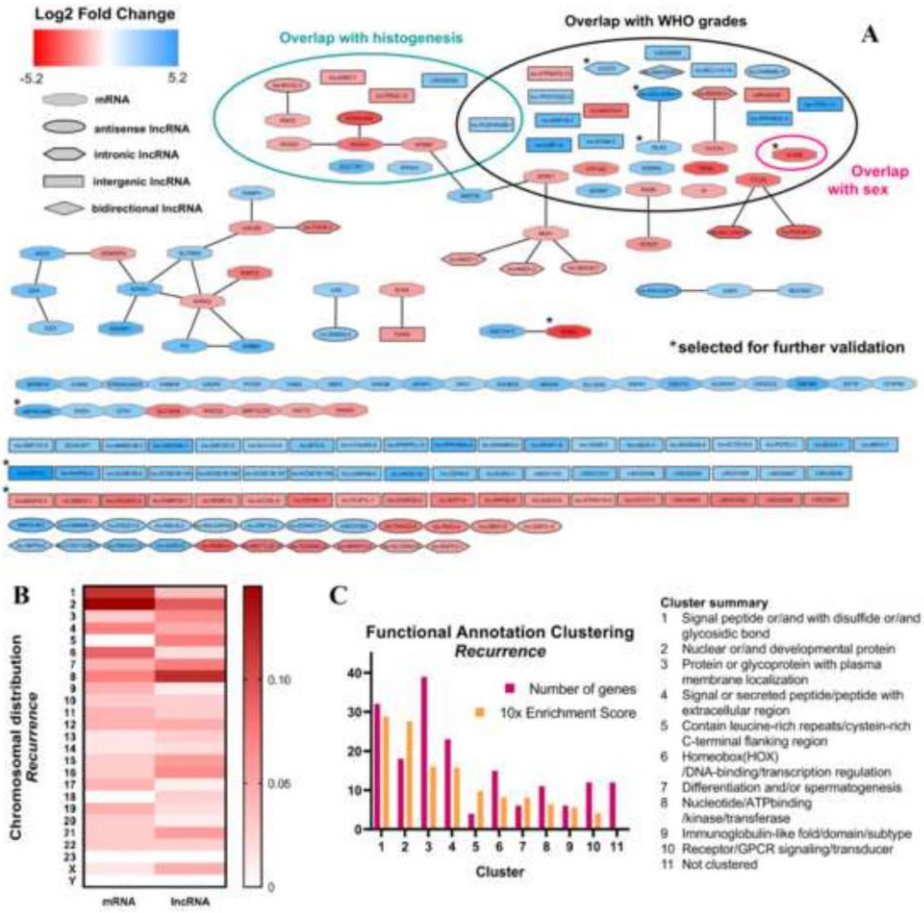

Figure 3

Click here to access/download;Figure;Figure 3.tif

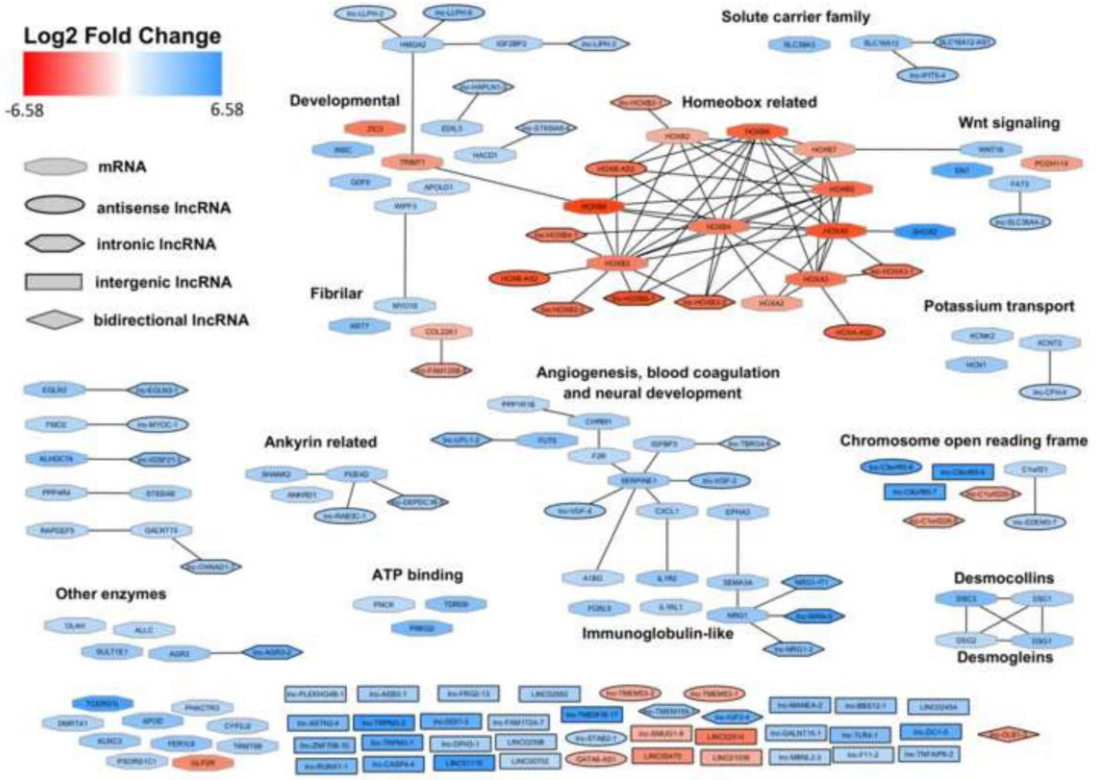

Figure 4

Click here to access/download;Figure;Figure 4.tif

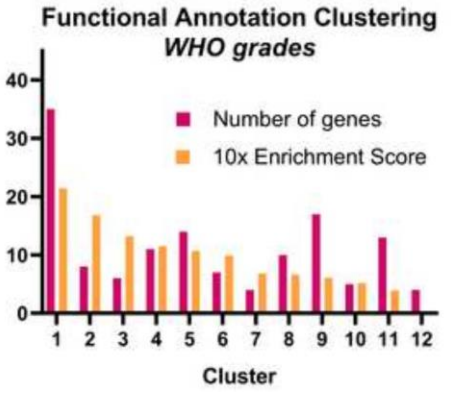

Cluster summary

1 Membrane component or/and with disulfide or/and with glycosidic bond
2 Ion (esp. K+/voltage dependent/channel) transport with BTB/POZ domain
3 C-type lectin-like and carbohydrate bonding
4 Signal-anchor/Golgi apparatus (membrane)/transferase
5 Lipoprotein/chemical synaptic transmission/palmitate
6 Activator/Homeobox (HOX) - DNA-binding region
7 Chemical synaptic transmission/cell junction
8 Secreted and extracellular protein
9 Transcription regulation (esp. from RNA pol II promoter)/HOX/activator
10 Oxidation-reduction process in mitochondrion
11 Metal-binding (esp. Zn)/Zinc-finger
12 Not clustered

Figure 5

Click here to access/download;Figure;Figure 5.tiff

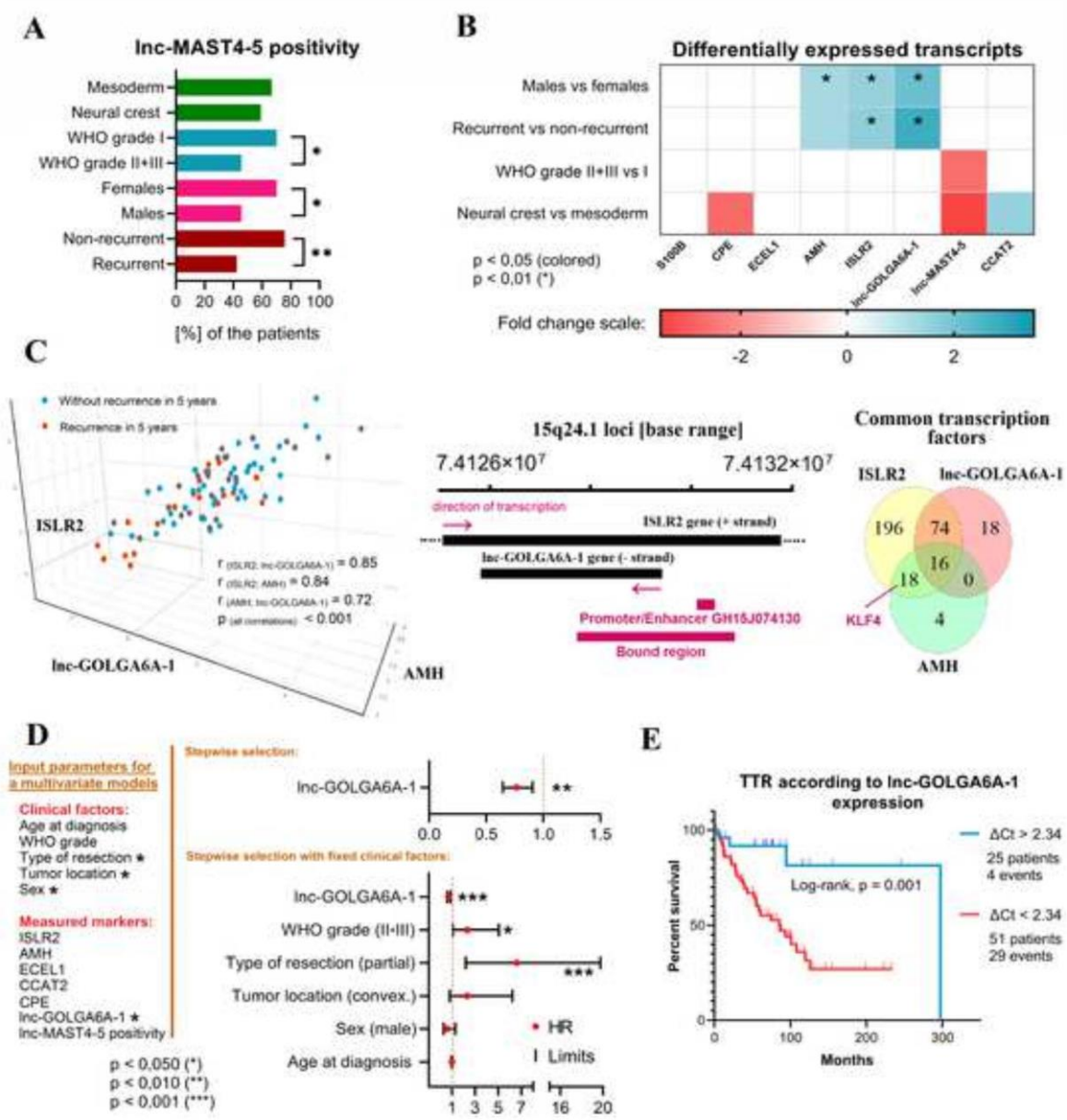

Table 1: The clinical-pathological features of all meningioma patients included in the data set

Cohort (n)		RNA-seq cohort (n = 64)				RT-qPCR validation cohort (n = 90)			
		Non-Recurrent	Recurrent	p-value	Total*	Non-Recurrent	Recurrent	p-value	Total*
Female/Male	n (%)	25/5 (83.3/16.7)	12/4 (75/25)	0.698	46/18 (71.9/28.1)	20/13 (60.6/39.4)	21/12 (63.6/36.4)	1	57/33 (63.3/36.7)
WHO grade I/II-III	n (%)	23/7 (76.7/23.3)	9/7 (56.2/43.8)	0.189	44/20 (68.8/31.2)	26/7 (78.8/21.2)	18/15 (54.5/45.5)	0.068	57/33 (63.3/36.7)
Skull base/ Convexitary meningioma	n (%)	16/14 (53.3/46.7)	7/9 (43.8/56.2)	0.757	32/32 (50/50)	16/17 (48.5/51.5)	10/23 (30.3/69.7)	0.208	45/45 (50/50)
Simpson grade I-III/IV-V	n (%)	27/3 (90/10)	8/7 (53.3/46.7)	0.009	52/11 (82.5/17.5)	28/3 (90.3/9.7)	23/8 (74.2/25.8)	0.184	65/18 (78.3/21.7)
Mesoderm/ Neural crest	n (%)	5/25 (16.7/83.3)	4/12 (25/75)	0.698	13/51 (20.3/79.7)	8/25 (24.2/75.8)	6/26 (18.8/81.2)	0.813	18/71 (20.2/79.8)
Age [years]	median (IQR)	57.5 (47.25-65)	47.5 (38-64.25)	0.235	59.5 (45.75-69.25)	57 (50-62)	54 (47-64)	0.653	57 (47.25-64)
Follow-up [months]	median (IQR)	82.9 (67.87-104.79)	47.8 (29.46-74.15)	0.003	65.9 (38.03-86.84)	95.4 (77.37-127.13)	40 (19.98-85.55)	<0.001	69.4 (33.05-97.97)
Time to relapse#	surv±SE (%)				68±5.6				80±5.7

IQR, interquartile range (1st quartile – 3rd quartile); surv±SE, 5-year survival ± standard error; WHO, World Health Organization; *, including patients with follow-up < 5 years without recurrence; #, Kaplan-Meier estimate of survival at the time of 5 years after surgery

Visual Abstract

Transcriptomic Profiling Revealed Lnc-GOLGA6A-1 as a Novel Prognostic Biomarker of Meningioma Recurrence

Study design

RNA-seq cohort
64 FFPE primary samples:
16 recurrent vs 30 non-recurrent
51 neural crest vs 13 mesodermal
18 males vs 46 females
WHO grades: I (44); II (17); III (3)

RT-qPCR validation cohort
90 FFPE primary samples
33 recurrent vs 33 non-recurrent
71 neural crest vs 18 mesodermal
33 males vs 57 females
WHO grades: I (57); II (26); III (7)

Cox regression models for recurrence risk estimation

Results

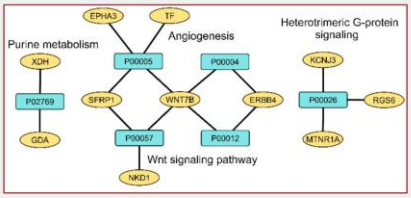

- Differential transcriptomic
- Pathways & Networks
- Potential *cis*-regulatory lncRNA/mRNA relationships:

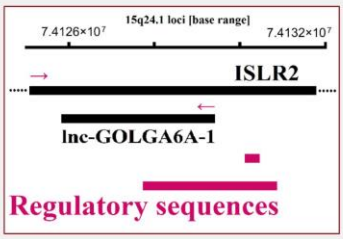

Crucial outcomes

- Distinct transcriptomic signatures of meningiomas in male and female patients and signatures associated with different histogenetic origins revealed for the first time
- lnc-GOLGA6A-1 is the most significant factor for recurrence risk estimation (1/HR = 1.31; p = 0.002)

Time to recurrence according to lnc-GOLGA6A-1 expression

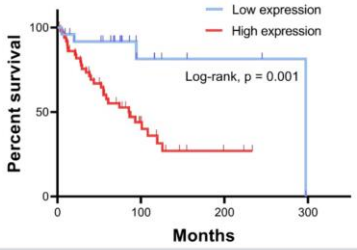

Nayak et al. *Neurosurgery*. December 2020

NEUROSURGERY
THE REGISTER OF THE NEUROSURGICAL MEME

APPENDIX 3

Původní práce

Stanovení exprese CEA, EGFR a hTERT v peritoneální laváži u pacientů s adenokarcinomem pankreatu metodou RT-PCR

M. Ghothim[1], J. Srovnal[2], L. Bébarová[3], J. Tesaříková[3], P. Skalický[3], D. Klos[3], A. Prokopová[2], M. Vahalíková[2], H. Slavík[2], J. Vrbková[2], Č. Neoral[3], R. Havlík[3], M. Hajdúch[2], M. Loveček[1]

[1] I. chirurgická klinika LF Univerzity Palackého Olomouc, přednosta: prof. MUDr. Č. Neoral, CSc.
[2] Laboratoř experimentální medicíny, Ústav molekulární a translační medicíny LF Univerzity Palackého Olomouc, ředitel doc. MUDr. M. Hajdúch, Ph.D.
[3] I. chirurgická klinika FN Olomouc, přednosta: prof. MUDr. Č. Neoral, CSc.

Souhrn

Úvod: Cílem práce je posoudit význam CEA, EGFR a hTERT jako markerů okultních nádorových buněk v břišní laváži v predikci léčebných výsledků u adenokarcinomu pankreatu, včetně stanovení jejich cut-off hodnot.
Metoda: Práce porovnává skupinu 87 pacientů operovaných pro duktální adenokarcinom pankreatu ve stadiu III - IV (UICC) u nichž byl proveden paliativní výkon (biliodigestivní spojka, odběr biologického materiálu pro následnou onkologickou léčbu) s kontrolní skupinou 24 pacientů. U všech pacientů byly odebrány vzorky peritoneální laváže za použití 100 ml fyziologického roztoku (phosphate buffered saline, pH=7,2) do transportních lahví obsahujících 1,5 ml 0,5M EDTA a 10 ml fetálního bovinního séra. Celková RNA všech vzorků byla purifikována a zpracována procesem reverzní transkripce. Okultní nádorové buňky v peritoneální laváži byly detekovány RT-PCR metodou využitím CEA, EGFR a hTERT. Sekundárním cílem studie bylo stanovení cut-off hodnot exprese těchto markerů. Pro statistické analýzy byly použity softwary R (www.r-project.org) a Statistica (StatSoft, Inc., USA).
Výsledky: Průměrná exprese CEA, EGFR a hTERT v peritoneální laváži kontrolní skupiny byla 2501, 716749, resp. 104 kopií mRNA/µg RNA. Prahové, cut-off hodnoty, byly stanoveny jako „průměr + 2x směrodatná odchylka". Hodnoty absolutní exprese byly dále normalizovány na expresi house-keepingového genu glyceraldehdyd-3-fosfát dehydrogenázy (GAPDH). Cut-off hodnoty testovaných markerů po normalizaci byly 4,89; 115,88 resp. 0,02 kopií mRNA genu/kopií mRNA GAPDH. V případě absolutní exprese testovaných markerů, pouze hTERT dokáže statisticky významně (p <0,001) odlišit obě analyzované skupiny, kdy pacienti s pokročilým adenokarcinomem pankreatu mají vyšší hodnotu exprese hTERT. Absolutní exprese CEA ani EGFR nevykazovala statisticky signifikantní rozdíly mezi skupinou s pokročilým karcinomem pankreatu a kontrolní skupinou. Použitím přesnějších - normalizovaných hodnot exprese testovaných markerů byla prokázána statisticky významně vyšší exprese CEA a hTERT (p<0,005, resp. p<0,001) u pacientů s pokročilým adenokarcinomem pankreatu v porovnání s kontrolní skupinou.
Závěr: Absolutní exprese hTERT v peritoneální laváži pacientů s pokročilým adenokarcinomem pankreatu byla signifikantně vyšší v porovnání s kontrolní skupinou. Naopak absolutní exprese CEA a EGFR nebyla signifikantně rozdílná.
Klíčová slova: karcinom pankreatu – okultní nádorové buňky – peritoneální laváž – RT-PCR – CEA – EGFR – hTERT

Summary

Determination of CEA, EGFR and hTERT expression in peritoneal lavage in patients with pancreatic adenocarcinoma using RT – PCR method

M. Ghothim, J. Srovnal, L. Bebarova, J. Tesarikova, P. Skalicky, D. Klos, A. Prokopova, M. Vahalikova, H. Slavik, J. Vrbkova, C. Neoral, R. Havlik, M. Hajduch, M. Lovecek

Introduction: The aim of this study is to assess the significance of CEA, EGFR and hTERT as markers of occult tumor cells for predicting treatment outcomes in pancreatic cancers, as well as determining the cut-off values of these markers individually in peritoneal lavage.
Method: The study compared 87 patients undergoing palliative operations (bypass surgery, biological sampling for subsequent oncological treatment) for either stage III or IV (UICC) pancreatic ductal adenocarcinomas with a control group of 24 healthy patients. Abdominal cavity lavage was performed at the beginning of the surgery in both groups, using 100 ml of physiological solution (phosphate buffered saline, pH 7.2). The samples were transported in bottles containing 1.5 ml 0.5 M EDTA and 10 ml of fetal bovine serum. Total RNA samples were all processed and purified by reverse transcription. Occult tumor cells in the peritoneal lavage were detected by the real-time RT-PCR method using CEA, EGFR and hTERT as markers of tumor cells. Another aim was to calculate the cut-off values of these markers. Statistical analysis was done using software R (www.r-project.org) and Statistica (StatSoft, Inc. USA).
Results: Mean expression of CEA, EGFR and hTERT in peritoneal lavage in the control group was 2501, 716749 and 104 copies of mRNA / mg RNA. Threshold, cut-off values were determined as the "mean + 2 times standard deviation". Absolute expression values were further normalized to expression of the house-keeping gene glyceraldehyde-3-phosphate dehydrogenase (GAPDH). After normalization, cut-off values of the tested markers were 4.89, 115.88 and 0.02 copies of mRNA/GAPDH mRNA. As regards absolute expression of the markers tested, only hTERT was able to statistically significantly (p<0.001) distinguish the analysed groups, where patients with advanced pancreatic adenocarcinoma had a higher expression of hTERT. Absolute expression of CEA or EGFR was not able to discriminate between the two groups. The more accurate normalized expression values of the test markers demonstrated a statistically significantly higher expression of hTERT (p<0.005) and CEA (p<0.001) in patients with advanced adenocarcinoma compared to the control group.
Conclusion: Absolute hTERT expression in peritoneal lavage of patients with advanced pancreatic cancer was significantly higher compared to the control group.
Key words: pancreatic adenocarcinoma – occult tumor cells – peritoneal lavage – RT-PCR – CEA – EGFR – hTERT

Rozhl Chir 2015;94:464–476

ÚVOD

Vedle uzlin, systémové krve a kostní dřeně je peritoneální dutina dalším sledovatelným kompartmentem v procesu šíření karcinomu pankreatu. Studie exprese markerů okultních epiteliálních nádorových buněk (karcinoembryonálního antigenu – CEA, receptoru pro epidermální růstový faktor – EGFR a lidské telomerázy – hTERT) v abdominální laváži nemocných s různými stádii adenokarcinomu pankreatu ukázala, že zvýšenou expresi EGFR a CEA v tomto kompartmentu je možno považovat za negativní prognostický faktor přežívání, korespondující s klinickým stadiem a gradem tumoru [1]. Publikací zaměřených na prognosticky významné markery okultních nádorových buněk metodou PCR v peritoneální laváži u pacientů s karcinomem pankreatu není mnoho a výsledky jsou často nejednoznačné [1,2,3,4,5,6,7,8,9]. Eguchi a spol. prokázal metodou PCR pozitivitu CEA ve vzorcích peritoneální laváže u 21,7 % (15/69) radikálně operovaných pacientů s rakovinou slinivky břišní, a tito pacienti měli kratší dobu přežití bez progrese onemocnění i celkovou dobu přežití (p=0,004 a p=0,01) [3]. Broll a spol. rovněž referuje o vysoké pozitivitě CEA (63 %) v peritoneální laváži pacientů s karcinomem pankreatu, ale současně nedoporučuje metodu PCR založenou na analýze CEA transkriptů pro detekci okultních nádorových buněk v peritoneální laváži pro vysokou míru falešně pozitivních výsledků (38 %) u kontrolních vzorků peritoneální laváže u zdravých osob [7]. Příčinou rozdílných výsledků i závěrů mohou být různé použité metody, různý výběr markerů a malé soubory testovaných vzorků (pacientů). Klos a spol. zjistili statistickou souvislost mezi expresí EGFR v portální krvi a klinickým stadiem (p<0,006), expresí EGFR v portální krvi a stupněm diferenciace primárního tumoru (p<0,045) a vysokou míru exprese EGFR v peritoneální laváži u pacientů s metastatickým postižením oproti pacientům bez přítomnosti metastáz (p<0,015), exprese EGFR (p=0,01) byla spojena s kratším celkovým přežíváním pacientů s adenokarcinomem pankreatu [4]. V peritoneální laváži byly testovány markery CEA a CA 19-9 jak RT-PCR tak biochemickými metodikami [10]. EGFR a hTERT dosud testovány nebyly.

Současná studie předkládá výsledky srovnání exprese markerů CEA, EGFR a hTERT v abdominální laváži u nemocných s pokročilým duktálním adenokarcinomem pankreatu a u kontrolní skupiny nemocných bez nádoru či zánětlivého onemocnění. Cílem studie bylo i stanovení a ověření cut-off hodnot pro tyto markery v peritoneální laváži.

METODA

Pacienti s adenokarcinomem pankreatu

Do studie bylo zařazeno 87 pacientů operovaných na I. chirurgické klinice FN Olomouc v letech 2007–2010 pro vývodový adenokarcinom pankreatu ve stadiu III - IV (UICC) – lokálně inoperabilní či generalizovaný, u nichž byl proveden paliativní výkon (bypassová operace, odběr biologického materiálu pro následnou onkologickou léčbu) a zároveň byl získán materiál z laváže dutiny břišní. Diagnóza adenokarcinomu pankreatu byla ověřena histologicky a do studie byli zahrnuti pouze pacienti s pooperačním statusem R2 výkonu (Tab. 1).

Kontrolní skupina

Kontrolní skupinu tvořilo 24 elektivně operovaných pacientů pro cholecystolithiasu bez známek akutního zánětu a bez nádorového onemocnění či anamnézy nádorového onemocnění, u nichž byla provedena v úvodu výkonu laváž dutiny břišní (Tab. 1). Studie byla schválena Etickou komisí Fakultní nemocnice v Olomouci, pacienti podepsali informovaný souhlas.

Odběr peritoneální laváže

Vzorky peritoneální laváže byly získány u všech 87 nemocných s pokročilým adenokarcinomem pankreatu a u všech 24 kontrolních subjektů použitím 100 ml fyziologického roztoku (phosphate buffered saline, pH=7,2) ihned po otevření břišní dutiny či v úvodu laparoskopického výkonu. Peritoneální laváž byla získána aspirací do sterilní stříkačky a poté přenesena do transportních lahví obsahujících 1,5 ml 0,5M EDTA a 10 ml fetálního bovinního séra. Odebraný materiál byl následně ihned transportován do laboratoře.

RNA purifikace a reverzní transkripce

Celková RNA byla izolována ze sedimentu peritoneální laváže fenol-chloroformovou metodou za použití kitu TRI Reagent (Molecular Research Center, Cincinnati, OH, USA), postupovalo se dle návodu výrobce. Pro reverzní transkripci byl použit 1µg získané RNA, po inkubaci s náhodnými hexamery (Promega, Madison, WI, USA) byla provedena reverzní transkripce za použití RevertAid Moloney Murine Leukemia Virus reverzní transkriptázy (Fermentas, Vilnius, Lithuania).

Real-time PCR

Real-time PCR amplifikace 100ng cDNA získané reverzní transkripcí byla provedena na přístroji Rotor Gene 3000 (Corbett Research, Sydney, Australia). Pro amplifikaci karcinoembryonálního antigenu (CEA, NM 004363), receptoru pro epidermální růstový faktor 1 (EGFR, NM_005228) a lidskou telomerázu (hTERT, NM_198253) byly navrženy specifické primery a taqman sondy (Generi-Biotech, Hradec Králové, Česká republika) [3]. Samotná PCR reakce byla amplifikovaná polymerázou HotStart Taq Polymerase (AB Gene, Epsom, UK). Pro absolutní kvantifikaci byly připraveny plazmidové standardy pCR 2.1Topo (Invitrogen, Carlsbad, California, USA), které v ředění sloužily k sestavení kalibrační křivky. Změřené hodnoty genové exprese testovaných markerů byly normalizovány jak na množství RNA vstupující do reverzní transkripce, tak vzhledem k expresi housekeepingového genu glyceraldehyd-3-fosfát dehydrogenázy (GAPDH).

Statistická analýza

Prahové, cut-off, hodnoty exprese CEA, EGFR a hTERT v peritoneální laváži byly stanoveny jako aritmetický průměr plus dvojnásobek směrodatné odchylky v souboru kontrolních zdravých subjektů. Exprese testovaných markerů u pacientů s adenokarcinomem pankreatu byly srovnány s hodnotami v kontrolním souboru prostřednictvím Wilcoxonova exaktního dvouvýběrového testu. Obě skupiny jsou porovnány rovněž graficky prostřednictvím krabicových grafů s vyznačenou prahovou hodnotou. Pro statistické výpočty a grafy byly použity softwary R (www.r-project.org) a STATISTICA (StatSoft, Inc., USA).

VÝSLEDKY

Průměrná exprese CEA, EGFR a hTERT v peritoneální laváži kontrolní skupiny byla 2501, 716749, resp. 104 kopií mRNA/µg RNA (Tab. 2). Hodnoty absolutní exprese byly dále normalizovány na expresi house-keepingového genu glycealdehdyd-3-fosfát dehydrogenázy (GAPDH). Cut-off hodnoty testovaných markerů po normalizaci byly 4,89, 115,88, resp. 0,02 kopií mRNA genu/kopií mRNA GAPDH.

Bylo provedeno porovnání exprese CEA, EGFR a hTERT mezi kontrolní skupinou a pacienty s pokročilým adenokarcinomem pankreatu (R2). V případě absolutní exprese testovaných markerů (Graf 1,2,3), pouze hTERT dokáže statisticky významně ($p<0,001$) odlišit obě analyzované skupiny, kdy pacienti s pokročilým adenokarcinomem pankreatu (R2) mají vyšší hodnotu exprese hTERT (Obr. 3). Absolutní exprese CEA ani EGFR nedokáže odlišit obě skupiny, hodnoty exprese obou markerů nevykazují statisticky signifikantní rozdíly mezi kontrolní skupinou a skupinou s pokročilým adenokarcinomem pankreatu.

Za využití přesnějších, normalizovaných hodnot exprese testovaných markerů Graf 4,5,6) byla prokázána statisticky významně vyšší exprese CEA a hTERT ($p<0,005$, resp. $p<0,001$) u pacientů s pokročilým adenokarcinomem pankreatu (R2) v porovnání s kontrolní skupinou (Graf 4 a 6).

Tab. 1: Charakteristika pacientů (ND – nestanoveno)
Tab. 1: Patients characteristics (ND - not determined)

	Počet	Pohlaví		Věk (medián)	Stádium		Grading			
		Muži	Ženy		III	IV	1	2	3	ND
Pacienti s adenokarcinomem pankreatu (R2)	87	49	38	65	26	61	1	26	44	16
Kontrolní skupina	24	8	16	50	ND	ND	ND	ND	ND	ND

Tab. 2: Cut-off hodnoty exprese CEA, EGFR a hTERT v peritoneální laváži
Tab. 2: Cut-off values of CEA, EGFR and hTERT gene expression in peritoneal lavage

	Absolutní exprese genu (kopie mRNA genu/µg RNA)				Normalizovaná exprese genu (kopie mRNA genu/mRNA GAPDH)		
Kategorie	CEA	EGFR	hTERT	GAPDH	CEA/GAPDH	EGFR/GAPDH	hTERT/GAPDH
Průměr	2501	716 749	104	125 248 876	0,49	25,42	0,0023
Směrodatná odchylka	7651	1 423 099	178	149 229 377	2,20	45,23	0,0078
Cut-off	**17800**	**3 550 000**	**460**	**423 700 000**	**4,89**	**115,88**	**0,0200**

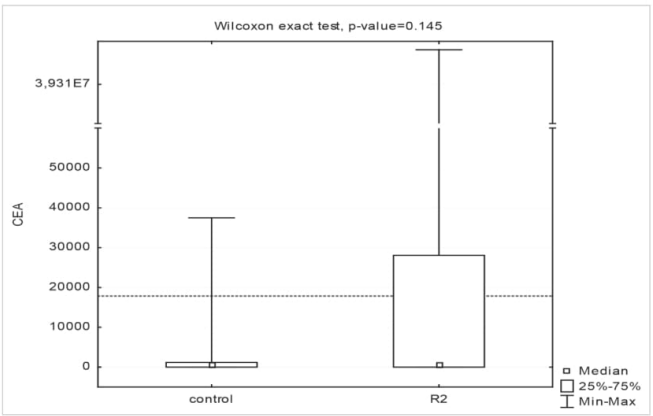

Graf 1: Absolutní exprese CEA (kopie mRNA genu/µg RNA) ve skupině kontrol a pacientů s pokročilým adenokarcinomem pankreatu
Přerušovaná linka představuje vypočtenou cut--off hodnotu.
Graph 1. Absolute expression of CEA (copy of mRNA of the gene/µg RNA) in the control group and in the group with advanced pancreatic carcinoma
The dotted line means the calculated cutt-off value.

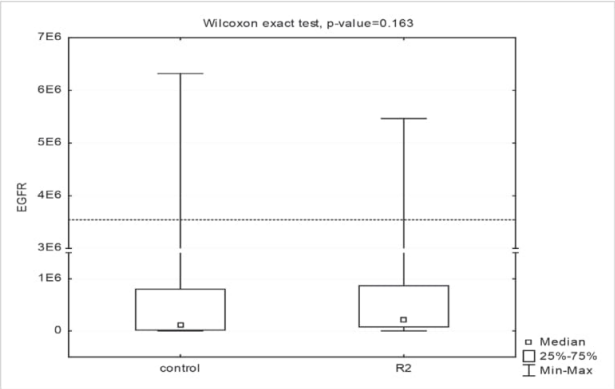

Graf 2: Absolutní exprese EGFR (kopie mRNA genu/µg RNA) ve skupině kontrol a pacientů s pokročilým adenokarcinomem pankreatu
Přerušovaná linka představuje vypočtenou cut-off hodnotu.
Graph 2. Absolute expression of EGFR (copy of mRNA of the gene/µg RNA) in the control group and in the group with advanced pancreatic carcinoma
The dotted line means the calculated cutt-off value.

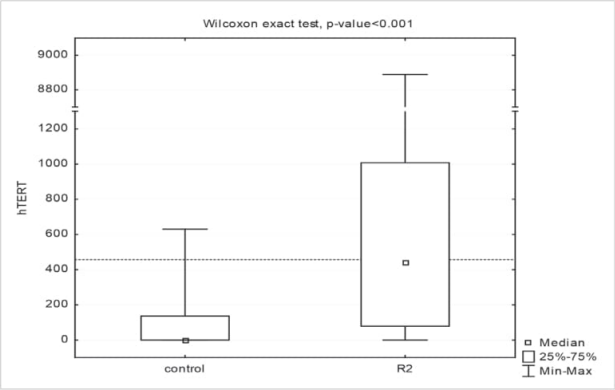

Graf 3: Absolutní exprese hTERT (kopie mRNA genu/µg RNA) ve skupině kontrol a pacientů s pokročilým adenokarcinomem pankreatu
Přerušovaná linka představuje vypočtenou cut-off hodnotu.
Graph 3. Absolute expression of hTERT (copy of mRNA of the gene/µg RNA) in the control group and in the group with advanced pancreatic carcinoma
The dotted line means the calculated cutt-off value.

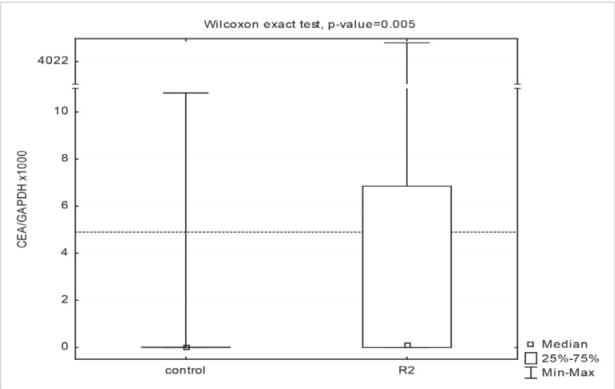

Graf 4: Normalizovaná exprese CEA (kopie mRNA genu/ kopie mRNA GAPDH) ve skupině kontrol a pacientů s pokročilým adenokarcinomem pankreatu
Přerušovaná linka představuje vypočtenou cut-off hodnotu**.**
Grahp 4. Normalized expression of CEA (copy of mRNA of the gene/copy of mRNA GAPDH) in the control group and in the group with advanced pancreatic carcinoma
The dotted line means the calculated cutt-off value.

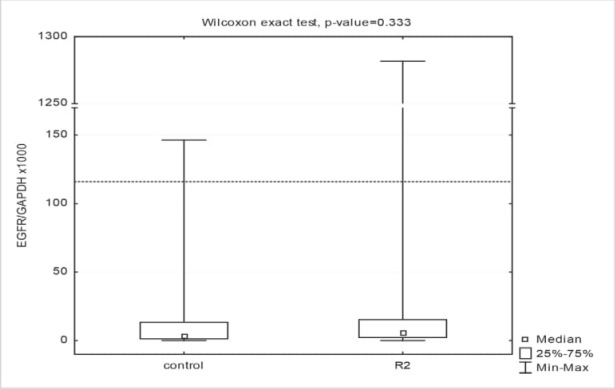

Graf 5: Normalizovaná exprese EGFR (kopie mRNA genu/ kopie mRNA GAPDH) ve skupině kontrol a pacientů s pokročilým adenokarcinomem pankreatu
Přerušovaná linka představuje vypočtenou cut-off hodnotu.
Graph 5. Normalized expression of EGFR (copy of mRNA of the gene/copy of mRNA GAPDH) in the control group and in the group with advanced pancreatic carcinoma
The dotted line means the calculated cutt-off value.

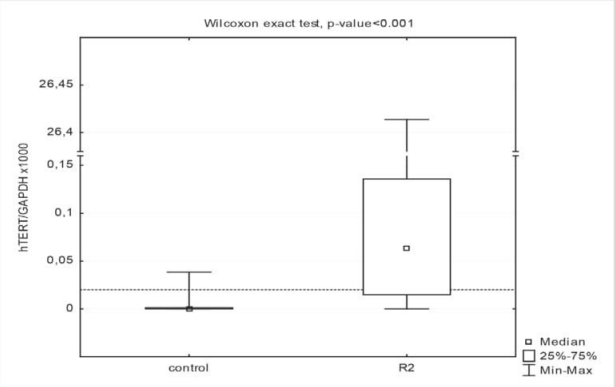

Graf 6: Normalizovaná exprese hTERT (kopie mRNA genu/ kopie mRNA GAPDH) ve skupině kontrol a pacientů s pokročilým adenokarcinomem pankreatu
Přerušovaná linka představuje vypočtenou cut-off hodnotu.
Graph 6. Normalized expression of hTERT (copy of mRNA of the gene/copy of mRNA GAPDH) in the control group and in the group with advanced pancreatic carcinoma
The dotted line means the calculated cutt-off value.

DISKUZE

Cílem studie bylo stanovit hodnoty exprese CEA, EGFR a hTERT jako potenciálních markerů okultních nádorových buněk u nemocných s pokročilým karcinomem pankreatu v abdominální laváži – kompartmentu břišní dutiny – a hodnoty exprese týchž markerů u kontrolní skupiny [2,3,4,5]. Ke stanovení bylo využito metod založených na principu RT – PCR.

Předpokladem studie byla hypotéza, že přítomnost markerů nádorových buněk v populaci zdravé a v populaci s pokročilým karcinomem pankreatu bude rozdílná. Záměrem je využitím zmíněné metodiky ověřit diskriminační schopnosti těchto markerů pro skupinu nemocných s pokročilým karcinomem.

Ačkoliv část naší skupiny prokázala nedávno statisticky významné rozdíly v expresi EGFR u nemocných s metastatickým postižením oproti nemocným s lokalizovaným onemocněním jak v portální krvi, tak v abdominální laváži, současná studie porovnáním těchto výsledků s kontrolní zdravou skupinou zjišťuje, že není statisticky významný rozdíl v expresi tohoto markeru mezi oběma nyní sledovanými skupinami [1,4]. Klos a spol. prokázali zvýšenou expresi EGFR u pokročilých stadií karcinomu pankreatu a statisticky významně vyšší u pokročilých stadií oproti méně pokročilým stadiím, i v korelaci s dobou přežití. Havlík a spol. prokázali, že EGFR a CEA pozitivita v peritoneální laváži koresponduje s klinickým stadiem a gradem tumoru ale i kratším přežitím u pokročilých stadií. Za překvapivý výsledek považujeme zjištění zejména u EGFR v naší studii. Ta ukazuje na srovnatelnou expresi jak absolutní tak normalizovanou v obou skupinách a tím velmi limituje využití exprese EGFR jako markeru okultních nádorových buněk v abdominální laváži. U markeru CEA jsme prokázali sice rozdílnou expresi v kontrolní skupině a u nemocných s pokročilým karcinomem pankreatu jak absolutní tak normalizovanou, nicméně statisticky významný rozdíl byl jen u normalizované. Toto je ve shodě s publikovanými závěry Brolla a spol., který rovněž referuje o vyšší pozitivitě CEA (63 %) v peritoneální laváži pacientů s karcinomem pankreatu, ale současně poukazuje na vysokou míru falešně pozitivních výsledků (38 %) u kontrolních vzorků peritoneální laváže u zdravých osob [7].

Výsledky naší studie potvrzují schopnosti diferenciace mezi zdravou skupinou a skupinou s pokročilým karcinomem pankreatu (stadia III a IV) jen u markeru hTERT, kdy byla prokázána statisticky významně vyšší absolutní exprese hTERT ($p<0,001$) i normalizovaná exprese hTERT ($p<0,001$) a u markeru CEA jen normalizovaná exprese CEA ($p<0,005$) v peritoneální laváži u pacientů s pokročilým adenokarcinomem pankreatu (R2) v porovnání s kontrolní skupinou. Aktuálně Campa a spol. potvrdil, že polymorfismus v genu TERT je spojený s rizikem karcinomu pankreatu na základě hloubkové analýzy genetické variability TERT u subjektů s karcinomem pankreatu a kontrolního souboru [11]. Expresi EGFR jak absolutní tak normalizovanou v naší studii nelze použít k odlišení obou studovaných skupin. Absolutní exprese CEA též nevykazovala statisticky signifikantní rozdíly u obou skupin. Konvenční cytologie, imunohistochemie i molekulárně-biologické metody zatím tedy poskytují rozporuplné výsledky v případě prognostického významu okultních nádorových buněk v peritoneální laváži u pacientů s adenokarcinomem pankreatu. Je zřejmé, že další pokrok v této oblasti úzce souvisí s potřebou standardizace metod a postupů, s validací výsledků v nezávislých ověřovacích studiích a s vývojem nových detekčních metod s optimální senzitivitou a specifitou umožňující přímou vizualizaci a následnou charakterizaci detekovaných nádorových buněk.

Lze tedy říci, že na základě prezentovaných výsledků pro detekci nádorových buněk u adenokarcinomu pankreatu v abdominální laváži využitím RT-PCR by mohl být použitelný marker hTERT, naopak průkaz exprese CEA a EGFR nesplňuje požadavky na odlišení kontrolní zdravé skupiny od skupiny s pokročilým adenokarcinomem pankreatu.

ZÁVĚR

Exprese hTERT v peritoneální laváži, jak absolutní tak normalizovaná, dosahuje statisticky signifikantního rozdílu a mohla by tak být kandidátním markerem pro identifikaci pacientů s pokročilým pankreatickým adenokarcinomem a s malým benefitem z radikálního chirurgického výkonu. Další studie se zaměřením na hTERT

budou nutné k potvrzení tohoto závěru. V dané studii však byl zjištěn prakticky zanedbatelný rozdíl jak v absolutní, tak normalizované expresi EGFR v peritoneální laváži a též nebyl zjištěn statisticky významný rozdíl v absolutní expresi CEA u kontrolní skupiny a u nemocných s pokročilým adenokarcinomem pankreatu.

Zkratky

UICC Union for International Cancer Control
EDTA ethylenediaminetetraacetic acid
RT-PCR reverse transcription polymerase chain reaction
RNA ribonucleic acid
DNA deoxyribonucleic acid

Práce byla podpořena granty: IGA_LF_2015_002, IGA_UP_2015_010, IGA LF 2014_030, CZ.1.07/2.3.00/30.0004, NPU LO1304 a TAČR TE0200005.

Konflikt zájmů

Autoři článku prohlašují, že nejsou v souvislosti se vznikem tohoto článku ve střetu zájmů a že tento článek nebyl publikován v žádném jiném časopise.

LITERATURA

1. Havlik R, Srovnal J, Klos D, et al. Occult tumour cells in peritoneal lavage are a negative prognostic factor in pancreatic cancer. Biomed Pap Med Fac Univ Palacky Olomouc Czech Repub 2013;157:233–8.
2. Okami J, Dohno K, Sakon M, et al. Genetic detection for micrometastases in lymph node of biliary tract carcinoma. Clin Cancer Res 2000;6:2326–32.
3. Eguchi H, Ohigashi H, Takahashi H, et al. Presence of minute cancer cell dissemination in peritoneal lavage fluid detected by reverse transcription PCR is an independent prognostic factor in patients with resectable pancreatic cancer. Surgery 2009;146:888–95.
4. Klos D, Loveček M, Srovnal J, et al. Možnosti využití stanovení minimální reziduální choroby u adenokarcinomu pankreatu pomocí metodiky real-time RT-PCR – pilotní studie. Časopis lékařů českých 2010;149:69–73.
5. Grochola LF, Greither T, Taubert HW, et al. Prognostic relevance of hTERT mRNA expression in ductal adenocarcinoma of the pancreas. Neoplasia 2008;10:973–6.
6. Vogel I, Kalthoff H, Henne-Bruns D, et al. Detection and prognostic impact of disseminated tumor cells in pancreatic carcinoma. Pancreatology 2002;2:79–88.
7. Broll R, Weschta M, Windhoevel U, et al. Prognostic significance of free gastrointestinal tumor cells in peritoneal lavage detected by immunocytochemistry and polymerase chain reaction. Langenbecks Arch Surg 2001;386:285–92.
8. Makary MA, Warshaw AL, Centeno BA, et al. Implications of peritoneal cytology for panceratic cancer management. Arch Surg 1998;133:361–5.
9. Yamada S, Fujii T, Kanda M, et al. Value of peritoneal cytology in potentially resectable pancreatic cancer. Br J Surg. 2013;100:1791–6.
10. Hoskovec D, Varga J, Konečná E, et al. Levels of CEA and Ca 19 - 9 in the sera and peritoneal cavity in patients with gastric and pancreatic cancers. Acta Cir Bras 2012;27:410–6.
11. Campa D, Rizzato C, Stolzenberg-Solomon RZ, et al. The TERT gene harbors multiple variants associated with pancreatic cancer susceptibility. Int J Cancer 2015;137:2175–83.

MUDr. Martin Loveček, Ph.D.
I.chirurgická klinika LF UP a FN Olomouc
I.P. Pavlova 6,
775 20 Olomouc
e-mail: mlovecek@seznam.cz

Komentář ke článku

„Stanovení exprese CEA, EGFR a hTERT jako markerů nádorových buněk v peritoneální laváži u pacientů s adenokarcinomem pankreatu metodou RT-PCR“ autorů Ghothim a kolektiv

Článek srovnání hladin exprese uvedených genů detekovaných v peritoneální laváži mezi skupinou 87 pacientů s pokročilým karcinomem pankreatu a kontrolní skupinou 24 pacientů operovanou pro žlučové kameny. Jako výsledek byl získán statisticky významný rozdíl exprese mezi oběma skupinami, a to při porovnání absolutní exprese u genu hTERT a při porovnání normalizovaných expresí u genů CEA a EGFR.

Jedná se čistě o metodickou práci, která sice nenaplňuje rysy nového postupu či nového využití metodologie, avšak která je po technické stránce precizně provedena. Otázkou je využitelnost získaných výsledků pro diagnostiku či terapii onemocnění, což, bohužel, bývá častým problémem u obdobně koncipovaných článků. Nadšení z prostého faktu odhalení statistické významnosti výskytu studovaných biomarkerů tak poněkud zastiňuje klinickou využitelnost (clinical utility). Je cílem práce zjistit prostou přítomnost okultních nádorových buněk v peritoneální laváži? Či je cílem zjistit, zda okultní nádorové buňky přítomné v laváži vykazují právě tyto a nikoli jiné markery? Jaká je potom prognostická hodnota hladin těchto genů v pankreatické tkáni, a v čem je tedy výhoda vyšetřování laváže? Jaký klinický smysl dává volba kontrolní skupiny tvořená pacienty s předpokladem normální zdravé tkáně v případě peritoneální laváže prováděné u pacientů operovaných pro suspektní pankreatické léze?

Je nepochybné, že v případě maligního onemocnění vykazuje velké množství genů významné rozdíly v expresi při srovnání s nenádorovou tkání, a proto fakt statistické významnosti nalezených rozdílů u pacientů a „zdravých“ kontrol není bez hlubšího klinického kontextu sledovaných biomarkerů nikterak překvapivý.

Výsledkem zcela legitimního a po metodické stránce špičkově provedeného výzkumného záměru je tak solidní technická zpráva demonstrující schopnost vyšetřování exprese několika vybraných genů v peritoneální laváži, nikoli zjištění zasazující danou metodiku do klinického kontextu. K obhajobě autorů je však třeba říci, že výše uvedené výhrady lze aplikovat i na řadu současných prací vycházejících v renomovaných časopisech s vysokým impakt faktorem, tedy se jistě nejedná o odchylku, nýbrž o poněkud nešťastný trend současné doby, pro kterou je okouzlení nově nastupujícími technikami tak typické.

RNDr. Marek Minárik Ph.D.
Genomac výzkumný ústav, s.r.o.
e-mail: mminarik@genomac.cz